CITATION REPORT List of articles citing

In-gel digestion for mass spectrometric characterization of proteins and proteomes

DOI: 10.1038/nprot.2006.468 Nature Protocols, 2006, 1, 2856-60.

Source: https://exaly.com/paper-pdf/40436414/citation-report.pdf

Version: 2024-04-23

This report has been generated based on the citations recorded by exaly.com for the above article. For the latest version of this publication list, visit the link given above.

The third column is the impact factor (IF) of the journal, and the fourth column is the number of citations of the article.

#	Paper	IF	Citations
2275	1,2-Dichloroethane Exposure Alters the Population Structure, Metabolism, and Kinetics of a Trichloroethene-Dechlorinating Dehalococcoides mccartyi Consortium.		
2274	Production and Transduction of a Human Recombinant Globin Chain into Proerythroid K562 Cells To Replace Missing Endogenous Globin.		
2273	Photoactivatable Glycolipid Probes for Identifying MycolateProtein Interactions in Live Mycobacteria.		
2272	Covalent Targeting of Ras G12C by Rationally Designed Peptidomimetics.		
2271	Selective Photoaffinity Probe That Enables Assessment of Cannabinoid CB2 Receptor Expression and Ligand Engagement in Human Cells.		
2270	Nucleation and Propagation of Heterochromatin by the Histone Methyltransferase PRC2: Geometric Constraints and Impact of the Regulatory Subunit JARID2.		
2269	Biosynthesis of an Anti-Addiction Agent from the Iboga Plant.		
2268	•		
2267	Abstract.		2
2266	Evidence that SpoIVFB is a novel type of membrane metalloprotease governing intercompartmental communication during Bacillus subtilis sporulation. 2000 , 182, 3305-9		61
2265	A practical recipe for stable isotope labeling by amino acids in cell culture (SILAC). <i>Nature Protocols</i> , 2006 , 1, 2650-60	18.8	711
2264	Salt-induced changes in the plasma membrane proteome of the halotolerant alga Dunaliella salina as revealed by blue native gel electrophoresis and nano-LC-MS/MS analysis. 2007 , 6, 1459-72		123
2263	New method for characterizing highly disulfide-bridged peptides in complex mixtures: application to toxin identification from crude venoms. 2007 , 6, 3216-23		74
2262	Gel-free sample preparation for the nanoscale LC-MS/MS analysis and identification of low-nanogram protein samples. 2007 , 30, 2210-6		15
2261	High-sensitivity analysis of specific peptides in complex samples by selected MS/MS ion monitoring and linear ion trap mass spectrometry: application to biological studies. 2007 , 42, 1391-403		65
2260	Mass spectrometry-based functional proteomics: from molecular machines to protein networks. 2007 , 4, 807-15		193
2259	Two-dimensional gel electrophoresis for identifying proteins that bind DNA or RNA. <i>Nature Protocols</i> , 2007 , 2, 1839-48	18.8	9

(2008-2007)

2258	Reprogramming the amino-acid substrate specificity of orthogonal aminoacyl-tRNA synthetases to expand the genetic code of eukaryotic cells. <i>Nature Protocols</i> , 2007 , 2, 2590-600	19
2257	Analysis of O-glycan heterogeneity in IgA1 myeloma proteins by Fourier transform ion cyclotron resonance mass spectrometry: implications for IgA nephropathy. 2007 , 389, 1397-407	77
2256	Stain efficiency and MALDI-TOF MS compatibility of seven visible staining procedures. 2008 , 390, 1765-73	25
2255	Isolation, characterization and molecular cloning of duplex-specific nuclease from the hepatopancreas of the Kamchatka crab. 2008 , 9, 14	45
2254	The chicken egg yolk plasma and granule proteomes. 2008 , 8, 178-91	141
2253	Variability of polymorphic families of three types of xylanase inhibitors in the wheat grain proteome. 2008 , 8, 1692-705	20
2252	Proteomic analysis of the chicken egg vitelline membrane. 2008 , 8, 2322-32	106
2251	Quantitative phosphoproteome analysis of a mouse liver cell line reveals specificity of phosphatase inhibitors. 2008 , 8, 4534-46	89
2250	Peptide separation with immobilized pI strips is an attractive alternative to in-gel protein digestion for proteome analysis. 2008 , 8, 4862-72	148
2249	Protein identification pipeline for the homology-driven proteomics. 2008 , 71, 346-56	70
2248	On-gel fluorescent visualization and the site identification of S-nitrosylated proteins. 2008 , 377, 150-5	34
2247	One-step procedure for peptide extraction from in-gel digestion sample for mass spectrometric analysis. 2008 , 80, 9797-805	15
2246	Detergent-based but gel-free method allows identification of several hundred membrane proteins in single LC-MS runs. 2008 , 7, 5028-32	72
2245	Molecular characterization of the major hemelipoglycoprotein in ixodid ticks. 2008 , 17, 197-208	30
2244	Transcriptional regulation of beta2-microglobulin demonstrated via a novel genomic and proteomic analysis of percutaneously collected peripheral atheroma. 2008 , 1, 240-4	2
2243	Differential proteome of bone marrow mesenchymal stem cells from osteoarthritis patients. 2008 , 16, 929-35	20
2242	The sea urchin (Strongylocentrotus purpuratus) test and spine proteomes. 2008 , 6, 22	92
2241	In-depth, high-accuracy proteomics of sea urchin tooth organic matrix. 2008 , 6, 33	63

2240	A proteomic approach identified growth hormone-dependent nutrition markers in children with idiopathic short stature. 2008 , 6, 35	18
2239	Proteomics and its Application to the Human-Pathogenic Fungi Aspergillus fumigatus and Candida albicans. 2008 , 155-186	1
2238	Chromatin Central: towards the comparative proteome by accurate mapping of the yeast proteomic environment. 2008 , 9, R167	96
2237	Human and Animal Relationships. 2008,	2
2236	Separating the wheat from the chaff: unbiased filtering of background tandem mass spectra improves protein identification. 2008 , 7, 3382-95	35
2235	Phosphorylation of SUMO-1 occurs in vivo and is conserved through evolution. 2008 , 7, 4050-7	30
2234	Distinction between human cytochrome P450 (CYP) isoforms and identification of new phosphorylation sites by mass spectrometry. 2008 , 7, 4678-88	46
2233	Stable isotope labeling by amino acids in cell culture (SILAC) and proteome quantitation of mouse embryonic stem cells to a depth of 5,111 proteins. 2008 , 7, 672-83	242
2232	Comparison of the membrane subproteomes during growth of a new pseudomonas strain on lysogeny broth medium, glucose, and phenol. 2008 , 7, 4278-88	14
2231	Amino Acid Sequence Database Suitable for the Protein and Proteome Analysis. 2008 , 5, 267-275	1
2230	Ordered organelle degradation during starvation-induced autophagy. 2008 , 7, 2419-28	145
2229	Identification of a synaptosome-associated form of BAG3 protein. 2008 , 7, 3104-5	19
2228	TSG-6 transfers proteins between glycosaminoglycans via a Ser28-mediated covalent catalytic mechanism. 2008 , 283, 33919-26	23
2227	Protein polymorphism between 2 Picea abies populations revealed by 2-dimensional gel electrophoresis and tandem mass spectrometry. 2008 , 99, 364-75	9
2226	A SILAC-based DNA protein interaction screen that identifies candidate binding proteins to functional DNA elements. 2009 , 19, 284-93	125
2225	The transfer of heavy chains from bikunin proteins to hyaluronan requires both TSG-6 and HC2. 2008 , 283, 18530-7	30
2224	Vacuole membrane protein 1 is an endoplasmic reticulum protein required for organelle biogenesis, protein secretion, and development. 2008 , 19, 3442-53	45
2223	Aspergillus nidulans ArfB plays a role in endocytosis and polarized growth. 2008 , 7, 1278-88	42

(2009-2008)

2222	Oligosaccharide profiles of the prostate specific antigen in free and complexed forms from the prostate cancer patient serum and in seminal plasma: a glycopeptide approach. 2008 , 18, 2-8	89
2221	4-Chloro-alpha-cyanocinnamic acid is an advanced, rationally designed MALDI matrix. 2008 , 105, 12200-5	129
2220	Akt1 intramitochondrial cycling is a crucial step in the redox modulation of cell cycle progression. 2009 , 4, e7523	56
2219	Actin remodeling by ADF/cofilin is required for cargo sorting at the trans-Golgi network. 2009 , 187, 1055-69	87
2218	Activation of dual oxidases Duox1 and Duox2: differential regulation mediated by camp-dependent protein kinase and protein kinase C-dependent phosphorylation. 2009 , 284, 6725-34	149
2217	Aldosterone increases oxidant stress to impair guanylyl cyclase activity by cysteinyl thiol oxidation in vascular smooth muscle cells. 2009 , 284, 7665-72	82
2216	Proteomic analysis of the human receptive versus non-receptive endometrium using differential in-gel electrophoresis and MALDI-MS unveils stathmin 1 and annexin A2 as differentially regulated. 2009 , 24, 2607-17	100
2215	Core glycosylation of collagen is initiated by two beta(1-O)galactosyltransferases. 2009 , 29, 943-52	99
2214	Inhibition of the soluble epoxide hydrolase by tyrosine nitration. 2009 , 284, 28156-28163	24
2213	Dephosphorylation of major sperm protein (MSP) fiber protein 3 by protein phosphatase 2A during cell body retraction in the MSP-based amoeboid motility of Ascaris sperm. 2009 , 20, 3200-8	21
2212	Stable isotope labeling by amino acids in cell culture (SILAC) and quantitative comparison of the membrane proteomes of self-renewing and differentiating human embryonic stem cells. 2009 , 8, 959-70	98
2211	Theoretical and experimental analysis links isoform-specific ERK signalling to cell fate decisions. 2009 , 5, 334	62
22 10	Differential Proteomics Identifies Protein Biomarkers That Predict Local Relapse of Head and Neck Squamous Cell Carcinomas. 2009 , 15, 7666-7675	53
2209	Systems-wide analysis of a phosphatase knock-down by quantitative proteomics and phosphoproteomics. 2009 , 8, 1908-20	88
2208	Unique features of plant cleavage and polyadenylation specificity factor revealed by proteomic studies. 2009 , 151, 1546-56	20
2207	Comparative proteomics analysis of cardiac muscle samples from pufferfish Takifugu rubripes exposed to excessive fluoride: initial molecular response to fluorosis. 2009 , 19, 468-75	6
2206	The exosome associates cotranscriptionally with the nascent pre-mRNP through interactions with heterogeneous nuclear ribonucleoproteins. 2009 , 20, 3459-70	31
2205	Role of annexin A2 in cellular entry of rabbit vesivirus. 2009 , 90, 2724-2730	21

2204	Artifactual sulfation of silver-stained proteins: implications for the assignment of phosphorylation and sulfation sites. 2009 , 8, 506-18	24
2203	Large-scale proteomics analysis of the human kinome. 2009 , 8, 1751-64	236
2202	An enhanced mass spectrometry approach reveals human embryonic stem cell growth factors in culture. 2009 , 8, 421-32	72
2201	Regulation of vascular contractility and blood pressure by the E2F2 transcription factor. 2009 , 120, 1213-21	22
2200	The Mre11-Rad50-Nbs1 complex mediates activation of TopBP1 by ATM. 2009 , 20, 2351-60	57
2199	Complement factor H binding by different Lyme disease and relapsing fever Borrelia in animals and human. 2009 , 2, 134	34
2198	Off-target decoding of a multitarget kinase inhibitor by chemical proteomics. 2009 , 10, 1163-74	14
2197	The development of a two-leveled two cross interface for on-line coupling solid-phase extraction and capillary electrophoresis-mass spectrometry. 2009 , 30, 1675-83	17
2196	A novel approach to tag and identify geranylgeranylated proteins. 2009 , 30, 3598-606	57
2195	Enrichment of protein-RNA crosslinks from crude UV-irradiated mixtures for MS analysis by on-line chromatography using titanium dioxide columns. 2009 , 91, 297-309	20
2194	Analysis of autophosphorylation sites in the recombinant catalytic subunit alpha of cAMP-dependent kinase by nano-UPLC-ESI-MS/MS. 2009 , 395, 1713-20	28
2193	Global analysis of cellular protein translation by pulsed SILAC. 2009 , 9, 205-9	265
2192	Insights into yeast adaptive response to the agricultural fungicide mancozeb: a toxicoproteomics approach. 2009 , 9, 657-70	61
2191	Mass spectrometry-based absolute quantification of microsomal cytochrome P450 2D6 in human liver. 2009 , 9, 2313-23	61
2190	Isolation of intact proteins from acid-degradable polyacrylamide gel. 2009 , 9, 3765-71	5
2189	A "fluorescence switch" technique increases the sensitivity of proteomic detection and identification of S-nitrosylated proteins. 2009 , 9, 5359-70	40
2188	A MS data search method for improved 15N-labeled protein identification. 2009 , 9, 4265-70	20
2187	High-accuracy identification and bioinformatic analysis of in vivo protein phosphorylation sites in yeast. 2009 , 9, 4642-52	103

(2009-2009)

2186	Proteomic analysis from haploid and diploid embryos of Quercus suber L. identifies qualitative and quantitative differential expression patterns. 2009 , 9, 4355-67		34
2185	Adaptation to beta-myrcene catabolism in Pseudomonas sp. M1: an expression proteomics analysis. 2009 , 9, 5101-11		12
2184	Gram-positive bacteria produce membrane vesicles: proteomics-based characterization of Staphylococcus aureus-derived membrane vesicles. 2009 , 9, 5425-36		380
2183	Proteomic and functional characterization of the outer membrane vesicles from the gastric pathogen Helicobacter pylori. 2009 , 3, 785-96		56
2182	Shotgun proteomics approach to characterizing the embryonic proteome of the silkworm, Bombyx mori, at labrum appearance stage. 2009 , 18, 649-60		17
2181	Synthetic protein scaffolds provide modular control over metabolic flux. 2009 , 27, 753-9		920
2180	Proteomics strategy for quantitative protein interaction profiling in cell extracts. 2009, 6, 741-4		121
2179	Multiplex peptide stable isotope dimethyl labeling for quantitative proteomics. <i>Nature Protocols</i> , 2009 , 4, 484-94	18.8	1072
2178	Use of in vivo biotinylation to study protein-protein and protein-DNA interactions in mouse embryonic stem cells. <i>Nature Protocols</i> , 2009 , 4, 506-17	18.8	112
2177	A sensitive mass spectrometric method for hypothesis-driven detection of peptide post-translational modifications: multiple reaction monitoring-initiated detection and sequencing (MIDAS). <i>Nature Protocols</i> , 2009 , 4, 870-7	18.8	85
2176	Proteome analysis of the moss Physcomitrella patens (Hedw.) B.S.G. 2009 , 74, 480-90		5
2175	Novel shuttling domain in a regulator (RSC1A1) of transporter SGLT1 steers cell cycle-dependent nuclear location. 2009 , 10, 1599-618		12
2174	Analysis of the secretome of the soybean symbiont Bradyrhizobium japonicum. 2009 , 140, 51-8		41
2173	Changes in the 2-DE protein profile during zygotic embryogenesis in the Brazilian Pine (Araucaria angustifolia). 2009 , 72, 337-52		54
2172	Comparative analysis of synovial fluid and plasma proteomes in juvenile arthritisproteomic patterns of joint inflammation in early stage disease. 2009 , 72, 656-76		23
2171	Comparative proteome analysis to explore p53 pathway disruption in head and neck carcinogenesis. 2009 , 72, 803-14		8
2170	Ligand-induced Flt3-downregulation modulates cell death associated proteins and enhances chemosensitivity to idarubicin in THP-1 acute myeloid leukemia cells. 2009 , 33, 276-87		11
2169	Proteolysis of the proofreading subunit controls the assembly of Escherichia coli DNA polymerase III catalytic core. 2009 , 1794, 1606-15		8

2168	exemplified by analysis of in vitro phosphorylated Plasmodium falciparum glideosome-associated protein 45 by nano-ultra performance liquid chromatography-tandem mass spectrometry. 2009 , 393, 41-7	22
2167	System-wide changes to SUMO modifications in response to heat shock. 2009 , 2, ra24	367
2166	Analysis of nuclear protein complexes comprising ⊞ctinin-4 by 2D-electrophoresis and mass spectrometry. 2009 , 3, 431-437	1
2165	Quantitative analysis of the human spindle phosphoproteome at distinct mitotic stages. 2009 , 8, 4553-63	97
2164	Sesterterpenes as tubulin tyrosine ligase inhibitors. First insight of structure-activity relationships and discovery of new lead. 2009 , 52, 3814-28	41
2163	In-gel trypsin digest of gel-fractionated proteins. 2009 , 2009, pdb.prot5110	12
2162	Respiratory arsenate reductase as a bidirectional enzyme. 2009 , 382, 298-302	90
2161	Cysteine-rich venom proteins from the snakes of Viperinae subfamily - molecular cloning and phylogenetic relationship. 2009 , 53, 162-8	23
2160	Shotgun proteomics in neuroscience. 2009 , 63, 12-26	44
2159	Genetically Derepressed Nucleoplasmic Stellate Protein in Spermatocytes of D. melanogaster interacts with the catalytic subunit of protein kinase 2 and carries histone-like lysine-methylated mark. 2009 , 389, 895-906	14
2158	Updated biological roles for matrix metalloproteinases and new "intracellular" substrates revealed by degradomics. 2009 , 48, 10830-45	172
2157	Citrate boosts the performance of phosphopeptide analysis by UPLC-ESI-MS/MS. 2009 , 8, 418-24	57
2156	Adipocyte fatty acid-binding protein suppresses cardiomyocyte contraction: a new link between obesity and heart disease. 2009 , 105, 326-34	149
2155	Differential proteomics of omental and subcutaneous adipose tissue reflects their unalike biochemical and metabolic properties. 2009 , 8, 1682-93	79
2154	Comparative proteomic analysis of responses to pathogen infection and wounding in Fagus sylvatica. 2009 , 8, 4077-91	35
2153	New proteins identified in epididymal fluid from the platypus (Ornithorhynchus anatinus). 2009 , 21, 1002-7	9
2152	Channel-interacting PDZ protein, 'CIPP', interacts with proteins involved in cytoskeletal dynamics. 2009 , 419, 289-300	6
2151	An optimal protocol to analyze the rat spinal cord proteome. 2009 , 4, 135-64	9

(2010-2009)

2150	PI3Kgamma controls oxidative bursts in neutrophils via interactions with PKCalpha and p47phox. 2009 , 419, 603-10	28
2149	Peptide mass fingerprinting after less specific in-gel proteolysis using MALDI-LTQ-Orbitrap and 4-chloro-alpha-cyanocinnamic acid. 2010 , 9, 2619-29	7
2148	Identification of pancreas-specific proteins in endoscopically (endoscopic pancreatic function test) collected pancreatic fluid with liquid chromatographytandem mass spectrometry. 2010 , 39, 889-96	23
2147	The phosphoproteome of toll-like receptor-activated macrophages. 2010 , 6, 371	113
2146	Establishment of a protein frequency library and its application in the reliable identification of specific protein interaction partners. 2010 , 9, 861-79	52
2145	Valvular aortic stenosis: a proteomic insight. 2010 , 4, 1-7	14
2144	Proteomic analysis of sea urchin (Strongylocentrotus purpuratus) spicule matrix. 2010 , 8, 33	98
2143	Lysozyme inhibitor conferring bacterial tolerance to invertebrate type lysozyme. 2010 , 67, 1177-88	32
2142	Part II: defining and quantifying individual and co-cultured intracellular proteomes of two thermophilic microorganisms by GeLC-MS2 and spectral counting. 2010 , 398, 391-404	10
2141	Part I: characterization of the extracellular proteome of the extreme thermophile Caldicellulosiruptor saccharolyticus by GeLC-MS2. 2010 , 398, 377-89	16
2140	Measuring the intra-individual variability of the plasma proteome in the chicken model of spontaneous ovarian adenocarcinoma. 2010 , 398, 737-49	24
2139	Recombinant expression of bioactive peptide lunasin in Escherichia coli. 2010 , 88, 177-86	21
2138	Shotgun strategy-based proteome profiling analysis on the head of silkworm Bombyx mori. 2010 , 39, 751-61	16
2137	Proteomic response of Escherichia coli to the alkaloid extract of Papaver polychaetum. 2010 , 60, 709-717	10
2136	Identification of four novel DC-SIGN ligands on Mycobacterium bovis BCG. 2010 , 1, 859-70	42
2135	Characterisation of the first wheat (Triticum aestivum L.) nucleotide pyrophosphatase/phosphodiesterase resembling mammalian counterparts. 2010 , 51, 326-336	6
2134	Identification of a sensitive anti-erythropoietin receptor monoclonal antibody allows detection of low levels of EpoR in cells. 2010 , 352, 126-39	62
2133	Flavin-containing monooxygenase-3: induction by 3-methylcholanthrene and complex regulation by xenobiotic chemicals in hepatoma cells and mouse liver. 2010 , 247, 60-9	30

2132	Cell wall proteome analysis of Mycobacterium smegmatis strain MC2 155. 2010 , 10, 121	52
2131	Protein solubility and differential proteomic profiling of recombinant Escherichia coli overexpressing double-tagged fusion proteins. 2010 , 9, 63	15
2130	Localization of proteins in the cell wall of Mycobacterium avium subsp. paratuberculosis K10 by proteomic analysis. 2010 , 8, 21	44
2129	Identification of a novel Plasmopara halstedii elicitor protein combining de novo peptide sequencing algorithms and RACE-PCR. 2010 , 8, 24	3
2128	Assembly and oligomerization of human ATP synthase lacking mitochondrial subunits a and A6L. 2010 , 1797, 1004-11	79
2127	Golgi apparatus casein kinase phosphorylates bioactive Ser-6 of bone morphogenetic protein 15 and growth and differentiation factor 9. 2010 , 584, 801-5	22
2126	Proteomics analysis of liver samples from puffer fish Takifugu rubripes exposed to excessive fluoride: an insight into molecular response to fluorosis. 2010 , 24, 21-8	9
2125	A novel polyacrylamide gel system for proteomic use offering controllable pore expansion by crosslinker cleavage. 2010 , 31, 585-92	22
2124	Biodegradation of MTBE by Achromobacter xylosoxidans MCM1/1 induces synthesis of proteins that may be related to cell survival. 2010 , 45, 794-798	22
2123	Vacuolar and cytosolic cytokinin dehydrogenases of Arabidopsis thaliana: heterologous expression, purification and properties. 2010 , 71, 1970-8	64
2122	Mineralized human primary osteoblast matrices as a model system to analyse interactions of prostate cancer cells with the bone microenvironment. 2010 , 31, 7928-36	96
2121	Mass spectrometric identification of dystrophin isoform Dp427 by on-membrane digestion of sarcolemma from skeletal muscle. 2010 , 404, 197-203	30
2120	Evolutionary conservation of heavy chain protein transfer between glycosaminoglycans. 2010 , 1804, 1011-9	11
2119	Activity-based profiling reveals reactivity of the murine thymoproteasome-specific subunit beta5t. 2010 , 17, 795-801	67
2118	Cloning, expression, purification, crystallization and preliminary X-ray diffraction analysis of glyoxalase I from Leishmania infantum. 2010 , 66, 571-4	8
2117	Proteomic analysis of endoscopically (endoscopic pancreatic function test) collected gastroduodenal fluid using in-gel tryptic digestion followed by LC-MS/MS. 2010 , 4, 715-25	21
2116	Global analysis of the rat and human platelet proteome - the molecular blueprint for illustrating multi-functional platelets and cross-species function evolution. 2010 , 10, 2444-57	29
2115	Sites and extent of selenomethionine incorporation into recombinant Cas6 protein by top-down and bottom-up proteomics with 14.5 T Fourier transform ion cyclotron resonance mass spectrometry. 2010 , 24, 2386-92	3

2114	Purification and expression of a protein elicitor from Alternaria tenuissima and elicitor-mediated defence responses in tobacco. 2010 , 156, 411-420	26
2113	Raman microspectroscopy reveals long-term extracellular activity of Chlamydiae. 2010 , 77, 687-700	80
2112	Proteome analysis of chloroplasts from the moss Physcomitrella patens (Hedw.) B.S.G. 2010 , 75, 1470-83	8
2111	SUMOylation of the GTPase Rac1 is required for optimal cell migration. 2010 , 12, 1078-85	131
2110	Positive feedback between p53 and TRF2 during telomere-damage signalling and cellular senescence. 2010 , 12, 1205-12	68
2109	Chromogranin A is an autoantigen in type 1 diabetes. 2010 , 11, 225-31	269
2108	High-stringency tandem affinity purification of proteins conjugated to ubiquitin-like moieties. Nature Protocols, 2010 , 5, 873-82	15
2107	Decoding signalling networks by mass spectrometry-based proteomics. 2010 , 11, 427-39	484
2106	Rapid pre-gel visualization of proteins with mass spectrometry compatibility. 2010 ,	
2105	Mass Spectrometry and its Applications to Functional Proteomics. 2010 , 307-323	
2104	☑-Syntrophin is a Cdk5 substrate that restrains the motility of insulin secretory granules. 2010 , 5, e12929	32
2103	Fibroblasts from PS1 mutated pre-symptomatic subjects and Alzheimer's disease patients share a unique protein levels profile. 2010 , 21, 431-44	4
2102	Two-dimensional gel electrophoretic protein profile analysis during seed development of Ocotea catharinensis: a recalcitrant seed species. 2010 , 22, 23-33	10
2101	Aspergillus RabB Rab5 integrates acquisition of degradative identity with the long distance movement of early endosomes. 2010 , 21, 2756-69	70
2100	The TSG-6/HC2-mediated transfer is a dynamic process shuffling heavy chains between glycosaminoglycans. 2010 , 285, 21988-93	15
2099	Biochemical characterization of the cell-biomaterial interface by quantitative proteomics. 2010 , 9, 2089-98	8
2098	Protein acyltransferase function of purified calreticulin. Part 1: characterization of propionylation of protein utilizing propoxycoumarin as the propionyl group donor. 2010 , 147, 625-32	12
2097	The second extracellular loop of pore-forming subunits of ATP-binding cassette transporters for basic amino acids plays a crucial role in interaction with the cognate solute binding protein(s). 2010 , 192, 2150-9	11

2096	An integrated phosphoproteomics work flow reveals extensive network regulation in early lysophosphatidic acid signaling. 2010 , 9, 1047-62	25
2095	Use of dimedone-based chemical probes for sulfenic acid detection methods to visualize and identify labeled proteins. 2010 , 473, 95-115	98
2094	Glycoprotein capture and quantitative phosphoproteomics indicate coordinated regulation of cell migration upon lysophosphatidic acid stimulation. 2010 , 9, 2337-53	13
2093	Prolyl 3-hydroxylase 1 null mice display abnormalities in fibrillar collagen-rich tissues such as tendons, skin, and bones. 2010 , 285, 17253-62	59
2092	Defining the transcriptome and proteome in three functionally different human cell lines. 2010 , 6, 450	269
2091	Unbiased identification of protein-bait interactions using biochemical enrichment and quantitative proteomics. 2010 , 2010, pdb.prot5400	5
2090	Transmembrane protein 147 (TMEM147) is a novel component of the Nicalin-NOMO protein complex. 2010 , 285, 26174-81	18
2089	The SILAC fly allows for accurate protein quantification in vivo. 2010 , 9, 2173-83	138
2088	Proteomics on an Orbitrap benchtop mass spectrometer using all-ion fragmentation. 2010 , 9, 2252-61	189
2087	N-CLAP: global profiling of N-termini by chemoselective labeling of the alpha-amine of proteins. 2010 , 2010, pdb.prot5528	6
2086	Dynamics of the skeletal muscle secretome during myoblast differentiation. 2010 , 9, 2482-96	214
2085	Megadalton complexes in the chloroplast stroma of Arabidopsis thaliana characterized by size exclusion chromatography, mass spectrometry, and hierarchical clustering. 2010 , 9, 1594-615	149
2084	Merging molecular electron microscopy and mass spectrometry by carbon film-assisted endoproteinase digestion. 2010 , 9, 1729-41	9
2083	Identification of Conus peptidylprolyl cis-trans isomerases (PPIases) and assessment of their role in the oxidative folding of conotoxins. 2010 , 285, 12735-46	25
2082	Expression of Heat Shock and Other Stress Response Proteins in Ticks and Cultured Tick Cells in Response to Anaplasma spp. Infection and Heat Shock. 2010 , 2010, 657261	29
2081	Proteomic Profiling of the Dystrophin-Deficient MDX Heart Reveals Drastically Altered Levels of Key Metabolic and Contractile Proteins. 2010 , 2010, 648501	26
2080	The physiological importance of photosynthetic ferredoxin NADP+ oxidoreductase (FNR) isoforms in wheat. 2010 , 61, 2669-81	31
2079	Phosphorylation of mouse immunity-related GTPase (IRG) resistance proteins is an evasion strategy for virulent Toxoplasma gondii. 2010 , 8, e1000576	184

(2010-2010)

2078	hereditary spastic paraplegia. 2010 , 8, e1000408	133
2077	Chemotactic activation of Dictyostelium AGC-family kinases AKT and PKBR1 requires separate but coordinated functions of PDK1 and TORC2. 2010 , 123, 983-92	37
2076	The acidic A-domain of Arabidopsis TOC159 occurs as a hyperphosphorylated protein. 2010 , 153, 1016-30	40
2075	Autophagy dysfunction and ubiquitin-positive protein aggregates in Dictyostelium cells lacking Vmp1. 2010 , 6, 100-9	58
2074	A capillary monolithic trypsin reactor for efficient protein digestion in online and offline coupling to ESI and MALDI mass spectrometry. 2010 , 82, 1434-43	7 ²
2073	Identification of NEEP21 as a Eamyloid precursor protein-interacting protein in vivo that modulates amyloidogenic processing in vitro. 2010 , 30, 15677-85	46
2072	Quantitative phosphoproteomics reveals widespread full phosphorylation site occupancy during mitosis. 2010 , 3, ra3	1106
2071	Combined proteomic approaches for the identification of specific amino acid residues modified by 4-hydroxy-2-nonenal under physiological conditions. 2010 , 9, 5770-81	23
2070	A proteome investigation of roxarsone degradation by Alkaliphilus oremlandii strain OhILAs. 2010 , 2, 133-9	15
2069	Enhanced characterization of serum autoantibody reactivity following HSP 60 immunization in a rat model of experimental autoimmune glaucoma. 2010 , 35, 900-8	27
2068	Identification of immunoreactive proteins of Dirofilaria immitis and D. repens recognized by sera from patients with pulmonary and subcutaneous dirofilariosis. 2010 , 59, 248-56	14
2067	Proteomics analysis of cellular imatinib targets and their candidate downstream effectors. 2010 , 9, 6033-43	25
2066	Comparative proteomics of kidney samples from puffer fish Takifugu rubripes exposed to excessive fluoride: an insight into molecular response to fluorosis. 2010 , 20, 345-54	11
2065	Enolase autoantibodies cross-reactive to viral proteins in a mouse model of biliary atresia. 2010 , 139, 1753-61	62
2064	Systems Biology in Drug Discovery and Development. 2010 ,	2
2063	Assessment of buffer systems for harvesting proteins from tissue interstitial fluid for proteomic analysis. 2010 , 9, 4161-9	14
2062	Immunoaffinity enrichment and liquid chromatography-selected reaction monitoring mass spectrometry for quantitation of carbonic anhydrase 12 in cultured renal carcinoma cells. 2010 , 82, 8998-9005	11
2061	Liquid chromatography electrospray ionization Fourier transform ion cyclotron resonance mass spectrometric characterization of N-linked glycans and glycopeptides. 2010 , 82, 6542-8	27

2060	Quantitative proteomics reveals a "poised quiescence" cellular state after triggering the DNA replication origin activation checkpoint. 2010 , 9, 5445-60	6
2059	SIRT1 is a redox-sensitive deacetylase that is post-translationally modified by oxidants and carbonyl stress. 2010 , 24, 3145-59	232
2058	Regulation of the autophagy protein LC3 by phosphorylation. 2010 , 190, 533-9	244
2057	TERRA transcripts are bound by a complex array of RNA-binding proteins. 2010 , 1, 33	101
2056	Mass spectrometric identification of phosphorylation sites in guanylyl cyclase A and B. 2010 , 49, 10137-45	24
2055	Proteomic identification of Hsc70 as a mediator of RGS9-2 degradation by in vivo interactome analysis. 2010 , 9, 1510-21	13
2054	Identification of Non-HLA antigens targeted by alloreactive antibodies in patients undergoing chronic hemodialysis. 2010 , 9, 1041-9	24
2053	Proteomic analysis for antiobesity potential of capsaicin on white adipose tissue in rats fed with a high fat diet. 2010 , 9, 2977-87	112
2052	Substrate-assisted inhibition of ubiquitin-like protein-activating enzymes: the NEDD8 E1 inhibitor MLN4924 forms a NEDD8-AMP mimetic in situ. 2010 , 37, 102-11	335
2051	Site-specific identification of SUMO-2 targets in cells reveals an inverted SUMOylation motif and a hydrophobic cluster SUMOylation motif. 2010 , 39, 641-52	215
2050	Identification of residues on Hsp70 and Hsp90 ubiquitinated by the cochaperone CHIP. 2010 , 395, 587-94	73
2049	Characterization of a functional DnaG-type primase in archaea: implications for a dual-primase system. 2010 , 397, 664-76	20
2048	Distinct regions of human eIF3 are sufficient for binding to the HCV IRES and the 40S ribosomal subunit. 2010 , 403, 185-96	28
2047	Molecular interactions in the retinal basement membrane system: a proteomic approach. 2010 , 29, 471-83	41
2046	Proteomic analysis of ACTN4-interacting proteins reveals it's a putative involvement in mRNA metabolism. 2010 , 397, 192-6	11
2045	Treslin collaborates with TopBP1 in triggering the initiation of DNA replication. 2010 , 140, 349-59	169
2044	The protein composition of mitotic chromosomes determined using multiclassifier combinatorial proteomics. 2010 , 142, 810-21	217
2043	A family of protein-deglutamylating enzymes associated with neurodegeneration. 2010 , 143, 564-78	221

(2011-2010)

2042	The Caenorhabditis elegans Ste20 kinase, GCK-3, is essential for postembryonic developmental timing and regulates meiotic chromosome segregation. 2010 , 344, 758-71	11
2041	Hyperglycemia alters the schwann cell mitochondrial proteome and decreases coupled respiration in the absence of superoxide production. 2010 , 9, 458-71	52
2040	Potential urinary biomarkers of disease activity in Crohn's disease. 2010 , 45, 1440-8	8
2039	Proteomic analysis of the murine liver in response to a combined exposure to psychological stress and 7,12-dimethylbenz(a)anthracene. 2010 , 9, 509-20	13
2038	Quantitative proteome and transcriptome analysis of the archaeon Thermoplasma acidophilum cultured under aerobic and anaerobic conditions. 2010 , 9, 4839-50	35
2037	Top-down and bottom-up proteomics of SDS-containing solutions following mass-based separation. 2010 , 9, 2863-70	119
2036	Cytotoxic copper(II) salicylaldehyde semicarbazone complexes: mode of action and proteomic analysis. 2010 , 2, 694-705	28
2035	Direct and indirect detection methods for the analysis of S-nitrosylated peptides and proteins. 2010 , 473, 265-80	16
2034	Antimicrobial activity of lipophilic avian eggshell surface extracts. 2010 , 58, 10156-61	19
2033	LC-MS/MS in Proteomics. 2010 ,	3
2032	A novel class of protease targets of phosphatidylethanolamine-binding proteins (PEBP): a study of the acylpeptide hydrolase and the PEBP inhibitor from the archaeon Sulfolobus solfataricus. 2010 , 6, 2498-507	8
2031	Proteomic analysis of proteins released from growth-arrested Candida albicans following exposure to caspofungin. 2010 , 48, 598-605	14
2030	Rapid microscale in-gel processing and digestion of proteins using surface acoustic waves. 2010 , 10, 1518-20	19
2029	Protein cage nanoparticles bearing the LyP-1 peptide for enhanced imaging of macrophage-rich vascular lesions. 2011 , 5, 2493-502	91
2028	Comparative analysis on the membrane proteome of Clostridium acetobutylicum wild type strain and its butanol-tolerant mutant. 2011 , 7, 1660-77	47
2027	Chemical proteomics reveals bolinaquinone as a clathrin-mediated endocytosis inhibitor. 2011 , 7, 480-5	24
2026	Metabolic priming by a secreted fungal effector. 2011 , 478, 395-8	371
		· ·

2024	Proteome of the Caenorhabditis elegans oocyte. 2011 , 10, 2300-5		12
2023	OspA-CD40 dyad: ligand-receptor interaction in the translocation of neuroinvasive Borrelia across the blood-brain barrier. 2011 , 1, 86		19
2022	TRPM1 forms complexes with nyctalopin in vivo and accumulates in postsynaptic compartment of ON-bipolar neurons in mGluR6-dependent manner. 2011 , 31, 11521-6		68
2021	Development and use of clickable activity based protein profiling agents for protein arginine deiminase 4. 2011 , 6, 466-76		34
2020	COP1 is a tumour suppressor that causes degradation of ETS transcription factors. 2011 , 474, 403-6		130
2019	Characterization of ubiquitination dependent dynamics in growth factor receptor signaling by quantitative proteomics. 2011 , 7, 3223-33		50
2018	Multiplexed Preparation of Biological Samples for Mass Spectrometry Using Gel Electrophoresis. 2011 , 91-105		
2017	cDNA cloning, structural, and functional analyses of venom phospholipases Aland a Kunitz-type protease inhibitor from steppe viper Vipera ursinii renardi. 2011 , 57, 332-41		28
2016	Isolation and identification of a snake venom metalloproteinase inhibitor from California ground squirrel (Spermophilus beecheyi) blood sera. 2011 , 58, 486-93		18
2015	Relative quantification of the proteomic changes associated with the mycotoxin zearalenone in the H295R steroidogenesis model. 2011 , 58, 533-42		13
2014	System-wide temporal characterization of the proteome and phosphoproteome of human embryonic stem cell differentiation. 2011 , 4, rs3		347
2013	Identifying and quantifying proteolytic events and the natural N terminome by terminal amine isotopic labeling of substrates. <i>Nature Protocols</i> , 2011 , 6, 1578-611	18.8	221
2012	Characterization of the phosphoproteome in androgen-repressed human prostate cancer cells by Fourier transform ion cyclotron resonance mass spectrometry. 2011 , 10, 3920-8		10
2011	Target Proteins: Bottom-Up and Top-Down Proteomics. 2011 , 89-100		2
2010	The pseudokinase domain of JAK2 is a dual-specificity protein kinase that negatively regulates cytokine signaling. 2011 , 18, 971-6		195
2009	Preparation and analysis of proteins and peptides using MALDI TOF/TOF mass spectrometry. 2011 , Chapter 16, Unit 16.13		15
2008	Argonaute Proteins. 2011,		1
2007	The Aspergillus fumigatus toxin fumagillin suppresses the immune response of Galleria mellonella larvae by inhibiting the action of haemocytes. 2011 , 157, 1481-1488		53

2006	Proteomic analysis of plasma derived from platelet buffy coats during storage at room temperature. An application of ProteoMinerlechnology. 2011 , 22, 252-69	12
2005	Nano LC-MS/MS: a robust setup for proteomic analysis. 2011 , 790, 115-26	40
2004	Nanoproteomics. 2011,	2
2003	The thylakoid membrane proteome of two marine diatoms outlines both diatom-specific and species-specific features of the photosynthetic machinery. 2011 , 10, 5338-53	102
2002	Guidelines for Molecular Analysis in Archive Tissues. 2011,	14
2001	The relative amounts of plasma transthyretin forms in familial transthyretin amyloidosis: a quantitative analysis by Fourier transform ion-cyclotron resonance mass spectrometry. 2011 , 18, 191-9	15
2000	Proteome analysis of cold acclimation in sunflower. 2011 , 10, 2330-46	50
1999	Implications of partial tryptic digestion in organic-aqueous solvent systems for bottom-up proteome analysis. 2011 , 703, 194-203	24
1998	Dissecting molecular events in thyroid neoplasia provides evidence for distinct evolution of follicular thyroid adenoma and carcinoma. 2011 , 179, 3066-74	13
1997	ADF/cofilin regulates secretory cargo sorting at the TGN via the Ca2+ ATPase SPCA1. 2011 , 20, 652-62	69
1996	Repo-Man coordinates chromosomal reorganization with nuclear envelope reassembly during mitotic exit. 2011 , 21, 328-42	139
1995	Human inter-⊞nhibitor is a substrate for factor XIIIa and tissue transglutaminase. 2011 , 1814, 1624-30	7
1994	Autodeimination of protein arginine deiminase 4 alters protein-protein interactions but not activity. 2011 , 50, 3997-4010	50
1993	Salicylic acid enhances Staphylococcus aureus extracellular adhesin protein expression. 2011 , 13, 1073-80	5
1992	The effect of storage at 25°C on proteins in human milk. 2011 , 21, 286-293	12
1991	Interactome study suggests multiple cellular functions of hepatoma-derived growth factor (HDGF). 2011 , 75, 588-602	24
1990	Quantitative in-depth analysis of the dynamic secretome of activated Jurkat T-cells. 2011 , 75, 561-71	15
1989	Identification and characterization of anti-microbial peptides from rabbit vaginal fluid. 2011 , 139, 176-86	13

1988	Analyzing protein-protein interactions by quantitative mass spectrometry. 2011 , 54, 387-95	51
1987	Identification of native Escherichia coli BL21 (DE3) proteins that bind to immobilized metal affinity chromatography under high imidazole conditions and use of 2D-DIGE to evaluate contamination pools with respect to recombinant protein expression level. 2011 , 78, 216-24	10
1986	Comparative proteomic analysis identifies a role for SUMO in protein quality control. 2011, 4, rs4	136
1985	Proteomic analysis of urine from male dogs during early stages of tubulointerstitial injury in a canine model of progressive glomerular disease. 2011 , 40, 222-36	35
1984	Identification of bacterial target proteins for the salicylidene acylhydrazide class of virulence-blocking compounds. 2011 , 286, 29922-31	78
1983	Preparation of multiprotein complexes from Arabidopsis chloroplasts using tandem affinity purification. 2011 , 775, 31-49	7
1982	Systems-wide proteomic analysis in mammalian cells reveals conserved, functional protein turnover. 2011 , 10, 5275-84	179
1981	Proteomic analysis of mouse oocytes reveals 28 candidate factors of the "reprogrammome". 2011 , 10, 2140-53	70
1980	Oxidative stress-dependent oligomeric status of erythrocyte peroxiredoxin II (PrxII) during storage under standard blood banking conditions. 2011 , 93, 845-53	35
1979	Soybeans as bioreactors for biopharmaceuticals and industrial proteins. 2011 , 10, 1733-52	13
1978	Quantitative proteomics identify novel miR-155 target proteins. 2011 , 6, e22146	26
1977	MicroRNA-96 directly inhibits ⊞globin expression in human erythropoiesis. 2011 , 6, e22838	51
1976	Proteomic interrogation of human chromatin. 2011 , 6, e24747	31
1975	The soluble recombinant Neisseria meningitidis adhesin NadA(B51-405) stimulates human monocytes by binding to extracellular Hsp90. 2011 , 6, e25089	18
1974	Phenotypic and genome-wide analysis of an antibiotic-resistant small colony variant (SCV) of Pseudomonas aeruginosa. 2011 , 6, e29276	63
1973	The presence of IGHG1 in human pancreatic carcinomas is associated with immune evasion mechanisms. 2011 , 40, 753-61	30
1972	Protein acyltransferase function of purified calreticulin: the exclusive role of P-domain in mediating protein acylation utilizing acyloxycoumarins and acetyl CoA as the acyl group donors. 2011 , 18, 507-17	7
1971	The kinesin KIF9 and reggie/flotillin proteins regulate matrix degradation by macrophage podosomes. 2011 , 22, 202-15	47

1970	Btk regulation in human and mouse B cells via protein kinase C phosphorylation of IBtk[]2011, 117, 6520-31	22
1969	Rapid characterization of N-linked glycosylation site using non-specific protease digestion of gel-separated glycoproteins and matrix-assisted laser desorption/ionization tandem time-of-flight mass spectrometry. 2011 , 17, 573-9	2
1968	Divergence in enzyme regulation between Caenorhabditis elegans and human tyrosine hydroxylase, the key enzyme in the synthesis of dopamine. 2011 , 434, 133-41	14
1967	Proteomics of extremophiles. 2011 , 13, 1934-55	16
1966	A high-definition native polyacrylamide gel electrophoresis system for the analysis of membrane complexes. 2011 , 67, 181-94	34
1965	R3F, a novel membrane-associated glycogen targeting subunit of protein phosphatase 1 regulates glycogen synthase in astrocytoma cells in response to glucose and extracellular signals. 2011 , 118, 596-610	14
1964	Fungal proteomics: from identification to function. 2011 , 321, 1-9	43
1963	Use of stable isotope labeling by amino acids in cell culture as a spike-in standard in quantitative proteomics. <i>Nature Protocols</i> , 2011 , 6, 147-57	232
1962	Interaction between MAK-V protein kinase and synaptopodin. 2011 , 76, 196-201	3
1961	WW domain-mediated interaction with Wbp2 is important for the oncogenic property of TAZ. 2011 , 30, 600-10	84
1960	SHARPIN forms a linear ubiquitin ligase complex regulating NF-B activity and apoptosis. 2011, 471, 637-41	526
1959	Acetylation-dependent regulation of endothelial Notch signalling by the SIRT1 deacetylase. 2011 , 473, 234-8	298
1958	The role of higher-order protein structure in supporting binding by heteroclitic monoclonal antibodies: the monoclonal antibody KIM185 to CD18 also binds C4-binding protein. 2011 , 49, 38-47	4
1957	Interleukin-2 signaling pathway analysis by quantitative phosphoproteomics. 2011 , 75, 177-91	34
1956	Eggplant polyphenol oxidase multigene family: cloning, phylogeny, expression analyses and immunolocalization in response to wounding. 2011 , 72, 2275-87	42
1955	Characterization of brassinosteroid-regulated proteins in a nuclear-enriched fraction of Arabidopsis suspension-cultured cells. 2011 , 49, 985-95	12
1954	Ddc1 checkpoint protein and DNA polymerase e interact with nick-containing DNA repair intermediate in cell free extracts of Saccharomyces cerevisiae. 2011 , 10, 815-25	8
1953	Proteome analysis of the fungus Aspergillus carbonarius under ochratoxin A producing conditions. 2011 , 147, 162-9	15

1952	Purification and biochemical characterization of a moderately halotolerant NADPH dependent xylose reductase from Debaryomyces nepalensis NCYC 3413. 2011 , 102, 9710-7	20
1951	A plasmodesmata-localized protein mediates crosstalk between cell-to-cell communication and innate immunity in Arabidopsis. 2011 , 23, 3353-73	176
1950	In vivo quantitative proteomics: the SILAC mouse. 2012 , 757, 435-50	69
1949	Disruption of a ciliary B9 protein complex causes Meckel syndrome. 2011 , 89, 94-110	114
1948	Bactericidal activity identified in 2S Albumin from sesame seeds and in silico studies of structure-function relations. 2011 , 30, 340-50	18
1947	A proteome analysis of the response of a Pseudomonas aeruginosa oxyR mutant to iron limitation. 2011 , 24, 523-32	17
1946	Surface-associated Hsp60 chaperonin of Leptospira interrogans serovar Autumnalis N2 strain as an immunoreactive protein. 2011 , 30, 1383-9	7
1945	100% protein sequence coverage: a modern form of surrealism in proteomics. 2011 , 41, 291-310	79
1944	Tools for phospho- and glycoproteomics of plasma membranes. 2011 , 41, 223-33	16
1943	Efficient electron transfer from hydrogen to benzyl viologen by the [NiFe]-hydrogenases of Escherichia coli is dependent on the coexpression of the iron-sulfur cluster-containing small subunit. 2011 , 193, 893-903	44
1942	In-depth analysis of the chicken egg white proteome using an LTQ Orbitrap Velos. 2011, 9, 7	107
1941	The ColRS system is essential for the hunger response of glucose-growing Pseudomonas putida. 2011 , 11, 170	11
1940	The respiratory molybdo-selenoprotein formate dehydrogenases of Escherichia coli have hydrogen: benzyl viologen oxidoreductase activity. 2011 , 11, 173	44
1939	Proteomic profile of culture filtrate from the Brazilian vaccine strain Mycobacterium bovis BCG Moreau compared to M. bovis BCG Pasteur. 2011 , 11, 80	30
1938	Mass spectrometry-based proteomics of endoscopically collected pancreatic fluid in chronic pancreatitis research. 2011 , 5, 109-20	16
1937	Gel-based proteomics analysis of the heterogeneity of 20S proteasomes from four human pancreatic cancer cell lines. 2011 , 5, 484-92	8
1936	Lights and shadows of proteomic technologies for the study of protein species including isoforms, splicing variants and protein post-translational modifications. 2011 , 11, 590-603	17
1935	An approach for identification of phosphoproteins using the G-electrode-loading method in two-dimensional gel electrophoresis. 2011 , 11, 1545-9	3

(2011-2011)

1934	Quantitative proteomics (2-D DIGE) reveals molecular strategies employed by Burkholderia cenocepacia to adapt to the airways of cystic fibrosis patients under antimicrobial therapy. 2011 , 11, 1313-28	34
1933	Differential expression of adipose tissue proteins between obesity-susceptible and -resistant rats fed a high-fat diet. 2011 , 11, 1429-48	35
1932	One-source peptide/phosphopeptide standards for accurate phosphorylation degree determination. 2011 , 11, 490-4	14
1931	A cost-benefit analysis of multidimensional fractionation of affinity purification-mass spectrometry samples. 2011 , 11, 2603-12	27
1930	2-D DIGE analysis of the mitochondrial proteome from human skeletal muscle reveals time course-dependent remodelling in response to 14 consecutive days of endurance exercise training. 2011 , 11, 1413-28	56
1929	Quantitative proteomics by 2-DE, 16O/18O labelling and linear ion trap mass spectrometry analysis of lymph nodes from piglets inoculated by porcine circovirus type 2. 2011 , 11, 3452-69	21
1928	Optimization of cell lysis and protein digestion protocols for the analysis of HeLa S3 cells by LC-MS/MS. 2011 , 11, 4726-30	32
1927	Detection and expression analysis of recombinant proteins in plant-derived complex mixtures using nanoUPLC-MS(E). 2011 , 34, 2618-30	48
1926	Matrix-assisted laser desorption/ionisation mass spectrometric response factors of peptides generated using different proteolytic enzymes. 2011 , 46, 1233-40	20
1925	An antioxidant protein in Curcuma comosa Roxb. Rhizomes. 2011 , 124, 476-480	13
1924	Specificity analysis-based identification of new methylation targets of the SET7/9 protein lysine methyltransferase. 2011 , 18, 111-20	128
1924 1923		128 6
	methyltransferase. 2011 , 18, 111-20 An optimized magnetite microparticle-based phosphopeptide enrichment strategy for identifying	
1923	An optimized magnetite microparticle-based phosphopeptide enrichment strategy for identifying multiple phosphorylation sites in an immunoprecipitated protein. 2011 , 408, 19-31 Preventing arginine-to-proline conversion in a cell-line-independent manner during cell cultivation	6
1923 1922	An optimized magnetite microparticle-based phosphopeptide enrichment strategy for identifying multiple phosphorylation sites in an immunoprecipitated protein. 2011 , 408, 19-31 Preventing arginine-to-proline conversion in a cell-line-independent manner during cell cultivation under stable isotope labeling by amino acids in cell culture (SILAC) conditions. 2011 , 412, 123-5	6 39
1923 1922 1921	An optimized magnetite microparticle-based phosphopeptide enrichment strategy for identifying multiple phosphorylation sites in an immunoprecipitated protein. 2011, 408, 19-31 Preventing arginine-to-proline conversion in a cell-line-independent manner during cell cultivation under stable isotope labeling by amino acids in cell culture (SILAC) conditions. 2011, 412, 123-5 Proteomics by mass spectrometrygo big or go home?. 2011, 55, 832-41 Protein profiling identified dissociations between growth hormone-mediated longitudinal growth	6 39 12
1923 1922 1921 1920	An optimized magnetite microparticle-based phosphopeptide enrichment strategy for identifying multiple phosphorylation sites in an immunoprecipitated protein. 2011, 408, 19-31 Preventing arginine-to-proline conversion in a cell-line-independent manner during cell cultivation under stable isotope labeling by amino acids in cell culture (SILAC) conditions. 2011, 412, 123-5 Proteomics by mass spectrometrygo big or go home?. 2011, 55, 832-41 Protein profiling identified dissociations between growth hormone-mediated longitudinal growth and bone mineralization in short prepubertal children. 2011, 74, 89-100 Proteomic analysis of salicylic acid induced resistance to Mungbean Yellow Mosaic India Virus in	6 39 12 9

1916	Unraveling tobacco BY-2 protein complexes with BN PAGE/LC-MS/MS and clustering methods. 2011 , 74, 1201-17	15
1915	A proteomic approach to investigate the differential antigenic profile of two Coxiella burnetii strains. 2011 , 74, 1150-9	19
1914	Differential proteome analysis of mature and germinated embryos of Araucaria angustifolia. 2011 , 72, 302-11	40
1913	Human phenotypically distinct TGFBI corneal dystrophies are linked to the stability of the fourth FAS1 domain of TGFBIp. 2011 , 286, 4951-8	49
1912	Cyclin-dependent kinase-mediated phosphorylation of RBP1 and pRb promotes their dissociation to mediate release of the SAP30[mSin3[HDAC transcriptional repressor complex. 2011 , 286, 5108-18	21
1911	Quantitative mass spectrometry of DENV-2 RNA-interacting proteins reveals that the DEAD-box RNA helicase DDX6 binds the DB1 and DB2 3' UTR structures. 2011 , 8, 1173-86	144
1910	Differential expression of liver proteins between obesity-prone and obesity-resistant rats in response to a high-fat diet. 2011 , 106, 612-26	18
1909	Liquid chromatography and mass spectrometry in food allergen detection. 2011 , 74, 316-45	60
1908	Studies of the mechanistic details of the pH-dependent association of botulinum neurotoxin with membranes. 2011 , 286, 27011-8	19
1907	Quantitative proteomics identifies ferritin in the innate immune response of C. elegans. 2011 , 2, 120-30	38
1906	Cullin 4B protein ubiquitin ligase targets peroxiredoxin III for degradation. 2011 , 286, 32344-54	41
1905	Identification of peroxiredoxin-1 as a novel biomarker of abdominal aortic aneurysm. 2011 , 31, 935-43	63
1904	The malaria parasite progressively dismantles the host erythrocyte cytoskeleton for efficient egress. 2011 , 10, M111.010678	54
1903	Neural precursor cell-expressed developmentally down-regulated protein 4-2 (Nedd4-2) regulation by 14-3-3 protein binding at canonical serum and glucocorticoid kinase 1 (SGK1) phosphorylation sites. 2011 , 286, 37830-40	32
1902	Comparative proteomics analysis of midgut samples from Takifugu rubripes exposed to excessive fluoride: initial molecular response to fluorosis. 2011 , 21, 444-52	3
1901	Modeling human endometrial decidualization from the interaction between proteome and secretome. 2011 , 96, 706-16	45
1900	Crumbs regulates rhodopsin transport by interacting with and stabilizing myosin V. 2011 , 195, 827-38	50
1899	Proteomic survey of ubiquitin-linked nuclear proteins in interferon-stimulated macrophages. 2011 , 31, 619-28	8

1898	Herpes simplex virus 1 ICP4 forms complexes with TFIID and mediator in virus-infected cells. 2011 , 85, 5733-44	44
1897	Caspofungin primes the immune response of the larvae of Galleria mellonella and induces a non-specific antimicrobial response. 2011 , 60, 189-196	54
1896	Identification of outer membrane proteins from an Antarctic bacterium Pseudomonas syringae Lz4W. 2011 , 10, M110.004549	15
1895	Quantitative proteomic analysis of cellular protein modulation upon inhibition of the NEDD8-activating enzyme by MLN4924. 2011 , 10, M111.009183	54
1894	Direct regulation of Treslin by cyclin-dependent kinase is essential for the onset of DNA replication. 2011 , 193, 995-1007	88
1893	Carboxyl-group footprinting maps the dimerization interface and phosphorylation-induced conformational changes of a membrane-associated tyrosine kinase. 2011 , 10, M110.005678	24
1892	A robust method for quantitative high-throughput analysis of proteomes by 18O labeling. 2011 , 10, M110.00	3335
1891	Androgen-sensitive microsomal signaling networks coupled to the proliferation and differentiation of human prostate cancer cells. 2011 , 2, 956-78	12
1890	Chromatin affinity purification and quantitative mass spectrometry defining the interactome of histone modification patterns. 2011 , 10, M110.005371	66
1889	Quantitative proteomic analysis of chromatin reveals that Ctf18 acts in the DNA replication checkpoint. 2011 , 10, M110.005561	53
1888	Protein interactions of phosphatase and tensin homologue (PTEN) and its cancer-associated G20E mutant compared by using stable isotope labeling by amino acids in cell culture-based parallel affinity purification. 2011 , 286, 18093-103	22
1887	Covalent structural changes in unfolded GroES that lead to amyloid fibril formation detected by NMR: insight into intrinsically disordered proteins. 2011 , 286, 21796-805	8
1886	Activation of BlaR1 protein of methicillin-resistant Staphylococcus aureus, its proteolytic processing, and recovery from induction of resistance. 2011 , 286, 38148-38158	46
1885	Glycosylation increases the thermostability of human aquaporin 10 protein. 2011 , 286, 31915-23	49
1884	Human lysophosphatidylcholine acyltransferases 1 and 2 are located in lipid droplets where they catalyze the formation of phosphatidylcholine. 2011 , 286, 21330-9	110
1883	Unambiguous characterization of site-specific phosphorylation of leucine-rich repeat Fli-I-interacting protein 2 (LRRFIP2) in Toll-like receptor 4 (TLR4)-mediated signaling. 2011 , 286, 10897-910	22
1882	Reduction in ribosomal protein synthesis is sufficient to explain major effects on ribosome production after short-term TOR inactivation in Saccharomyces cerevisiae. 2011 , 31, 803-17	30
1881	Invasion of Cryptococcus neoformans into human brain microvascular endothelial cells is mediated through the lipid rafts-endocytic pathway via the dual specificity tyrosine phosphorylation-regulated kinase 3 (DYRK3). 2011 , 286, 34761-9	54

1880	The RNA polymerase II C-terminal domain promotes splicing activation through recruitment of a U2AF65-Prp19 complex. 2011 , 25, 972-83	118
1879	Sample preparation techniques for the untargeted LC-MS-based discovery of peptides in complex biological matrices. 2011 , 2011, 245291	58
1878	Lysine acetylation is a widespread protein modification for diverse proteins in Arabidopsis. 2011 , 155, 1769-78	149
1877	Substantial histone reduction modulates genomewide nucleosomal occupancy and global transcriptional output. 2011 , 9, e1001086	140
1876	Dicer-dependent and -independent Argonaute2 protein interaction networks in mammalian cells. 2012 , 11, 1442-56	43
1875	Comparative proteomic analysis of Lactobacillus plantarum WCFS1 and atsR mutant strains under physiological and heat stress conditions. 2012 , 13, 10680-96	25
1874	Microbial reduction of chromate in the presence of nitrate by three nitrate respiring organisms. 2012 , 3, 416	34
1873	Tomato TFT1 is required for PAMP-triggered immunity and mutations that prevent T3S effector XopN from binding to TFT1 attenuate Xanthomonas virulence. 2012 , 8, e1002768	42
1872	The major autolysin Acm2 from Lactobacillus plantarum undergoes cytoplasmic O-glycosylation. 2012 , 194, 325-33	36
1871	Chloride channel ClC-2 modulates tight junction barrier function via intracellular trafficking of occludin. 2012 , 302, C178-87	44
1870	A combination of H2A.Z and H4 acetylation recruits Brd2 to chromatin during transcriptional activation. 2012 , 8, e1003047	70
1869	Contactin-associated protein-2 antibodies in non-paraneoplastic cerebellar ataxia. 2012 , 83, 437-40	91
1868	The Pseudomonas aeruginosa N-acylhomoserine lactone quorum sensing molecules target IQGAP1 and modulate epithelial cell migration. 2012 , 8, e1002953	67
1867	Screening the banana biodiversity for drought tolerance: can an in vitro growth model and proteomics be used as a tool to discover tolerant varieties and understand homeostasis. 2012 , 3, 176	71
1866	Analysis of PSPHL as a Candidate Gene Influencing the Racial Disparity in Endometrial Cancer. 2012 , 2, 65	18
1865	Quantitative proteomics profiling of murine mammary gland cells unravels impact of annexin-1 on DNA damage response, cell adhesion, and migration. 2012 , 11, 381-93	35
1864	The Ndc80 internal loop is required for recruitment of the Ska complex to establish end-on microtubule attachment to kinetochores. 2012 , 125, 3243-53	52
1863	Isolation and proteomic characterization of the mouse sperm acrosomal matrix. 2012 , 11, 758-74	41

1862	Deciphering the magainin resistance process of Escherichia coli strains in light of the cytosolic proteome. 2012 , 56, 1714-24	37
1861	On marathons and Sprints: an integrated quantitative proteomics and transcriptomics analysis of differences between slow and fast muscle fibers. 2012 , 11, M111.010801	65
1860	Methylation of CenH3 arginine 37 regulates kinetochore integrity and chromosome segregation. 2012 , 109, 9029-34	47
1859	Comparative evaluation of T11 target structure and its deglycosylated derivative nullifies the importance of glycan moieties in immunotherapeutic efficacy. 2012 , 44, 259-68	5
1858	RUNX3 interactome reveals novel centrosomal targeting of RUNX family of transcription factors. 2012 , 11, 1938-47	16
1857	MINOS1 is a conserved component of mitofilin complexes and required for mitochondrial function and cristae organization. 2012 , 23, 247-57	141
1856	Genome-wide Runx2 occupancy in prostate cancer cells suggests a role in regulating secretion. 2012 , 40, 3538-47	35
1855	Canid progesterone receptors lack activation function 3 domain-dependent activity. 2012 , 153, 6104-13	4
1854	Role for Rif1 in the checkpoint response to damaged DNA in Xenopus egg extracts. 2012 , 11, 1183-94	12
1853	Effect of asynchronous transfer on bovine embryonic development and relationship with early cycle uterine proteome profiles. 2012 , 24, 962-72	30
1852	Mechanistic studies on activation of ubiquitin and di-ubiquitin-like protein, FAT10, by ubiquitin-like modifier activating enzyme 6, Uba6. 2012 , 287, 15512-22	33
1851	Modulation of conotoxin structure and function is achieved through a multienzyme complex in the venom glands of cone snails. 2012 , 287, 34288-303	33
1850	Novel Podoviridae family bacteriophage infecting Weissella cibaria isolated from Kimchi. 2012 , 78, 7299-308	29
1849	Biotinylation of lysine method identifies acetylated histone H3 lysine 79 in Saccharomyces cerevisiae as a substrate for Sir2. 2012 , 109, E916-25	16
1848	Mutation in cyclophilin B that causes hyperelastosis cutis in American Quarter Horse does not affect peptidylprolyl cis-trans isomerase activity but shows altered cyclophilin B-protein interactions and affects collagen folding. 2012 , 287, 22253-65	63
1847	A single rainbow trout cobalamin-binding protein stands in for three human binders. 2012 , 287, 33917-25	11
1846	Surface multiheme c-type cytochromes from Thermincola potens and implications for respiratory metal reduction by Gram-positive bacteria. 2012 , 109, 1702-7	129
1845	Absolute quantitation of isoforms of post-translationally modified proteins in transgenic organism. 2012 , 11, 272-85	21

1844	A sensitive gel-based global O-glycomics approach reveals high levels of mannosyl glycans in the high mass region of the mouse brain proteome. 2012 , 393, 709-17	18
1843	Ribulose-1,5-bis-phosphate carboxylase/oxygenase accumulation factor1 is required for holoenzyme assembly in maize. 2012 , 24, 3435-46	80
1842	Optimization of an Efficient Protein Extraction Protocol Compatible with Two-Dimensional Electrophoresis and Mass Spectrometry from Recalcitrant Phenolic Rich Roots of Chickpea (Cicer arietinum L.). 2012 , 2012, 536963	21
1841	Quantitative proteomics reveals dynamic changes in the plasma membrane during Arabidopsis immune signaling. 2012 , 11, M111.014555	79
1840	Mitogen-activated protein kinase (MAPK/ERK) regulates adenomatous polyposis coli during growth-factor-induced cell extension. 2012 , 125, 1247-58	8
1839	Importin-□negatively regulates multiple aspects of mitosis including RANGAP1 recruitment to kinetochores. 2012 , 196, 435-50	43
1838	AUF1/hnRNP D is a novel protein partner of the EBER1 noncoding RNA of Epstein-Barr virus. 2012 , 18, 2073-82	58
1837	Mass spectrometry-based proteomic analysis of middle-aged vs. aged vastus lateralis reveals increased levels of carbonic anhydrase isoform 3 in senescent human skeletal muscle. 2012 , 30, 723-33	57
1836	Mass spectrometric characterization of the sarcoplasmic reticulum from rabbit skeletal muscle by on-membrane digestion. 2012 , 19, 252-63	13
1835	Upregulation of the I-form of 14-3-3 protein in telencephalon of goldfish (Carassius auratus): its possible role in spatial learning. 2012 , 23, 840-5	1
1834	Proteomic responses of Roseobacter litoralis OCh149 to starvation and light regimen. 2012 , 27, 430-42	12
1833	Exploration of the sea urchin coelomic fluid via combinatorial peptide ligand libraries. 2012 , 222, 93-104	8
1832	Proteomics of the rodent malaria parasite using matrix-assisted laser desorption/ionization quadrupole ion trap time-of-flight tandem mass spectrometry. 2012 , 28, 813-7	1
1831	Mitotic chromosomes are compacted laterally by KIF4 and condensin and axially by topoisomerase II⊞ 2012 , 199, 755-70	118
1830	Next-generation sequencing-based transcriptomic and proteomic analysis of the common reed, Phragmites australis (Poaceae), reveals genes involved in invasiveness and rhizome specificity. 2012 , 99, 232-47	39
1829	Mutational, proteomic and metabolomic analysis of a plant growth promoting copper-resistant Pseudomonas spp. 2012 , 335, 140-8	12
1828	Ethylene glycol metabolism by Pseudomonas putida. 2012 , 78, 8531-9	55
1827	Structure of a RING E3 ligase and ubiquitin-loaded E2 primed for catalysis. 2012 , 489, 115-20	339

1826	A high-throughput approach for measuring temporal changes in the interactome. 2012 , 9, 907-9	236
1825	Positive correlation between serum immunoreactivity to Demodex-associated Bacillus proteins and erythematotelangiectatic rosacea. 2012 , 167, 1032-6	55
1824	Toward stable genetic engineering of human O-glycosylation in plants. 2012 , 160, 450-63	29
1823	Proteomic analysis of trichloroethylene-induced alterations in expression, distribution, and interactions of SET/TAF-I\u00e4nd two SET/TAF-I\u00a4ning proteins, eEF1A1 and eEF1A2, in hepatic L-02 cells. 2012 , 263, 259-72	7
1822	Expert system for computer-assisted annotation of MS/MS spectra. 2012 , 11, 1500-9	53
1821	Cell type-dependent effects of andrographolide on human cancer cell lines. 2012, 91, 751-760	17
1820	Detergent selection for enhanced extraction of membrane proteins. 2012 , 86, 12-20	100
1819	Multidimensional liquid chromatography platform for profiling alterations of clusterin N-glycosylation in the plasma of patients with renal cell carcinoma. 2012 , 1256, 121-8	19
1818	Pine nut allergy: clinical features and major allergens characterization. 2012 , 56, 1884-93	13
1817	Metabolic and proteomic adaptation of Lactobacillus rhamnosus strains during growth under cheese-like environmental conditions compared to de Man, Rogosa, and Sharpe medium. 2012 , 12, 3206-18	46
1816	Proteomic analyses of transgenic LQT1 and LQT2 rabbit hearts elucidate an increase in expression and activity of energy producing enzymes. 2012 , 75, 5254-65	10
1815	Interplay between oncogenic K-Ras and wild-type H-Ras in Caco2 cell transformation. 2012 , 75, 5356-69	6
1814	Mass spectrometry-based label free quantification of gel separated proteins. 2012, 75, 5544-53	11
1813	Quantitative proteomic analysis of differentially expressed proteins in the toxicity-lost mutant of Alexandrium catenella (Dinophyceae) in the exponential phase. 2012 , 75, 5564-77	38
1812	Proteomic analysis of liver mitochondria of apolipoprotein E knockout mice treated with metformin. 2012 , 77, 167-75	21
1811	Identification of aero-allergens from Rhizopus oryzae: an immunoproteomic approach. 2012 , 77, 455-68	28
1810	Protein haptenation by amoxicillin: high resolution mass spectrometry analysis and identification of target proteins in serum. 2012 , 77, 504-20	61
1809	Quantitative proteomic analysis of yeast DNA replication proteins. 2012 , 57, 196-202	16

1808	Expression and purification of coronavirus envelope proteins using a modified I-barrel construct. 2012 , 85, 133-41	19
1807	Mitochondrial function and energy metabolism in umbilical cord blood- and bone marrow-derived mesenchymal stem cells. 2012 , 21, 575-88	54
1806	Long noncoding RNAs are rarely translated in two human cell lines. 2012 , 22, 1646-57	292
1805	Prunasin hydrolases during fruit development in sweet and bitter almonds. 2012 , 158, 1916-32	32
1804	A chemical proteomics approach reveals Hsp27 as a target for proapoptotic clerodane diterpenes. 2012 , 8, 2637-44	16
1803	Heat shock proteins as key biological targets of the marine natural cyclopeptide perthamide C. 2012 , 8, 1412-7	10
1802	Human complement C3 is a substrate for transglutaminases. A functional link between non-protease-based members of the coagulation and complement cascades. 2012 , 51, 4735-42	20
1801	Rho-associated coiled-coil kinase (ROCK) protein controls microtubule dynamics in a novel signaling pathway that regulates cell migration. 2012 , 287, 43620-9	54
1800	A comparative proteomic study of human skin suction blister fluid from healthy individuals using immunodepletion and iTRAQ labeling. 2012 , 11, 3715-27	45
1799	Roles of proteins, polysaccharides, and phenolics in haze formation in white wine via reconstitution experiments. 2012 , 60, 10666-73	53
1798	Identification of an IgE reactive peptide in hen egg riboflavin binding protein subjected to simulated gastrointestinal digestion. 2012 , 60, 5215-20	9
1797	Calcium-dependent interaction of calmodulin with human 80S ribosomes and polyribosomes. 2012 , 51, 6718-27	6
1796	Structural Insights into retinal guanylylcyclase-GCAP-2 interaction determined by cross-linking and mass spectrometry. 2012 , 51, 4932-49	18
1795	Catabolic pathway of gamma-caprolactone in the biocontrol agent Rhodococcus erythropolis. 2012 , 11, 206-16	35
1794	Triple SILAC to determine stimulus specific interactions in the Wnt pathway. 2012 , 11, 982-94	56
1793	Mapping protein receptor-ligand interactions via in vivo chemical crosslinking, affinity purification, and differential mass spectrometry. 2012 , 56, 161-5	12
1792	Four proteins governing overangiogenic endothelial cell phenotype in patients with multiple myeloma are plausible therapeutic targets. 2012 , 31, 2258-69	26
1791	Post-translational oxidative modification and inactivation of mitochondrial complex I in epileptogenesis. 2012 , 32, 11250-8	60

1790	Identifying cellular targets of small-molecule probes and drugs with biochemical enrichment and SILAC. 2012 , 803, 129-40	24
1789	S-glutathionylation of the Na,K-ATPase catalytic Bubunit is a determinant of the enzyme redox sensitivity. 2012 , 287, 32195-205	86
1788	Crystal structure of the lectin of Camptosema pedicellatum: implications of a conservative substitution at the hydrophobic subsite. 2012 , 152, 87-98	8
1787	In vivo quantitative proteome profiling: planning and evaluation of SILAC experiments. 2012, 893, 175-99	14
1786	A systematic investigation into the nature of tryptic HCD spectra. 2012 , 11, 5479-91	85
1785	Myosin light chain 3f attenuates age-induced decline in contractile velocity in MHC type II single muscle fibers. 2012 , 11, 203-12	15
1784	Mutation of Phe413 to Tyr in catalase KatE from Escherichia coli leads to side chain damage and main chain cleavage. 2012 , 525, 207-14	0
1783	Stabilization of the Escherichia coli DNA polymerase III \(\bar{B}\) ubunit by the \(\bar{B}\) ubunit favors in vivo assembly of the Pol III catalytic core. 2012 , 523, 135-43	12
1782	Minimization of side reactions during Lys Tag derivatization of C-terminal lysine peptides. 2012 , 712, 101-7	
1781	Regulation of the interferon-inducible 2'-5'-oligoadenylate synthetases by adenovirus VA(I) RNA. 2012 , 422, 635-649	28
1780	Production and characterization of a novel monoclonal antibody against Vibrio parahaemolyticus F0F1 ATP synthase's delta subunit and its application for rapid identification of the pathogen. 2012 , 88, 77-82	9
1779	Chemical labelling of active serum thioester proteins for quantification. 2012 , 217, 256-64	4
1778	Attenuated metabolism is a hallmark of obesity as revealed by comparative proteomic analysis of human omental adipose tissue. 2012 , 75, 783-95	34
1777	Longitudinal analysis of taurine induced effects on the tear proteome of contact lens wearers and dry eye patients using a RP-RP-Capillary-HPLC-MALDI TOF/TOF MS approach. 2012 , 75, 3177-90	28
1776	Analysis of N-glycosylation in maize cytokinin oxidase/dehydrogenase 1 using a manual microgradient chromatographic separation coupled offline to MALDI-TOF/TOF mass spectrometry. 2012 , 75, 4027-37	12
1775	Proteomic analysis of the soluble and the lysosomal+mitochondrial fractions from rat pancreas: Implications for cerulein-induced acute pancreatitis. 2012 , 1824, 1058-67	10
1774	Comparative proteomic analysis to dissect differences in signal transduction in activating TSH receptor mutations in the thyroid. 2012 , 44, 290-301	10
1773	Functional characterization of a synthetic hydrophilic antifungal peptide derived from the marine snail Cenchritis muricatus. 2012 , 94, 968-74	38

1772	A new vesicular scaffolding complex mediates the G-protein-coupled 5-HT1A receptor targeting to neuronal dendrites. 2012 , 32, 14227-41	24
1771	Comparison of in-gel protein separation techniques commonly used for fractionation in mass spectrometry-based proteomic profiling. 2012 , 33, 2516-26	31
1770	Adaptive response to acetic acid in the highly resistant yeast species Zygosaccharomyces bailii revealed by quantitative proteomics. 2012 , 12, 2303-18	30
1769	Investigation of serum proteome alterations in human glioblastoma multiforme. 2012 , 12, 2378-90	47
1768	Separation and study of the range of plasminogen isoforms in patients with prostate cancer. 2012 , 77, 1065-71	1
1767	Mapping of cis-regulatory sites in the promoter of testis-specific stellate genes of Drosophila melanogaster. 2012 , 77, 1285-93	3
1766	Comparison of total and cytoplasmic mRNA reveals global regulation by nuclear retention and miRNAs. 2012 , 13, 574	30
1765	Combining proteomics and transcriptome sequencing to identify active plant-cell-wall-degrading enzymes in a leaf beetle. 2012 , 13, 587	51
1764	NanoUPLC-MSE proteomic data assessment of soybean seeds using the Uniprot database. 2012 , 12, 82	48
1763	High molecular mass proteomics analyses of left ventricle from rats subjected to differential swimming training. 2012 , 12, 11	10
1762	In-depth proteomic analysis of a mollusc shell: acid-soluble and acid-insoluble matrix of the limpet Lottia gigantea. 2012 , 10, 28	64
1761	Thermoascus aurantiacus is a promising source of enzymes for biomass deconstruction under thermophilic conditions. 2012 , 5, 54	59
1760	Mass spectrometry tools for analysis of intermolecular interactions. 2012 , 896, 387-98	3
1759	Mutant p53 interactome identifies nardilysin as a p53R273H-specific binding partner that promotes invasion. 2012 , 13, 638-44	55
1758	Proteomic identification of in vivo interactors reveals novel function of skin cornification proteins. 2012 , 11, 3068-76	16
1757	Differential subcellular targeting of recombinant human Eproteinase inhibitor influences yield, biological activity and in planta stability of the protein in transgenic tomato plants. 2012 , 196, 53-66	21
1756	The protein composition of the digestive fluid from the venus flytrap sheds light on prey digestion mechanisms. 2012 , 11, 1306-19	63
1755	Comprehensive phosphoproteome analysis of INS-1 pancreatic I-cells using various digestion strategies coupled with liquid chromatography-tandem mass spectrometry. 2012 , 11, 2206-23	21

(2012-2012)

1754	Large-scale proteome comparative analysis of developing rhizomes of the ancient vascular plant equisetum hyemale. 2012 , 3, 131	16
1753	Quantitative- and phospho-proteomic analysis of the yeast response to the tyrosine kinase inhibitor imatinib to pharmacoproteomics-guided drug line extension. 2012 , 16, 537-51	7
1752	Identification of an amino-terminal fragment of apolipoprotein E4 that localizes to neurofibrillary tangles of the Alzheimer's disease brain. 2012 , 1475, 106-15	31
1751	Effects of left ventricular assist device (LVAD) placement on myocardial oxidative stress markers. 2012 , 21, 586-97	5
1750	Purification and primary structure determination of a galactose-specific lectin from Vatairea guianensis Aublet seeds that exhibits vasorelaxant effect. 2012 , 47, 2347-2355	17
1749	Proteome mapping of human skim milk proteins in term and preterm milk. 2012 , 11, 1696-714	78
1748	In-cell NMR in mammalian cells: part 3. 2012 , 895, 67-83	10
1747	Recent advances in platelet proteomics. 2012 , 9, 451-66	24
1746	Proteomic analysis of microvesicles derived from human mesenchymal stem cells. 2012 , 11, 839-49	295
1745	Identifying chromatin readers using a SILAC-based histone peptide pull-down approach. 2012 , 512, 137-60	9
1744	Comparative study of workflows optimized for in-gel, in-solution, and on-filter proteolysis in the analysis of plasma membrane proteins. 2012 , 11, 3030-4	55
1743	Three novel acetylation sites in the Foxp3 transcription factor regulate the suppressive activity of regulatory T cells. 2012 , 188, 2712-21	113
1742	Comprehensive quantification of monolignol-pathway enzymes in Populus trichocarpa by protein cleavage isotope dilution mass spectrometry. 2012 , 11, 3390-404	38
1741	Spatial distribution of cellular function: the partitioning of proteins between mitochondria and the nucleus in MCF7 breast cancer cells. 2012 , 11, 6080-101	21
1740	Integrin and Cell Adhesion Molecules. 2012,	2
1739	A proteomic survey of nonribosomal peptide and polyketide biosynthesis in actinobacteria. 2012 , 11, 85-94	30
1738	Proteomic analysis of proteins differentially expressed in conidia and mycelium of the entomopathogenic fungus Aschersonia placenta. 2012 , 58, 1327-34	4
1737	GOFAST: an integrated approach for efficient and comprehensive membrane proteome analysis. 2012 , 84, 9008-14	20

1736	Coupling a detergent lysis/cleanup methodology with intact protein fractionation for enhanced proteome characterization. 2012 , 11, 6008-18	63
1735	Comparative metaproteomics and diversity analysis of human intestinal microbiota testifies for its temporal stability and expression of core functions. 2012 , 7, e29913	147
1734	Comprehensive assessment of milk composition in transgenic cloned cattle. 2012 , 7, e49697	14
1733	Accelerated identification of proteins by mass spectrometry by employing covalent pre-gel staining with Uniblue A. 2012 , 7, e31438	7
1732	The centrosomal kinase Plk1 localizes to the transition zone of primary cilia and induces phosphorylation of nephrocystin-1. 2012 , 7, e38838	37
1731	Detection of the heterogeneous O-glycosylation profile of MT1-MMP expressed in cancer cells by a simple MALDI-MS method. 2012 , 7, e43751	11
1730	Verticillium longisporum infection affects the leaf apoplastic proteome, metabolome, and cell wall properties in Arabidopsis thaliana. 2012 , 7, e31435	90
1729	Identification and characterization of FAM124B as a novel component of a CHD7 and CHD8 containing complex. 2012 , 7, e52640	17
1728	Vinyl Sulfone: A Multi-Purpose Function in Proteomics. 2012 ,	2
1727	Vol 2, No 1 (2012). 2012 , 2,	
, ,	Vol 2, No 1 (2012). 2012 , 2, Proteomic Response to Arsenic Stress in Chromobacterium violaceum. 2012 , 2,	1
, ,		1
1726	Proteomic Response to Arsenic Stress in Chromobacterium violaceum. 2012 , 2, Identification of Potential Glycoprotein Biomarkers in Estrogen Receptor Positive (ER+) and Negative (ER-) Human Breast Cancer Tissues by LC-LTQ/FT-ICR Mass Spectrometry. 2012 , 3, 269-84	
1726 1725	Proteomic Response to Arsenic Stress in Chromobacterium violaceum. 2012 , 2, Identification of Potential Glycoprotein Biomarkers in Estrogen Receptor Positive (ER+) and Negative (ER-) Human Breast Cancer Tissues by LC-LTQ/FT-ICR Mass Spectrometry. 2012 , 3, 269-84	14
1726 1725 1724	Proteomic Response to Arsenic Stress in Chromobacterium violaceum. 2012, 2, Identification of Potential Glycoprotein Biomarkers in Estrogen Receptor Positive (ER+) and Negative (ER-) Human Breast Cancer Tissues by LC-LTQ/FT-ICR Mass Spectrometry. 2012, 3, 269-84 2-D DIGE analysis of UV-C radiation-responsive proteins in globe artichoke leaves. 2012, 12, 448-60 Proteomic analysis of the androgen receptor via MS-compatible purification of biotinylated protein	14
1726 1725 1724 1723	Proteomic Response to Arsenic Stress in Chromobacterium violaceum. 2012, 2, Identification of Potential Glycoprotein Biomarkers in Estrogen Receptor Positive (ER+) and Negative (ER-) Human Breast Cancer Tissues by LC-LTQ/FT-ICR Mass Spectrometry. 2012, 3, 269-84 2-D DIGE analysis of UV-C radiation-responsive proteins in globe artichoke leaves. 2012, 12, 448-60 Proteomic analysis of the androgen receptor via MS-compatible purification of biotinylated protein on streptavidin resin. 2012, 12, 43-53	14 9 5
1726 1725 1724 1723	Proteomic Response to Arsenic Stress in Chromobacterium violaceum. 2012, 2, Identification of Potential Glycoprotein Biomarkers in Estrogen Receptor Positive (ER+) and Negative (ER-) Human Breast Cancer Tissues by LC-LTQ/FT-ICR Mass Spectrometry. 2012, 3, 269-84 2-D DIGE analysis of UV-C radiation-responsive proteins in globe artichoke leaves. 2012, 12, 448-60 Proteomic analysis of the androgen receptor via MS-compatible purification of biotinylated protein on streptavidin resin. 2012, 12, 43-53 The ovarian cancer-derived secretory/releasing proteome: A repertoire of tumor markers. 2012, 12, 1883-91 Phosphorylation of calcineurin B-like (CBL) calcium sensor proteins by their CBL-interacting protein kinases (CIPKs) is required for full activity of CBL-CIPK complexes toward their target proteins.	14 9 5 24

(2012-2012)

1718	A multiplex quantitative proteomics strategy for protein biomarker studies in urinary exosomes. 2012 , 81, 1263-72	104
1717	Probing protein phosphatase substrate binding: affinity pull-down of ILKAP phosphatase 2C with phosphopeptides. 2012 , 8, 1452-60	7
1716	Proteomic profile of human aortic stenosis: insights into the degenerative process. 2012 , 11, 1537-50	44
1715	Galleria mellonella as a model for fungal pathogenicity testing. 2012 , 845, 469-85	56
1714	Purification and characterization of a mannose/N-acetyl-D-glucosamine-specific lectin from the seeds of Platymiscium floribundum Vogel. 2012 , 25, 443-9	15
1713	Alterations of the erythrocyte membrane proteome and cytoskeleton network during storagea possible tool to identify autologous blood transfusion. 2012 , 4, 882-90	11
1712	Analysis of proteins using DIGE and MALDI mass spectrometry. 2012 , 854, 47-66	13
1711	Symmetric dimethylation of H3R2 is a newly identified histone mark that supports euchromatin maintenance. 2012 , 19, 136-44	224
1710	Cyclostreptin derivatives specifically target cellular tubulin and further map the paclitaxel site. 2012 , 51, 329-41	17
1709	Chemical proteomics reveals heat shock protein 60 to be the main cellular target of the marine bioactive sesterterpene suvanine. 2012 , 13, 1953-8	21
1708	Tissue proteomics by one-dimensional gel electrophoresis combined with label-free protein quantification. 2012 , 11, 3680-9	29
1707	Secretome protein enrichment identifies physiological BACE1 protease substrates in neurons. 2012 , 31, 3157-68	236
1706	Multidimensional plasma protein separation technique for identification of potential Alzheimer's disease plasma biomarkers: a pilot study. 2012 , 119, 779-88	33
1705	Exposure of Staphylococcus aureus to silver(I) induces a short term protective response. 2012 , 25, 611-6	8
1704	Horizontal carryover of proteins on one-dimensional polyacrylamide gels may jeopardize gel-enhanced liquid chromatography mass spectrometry proteomic interpretations. 2012 , 421, 779-81	6
1703	Perfusion reversed-phase high-performance liquid chromatography for protein separation from detergent-containing solutions: an alternative to gel-based approaches. 2012 , 424, 97-107	8
1702	Demodex-associated bacterial proteins induce neutrophil activation. 2012 , 166, 753-60	41
1701	Adaptation of Pseudomonas aeruginosa to a pulsed light-induced stress. 2012 , 112, 502-11	12

1700	The proteome and gene expression profile of cementoblastic cells treated by bone morphogenetic protein-7 in vitro. 2012 , 39, 80-90	20
1699	Covalent binding of cisplatin impairs the function of Na(+)/K(+)-ATPase by binding to its cytoplasmic part. 2012 , 83, 1507-13	35
1698	Comprehensive proteomic analysis of human dentin. 2012 , 120, 259-68	41
1697	Functional characterization of UvrD helicases from Haemophilus influenzae and Helicobacter pylori. 2012 , 279, 2134-55	8
1696	Proteomic profiling of the hemolymph at the fifth instar of the silkworm Bombyx mori. 2012 , 19, 441-454	12
1695	Induction of Cr(VI) reduction activity in an Anoxybacillus strain under heat stress: a biochemical and proteomic study. 2012 , 331, 70-80	19
1694	Serum proteome analysis of vivax malaria: An insight into the disease pathogenesis and host immune response. 2012 , 75, 3063-80	38
1693	Inside human aortic stenosis: a proteomic analysis of plasma. 2012 , 75, 1639-53	25
1692	Assessment of Prunus persica fruit softening using a proteomics approach. 2012 , 75, 1618-38	38
1691	Differential protein profiling of synovial fluid from rheumatoid arthritis and osteoarthritis patients using LC-MALDI TOF/TOF. 2012 , 75, 2869-78	93
1690	Identification of a potential biomarker panel for the intake of the common dietary trans fat elaidic acid (trans B -C18:1). 2012 , 75, 2685-96	7
1689	Cell wall proteome of Clostridium thermocellum and detection of glycoproteins. 2012 , 167, 364-71	13
1688	Complement regulator C4BP binds to Staphylococcus aureus and decreases opsonization. 2012 , 50, 253-61	13
1687	Cytosol protein regulation in H295R steroidogenesis model induced by the zearalenone metabolites, ∃and ⊡zearalenol. 2012 , 59, 17-24	13
1686	Purification and kinetic characterization of two peroxidases of Selaginella martensii Spring. involved in lignification. 2012 , 52, 130-9	12
1685	Proteomic characterization of ovarian cancers identifying annexin-A4, phosphoserine aminotransferase, cellular retinoic acid-binding protein 2, and serpin B5 as histology-specific biomarkers. 2012 , 103, 747-55	40
1684	Expression of an apoplast-localized BURP-domain protein from soybean (GmRD22) enhances tolerance towards abiotic stress. 2012 , 35, 1932-47	56
1683	Hrip1, a novel protein elicitor from necrotrophic fungus, Alternaria tenuissima, elicits cell death, expression of defence-related genes and systemic acquired resistance in tobacco. 2012 , 35, 2104-20	46

(2013-2012)

1682	A low molecular weight proteome comparison of fertile and male sterile 8 anthers of Zea mays. 2012 , 10, 925-35	18
1681	In vitro evaluation of glass-glass ceramic thermoseed-induced hyperthermia on human osteosarcoma cell line. 2012 , 100, 64-71	18
1680	Proteomics in MBifBe disease. 2012 , 227, 308-12	20
1679	Proteomics applied to exercise physiology: a cutting-edge technology. 2012 , 227, 885-98	31
1678	Evaluation of Escherichia coli proteins that burden nonaffinity-based chromatography as a potential strategy for improved purification performance. 2012 , 28, 137-45	1
1677	Proteomic Analysis of PEG-Fractionated UV-C Stress-Response Proteins in Globe Artichoke. 2012 , 30, 111-122	7
1676	Proteomic analysis of peritrophic membrane (PM) from the midgut of fifth-instar larvae, Bombyx mori. 2012 , 39, 3427-34	32
1675	Functional analysis of light-regulated promoter region of AtPollgene. 2012 , 235, 411-32	11
1674	Whole gel processing procedure for GeLC-MS/MS based proteomics. 2013 , 11, 17	59
1673	Pre-analytical stability of the plasma proteomes based on the storage temperature. 2013 , 11, 10	29
1672	Differential proteomic analysis of drought stress response in leaves of common bean (Phaseolus vulgaris L.). 2013 , 78, 254-72	111
1671	Identification of Bilirubin Binding Site in Type I Collagen. 2013 , 19, 357-364	2
1670	Differentially expressed proteins during an incompatible interaction between common bean and the fungus Pseudocercospora griseola. 2013 , 32, 933-942	4
1669	Differential protease activity augments polyphagy in Helicoverpa armigera. 2013 , 22, 258-72	37
1668	Proteomic analysis of response to long-term continuous stress in roots of germinating soybean seeds. 2013 , 170, 470-9	29
1667	Biochemical and biological characterization of exosomes containing prominin-1/CD133. 2013 , 12, 62	83
1666	Reconfigurable infrared camouflage coatings from a cephalopod protein. 2013 , 25, 5621-5	124
1665	Orchestrated intron retention regulates normal granulocyte differentiation. 2013 , 154, 583-95	290

1664	Molecular Dermatology. 2013,	2
1663	Cell-selective labeling using amino acid precursors for proteomic studies of multicellular environments. 2013 , 10, 768-73	38
1662	A porin-like protein from oral secretions of Spodoptera littoralis larvae induces defense-related early events in plant leaves. 2013 , 43, 849-58	25
1661	Overcoming bottlenecks of enzymatic biofuel cell cathodes: crude fungal culture supernatant can help to extend lifetime and reduce cost. 2013 , 6, 1209-15	18
1660	Cell Senescence. 2013,	3
1659	Whole human genome proteogenomic mapping for ENCODE cell line data: identifying protein-coding regions. 2013 , 14, 141	45
1658	Natural variation in floral nectar proteins of two Nicotiana attenuata accessions. 2013, 13, 101	17
1657	Serine protease from midgut of Bombus terrestris males. 2013 , 82, 117-28	5
1656	Random UV mutagenesis approach for enhanced biodegradation of sulfonated azo dye, Green HE4B. 2013 , 169, 1467-81	9
1655	Eplt4 proteinaceous elicitor produced in Pichia pastoris has a protective effect against Cercosporidium sofinum infections of soybean leaves. 2013 , 169, 722-37	14
1654	Proteomic analysis of the mice hippocampus after preconditioning induced by N-methyl-D-aspartate (NMDA). 2013 , 50, 154-64	5
1653	Molecular cloning, expression, and in silico structural analysis of guinea pig IL-17. 2013 , 55, 277-87	10
1652	Quantitative proteomic analysis of ibuprofen-degrading Patulibacter sp. strain I11. 2013 , 24, 615-30	53
1651	Gene Regulation. 2013,	1
1650	Identification and confirmation of haptoglobin as a potential serum biomarker in hypertrophic cardiomyopathy using proteomic approaches. 2013 , 45, 341-7	5
1649	Dynamic changes in xylanases and [-1,4-endoglucanases secreted by Aspergillus niger An-76 in response to hydrolysates of lignocellulose polysaccharide. 2013 , 171, 832-46	16
1648	Proteomic analysis of synovial fluid: insight into the pathogenesis of knee osteoarthritis. 2013 , 37, 1045-53	17
1647	Molecular characterization and evolution of haemocyanin from the two freshwater shrimps Caridina multidentata (Stimpson, 1860) and Atyopsis moluccensis (De Haan, 1849). 2013 , 183, 613-24	14

(2013-2013)

1646	Elucidating heterogeneity of IgA1 hinge-region O-glycosylation by use of MALDI-TOF/TOF mass spectrometry: role of cysteine alkylation during sample processing. 2013 , 92, 299-312	40
1645	Polyacrylamide gel with switchable trypsin activity for analysis of proteins. 2013 , 85, 7024-8	6
1644	H-3, a new lectin from the marine sponge Haliclona caerulea: purification and mass spectrometric characterization. 2013 , 45, 2864-73	22
1643	Structures of Down syndrome kinases, DYRKs, reveal mechanisms of kinase activation and substrate recognition. 2013 , 21, 986-96	99
1642	Exclusive rewards in mutualisms: ant proteases and plant protease inhibitors create a lock-key system to protect Acacia food bodies from exploitation. 2013 , 22, 4087-100	26
1641	Detection of the antibacterial effect of essential oils on outer membrane proteins of Pseudomonas aeruginosa by lab-on-a-chip and MALDI-TOF/MS. 2013 , 28, 367-372	3
1640	Polybrominated diphenyl ethers do not affect metamorphosis but alter the proteome of the invasive slipper limpet Crepidula onyx. 2013 , 73, 273-81	3
1639	Performance evaluation of affinity ligands for depletion of abundant plasma proteins. 2013 , 939, 10-6	23
1638	Induced protein polymorphisms and nutritional quality of gamma irradiation mutants of sorghum. 2013 , 749, 66-72	21
1637	Unexpected histone H3 tail-clipping activity of glutamate dehydrogenase. 2013 , 288, 18743-57	34
1636	Lesser protein degradation machinery correlates with higher BM86 tick vaccine efficacy in Rhipicephalus annulatus when compared to Rhipicephalus microplus. 2013 , 31, 4728-35	32
1635	Simultaneous treatment with tebuconazole and abscisic acid induces drought and salinity stress tolerance in Arabidopsis thaliana by maintaining key plastid protein levels. 2013 , 12, 1266-81	15
1634	The influence of angiotensin-(1-7) Mas receptor agonist (AVE 0991) on mitochondrial proteome in kidneys of apoE knockout mice. 2013 , 1834, 2463-9	16
1633	Shotgun label-free quantitative proteomics of water-deficit-stressed midmature peanut (Arachis hypogaea L.) seed. 2013 , 12, 5048-57	28
1632	Heart Proteomics. 2013,	2
1631	Application of an improved proteomics method for abundant protein cleanup: molecular and genomic mechanisms study in plant defense. 2013 , 12, 3431-42	21
1630	Cytokeratin 8-MHC class I interactions: a potential novel immune escape phenotype by a lymph node metastatic carcinoma cell line. 2013 , 441, 618-23	17
1629	Analysis of the Streptococcus agalactiae exoproteome. 2013 , 89, 154-64	16

1628	Structural analysis of guanylyl cyclase-activating protein-2 (GCAP-2) homodimer by stable isotope-labeling, chemical cross-linking, and mass spectrometry. 2013 , 24, 1969-79	25
1627	Highly selective purification of three lipases from Geotrichum candidum 4013 and their characterization and biotechnological applications. 2013 , 98, 62-72	20
1626	Systems insight into the spore germination of Streptomyces coelicolor. 2013 , 12, 525-36	17
1625	Impact of benzo(a)pyrene, Cu and their mixture on the proteomic response of Mytilus galloprovincialis. 2013 , 144-145, 284-95	34
1624	Endogenous factor VIII synthesis from the intron 22-inverted F8 locus may modulate the immunogenicity of replacement therapy for hemophilia A. 2013 , 19, 1318-24	50
1623	In vitro activity of Neisseria meningitidis PglL O-oligosaccharyltransferase with diverse synthetic lipid donors and a UDP-activated sugar. 2013 , 288, 10578-87	20
1622	Genomically recoded organisms expand biological functions. 2013 , 342, 357-60	553
1621	Species differences take shape at nanoparticles: protein corona made of the native repertoire assists cellular interaction. 2013 , 47, 14367-75	61
1620	Experimental and computational analysis of the secretome of the hyperthermophilic archaeon Pyrococcus furiosus. 2013 , 17, 921-30	6
1619	Critical assessment of the spectroscopic activity assay for monitoring trypsin activity in organic-aqueous solvent. 2013 , 435, 131-6	11
1618	Two 🛮 xylanases from Aspergillus terreus: characterization and influence of phenolic compounds on xylanase activity. 2013 , 60, 46-52	32
1617	An alpha class glutathione S-transferase from pike liver. 2013 , 39, 498-503	2
1616	The proteome of the calcified layer organic matrix of turkey (Meleagris gallopavo) eggshell. 2013 , 11, 40	35
1615	Salt and UV-B induced changes in Anabaena PCC 7120: physiological, proteomic and bioinformatic perspectives. 2013 , 118, 105-14	33
1614	Dynamic protein phosphorylation during the growth of Xanthomonas campestris pv. campestris B100 revealed by a gel-based proteomics approach. 2013 , 167, 111-22	15
1613	Self-aliquoting microarray plates for accurate quantitative matrix-assisted laser desorption/ionization mass spectrometry. 2013 , 85, 9771-6	30
1612	Proteins differentially expressed in conidia and mycelia of the entomopathogenic fungus Metarhizium anisopliae sensu stricto. 2013 , 59, 443-8	9
1611	RT-PCR- and MALDI-TOF mass spectrometry-based identification and discrimination of isoforms homologous to pufferfish saxitoxin- and tetrodotoxin-binding protein in the plasma of non-toxic cultured pufferfish (Takifugu rubripes). 2013 , 77, 208-12	17

(2013-2013)

1610	Proteome analysis of functionally differentiated bovine (Bos indicus) mammary epithelial cells isolated from milk. 2013 , 13, 3189-204	21
1609	SILAC-based proteomics of human primary endothelial cell morphogenesis unveils tumor angiogenic markers. 2013 , 12, 3599-611	50
1608	Threshold-controlled ubiquitination of the EGFR directs receptor fate. 2013 , 32, 2140-57	125
1607	Mass spectrometry compatible surfactant for optimized in-gel protein digestion. 2013 , 85, 907-14	42
1606	Renal uptake of 99mTc-dimercaptosuccinic acid is dependent on normal proximal tubule receptor-mediated endocytosis. 2013 , 54, 159-65	39
1605	The ROK family regulator Rok7B7 pleiotropically affects xylose utilization, carbon catabolite repression, and antibiotic production in streptomyces coelicolor. 2013 , 195, 1236-48	47
1604	Longitudinal analysis of protein glycosylation and Dcasein phosphorylation in term and preterm human milk during the first 2 months of lactation. 2013 , 110, 105-15	25
1603	An improved method for the detection and enrichment of low-abundant membrane and lipid raft-residing proteins. 2013 , 79, 299-304	8
1602	Using multiple structural proteomics approaches for the characterization of prion proteins. 2013 , 81, 31-42	17
1601	An Efficient In-gel Digestion Protocol for Mass Spectral Analysis by MALDI-TOF-MS and MS/MS and Its Use for Proteomic Analysis of Vigna mungo Leaves. 2013 , 31, 47-54	6
1600	Effects of acute exercise over heart proteome from monogenic obese (ob/ob) mice. 2013, 228, 824-34	11
1599	Glycoproteomics-based cancer marker discovery adopting dual enrichment with Wisteria floribunda agglutinin for high specific glyco-diagnosis of cholangiocarcinoma. 2013 , 85, 1-11	38
1598	Identification of the phosphorylated residues in TveIF5A by mass spectrometry. 2013, 11, 378-84	3
1597	Autophosphorylation activity of a soluble hexameric histidine kinase correlates with the shift in protein conformational equilibrium. 2013 , 20, 1411-20	22
1596	A review of complementary separation methods and matrix assisted laser desorption ionization-mass spectrometry imaging: lowering sample complexity. 2013 , 1319, 1-13	13
1595	Tc-cAPX, a cytosolic ascorbate peroxidase of Theobroma cacao L.´engaged in the interaction with Moniliophthora perniciosa, the´causing agent of witches´ broom disease. 2013 , 73, 254-65	11
1594	The extracellular matrix locally regulates asynchronous concurrent lactation in tammar wallaby (Macropus eugenii). 2013 , 32, 342-51	12
1593	Displacement-weighted velocity analysis of gliding assays reveals that Chlamydomonas axonemal dynein preferentially moves conspecific microtubules. 2013 , 104, 1989-98	15

1592	Pseudopodial and 🛭 arrestin-interacting proteomes from migrating breast cancer cells upon PAR2 activation. 2013 , 80, 91-106	20
1591	Immunoreactivity of hen egg allergens: influence on in vitro gastrointestinal digestion of the presence of other egg white proteins and of egg yolk. 2013 , 136, 775-81	39
1590	The Rhesus macaque (Macaca mulatta) sperm proteome. 2013 , 12, 3052-67	37
1589	Hepatocystin/80K-H inhibits replication of hepatitis B virus through interaction with HBx protein in hepatoma cell. 2013 , 1832, 1569-81	11
1588	Tear proteome and protein network analyses reveal a novel pentamarker panel for tear film characterization in dry eye and meibomian gland dysfunction. 2013 , 78, 94-112	71
1587	Hydrogen peroxide induce modifications of human extracellular superoxide dismutase that results in enzyme inhibition. 2013 , 1, 24-31	54
1586	Genomic characterization of six novel Bacillus pumilus bacteriophages. 2013, 444, 374-83	27
1585	Changes in the hepatic mitochondrial and membrane proteome in mice fed a non-alcoholic steatohepatitis inducing diet. 2013 , 80, 107-22	21
1584	Alternative substrates selective for S-adenosylmethionine synthetases from pathogenic bacteria. 2013 , 536, 64-71	14
1583	CD98 marks a subpopulation of head and neck squamous cell carcinoma cells with stem cell properties. 2013 , 10, 477-88	35
1582	Immunoproteomic characterization of Ambrosia artemisiifolia pollen allergens in canine atopic dermatitis. 2013 , 155, 38-47	12
1581	Identification of phosphorylation sites in Hansenula polymorpha Pex14p by mass spectrometry. 2013 , 3, 6-10	8
1580	HMMC-1, a human monoclonal antibody to fucosylated core 1 O-glycan, suppresses growth of uterine endometrial cancer cells. 2013 , 104, 62-9	
1579	Detecting endogenous SUMO targets in mammalian cells and tissues. 2013 , 20, 525-31	155
1578	A novel prefractionation method combining protein and peptide isoelectric focusing in immobilized pH gradient strips. 2013 , 12, 1014-9	17
1577	Proteomic analysis of the tegument and excretory-secretory products of Dicrocoelium dendriticum (Digenea) adult worms. 2013 , 133, 411-20	15
1576	Intensive Protein Digestion Using Cross-Linked Trypsin Aggregates in Proteomics Analysis. 2013 , 78, 407-412	6
1575	Proteome reference map of Haloarcula hispanica and comparative proteomic and transcriptomic analysis of polyhydroxyalkanoate biosynthesis under genetic and environmental perturbations. 2013 , 12, 1300-15	7

1574	Effects of a pulsed light-induced stress on Enterococcus faecalis. 2013 , 114, 186-95	11
1573	In vivo SILAC-based proteomics reveals phosphoproteome changes during mouse skin carcinogenesis. 2013 , 3, 552-66	82
1572	Characterization of ⊞mannosidase from Dolichos lablab seeds: partial amino acid sequencing and N-glycan analysis. 2013 , 89, 7-15	12
1571	Centrosome isolation and analysis by mass spectrometry-based proteomics. 2013 , 525, 371-93	9
1570	Identifying specific protein-DNA interactions using SILAC-based quantitative proteomics. 2013 , 977, 137-57	15
1569	PPE38 of Mycobacterium marinum triggers the cross-talk of multiple pathways involved in the host response, as revealed by subcellular quantitative proteomics. 2013 , 12, 2055-66	20
1568	Using guanidine-hydrochloride for fast and efficient protein digestion and single-step affinity-purification mass spectrometry. 2013 , 12, 1020-30	33
1567	Analysis of the glycosylation pattern of plant copper amine oxidases by MALDI-TOF/TOF MS coupled to a manual chromatographic separation of glycans and glycopeptides. 2013 , 34, 2357-67	13
1566	Escherichia coli-based cell free production of flagellin and ordered flagellin display on virus-like particles. 2013 , 110, 2073-85	40
1565	Sialic acid capture-and-release and LC-MS(n) analysis of glycopeptides. 2013 , 951, 79-100	8
1564	Analysis of secreted proteins. 2013, 1002, 37-60	14
1563	Reprogramming- and pluripotency-associated membrane proteins in mouse stem cells revealed by label-free quantitative proteomics. 2013 , 86, 70-84	10
1562	Proteomic analysis of the proteins released from Staphylococcus aureus following exposure to Ag(I). 2013 , 27, 1644-8	9
1561	Global protein quantification of mouse heart tissue based on the SILAC mouse. 2013 , 1005, 39-52	11
1560	Detection of O-GlcNAc modifications on cardiac myofilament proteins. 2013 , 1005, 157-68	2
1559	A sequential extraction methodology for cardiac extracellular matrix prior to proteomics analysis. 2013 , 1005, 215-23	19
1558	A method for rapid production of heteromultimeric protein complexes in plants: assembly of protective bluetongue virus-like particles. 2013 , 11, 839-46	89
1557	An affinity pull-down approach to identify the plant cyclic nucleotide interactome. 2013 , 1016, 155-73	2

1556	Monitoring conformational changes in peroxisome proliferator-activated receptor by a genetically encoded photoamino acid, cross-linking, and mass spectrometry. 2013 , 56, 4252-63	18
1555	Application of label-free shotgun nUPLC-MS(E) and 2-DE approaches in the study of Botrytis cinerea mycelium. 2013 , 12, 3042-56	26
1554	A novel approach to the analysis of SUMOylation with the independent use of trypsin and elastase digestion followed by database searching utilising consecutive residue addition to lysine. 2013 , 27, 127-34	15
1553	Enhanced detection of ubiquitin isopeptides using reductive methylation. 2013 , 24, 421-30	11
1552	The loss of virulence of histone H1 overexpressing Leishmania donovani parasites is directly associated with a reduction of HSP83 rate of translation. 2013 , 88, 1015-31	12
1551	Relative quantification of proteasome activity by activity-based protein profiling and LC-MS/MS. Nature Protocols, 2013 , 8, 1155-68	62
1550	Antibodies to contactin-1 in chronic inflammatory demyelinating polyneuropathy. 2013, 73, 370-80	217
1549	Particles on the move: intracellular trafficking and asymmetric mitotic partitioning of nanoporous polymer particles. 2013 , 7, 5558-67	31
1548	14-3-3[boosts bleomycin-induced DNA damage response by inhibiting the drug-resistant activity of MVP. 2013 , 12, 2511-24	9
1547	Proteome analysis of silkworm, Bombyx mori, larval gonads: characterization of proteins involved in sexual dimorphism and gametogenesis. 2013 , 12, 2422-38	17
1546	Absolute quantification of E1, ubiquitin-like proteins and Nedd8-MLN4924 adduct by mass spectrometry. 2013 , 67, 139-47	11
1545	Systematic research on the pretreatment of peptides for quantitative proteomics using a CII microcolumn. 2013 , 13, 2229-37	23
1544	Tightly anchored tissue-mimetic matrices as instructive stem cell microenvironments. 2013, 10, 788-94	162
1543	Dysferlin interacts with calsequestrin-1, myomesin-2 and dynein in human skeletal muscle. 2013 , 45, 1927-38	21
1542	Oncogene-induced cellular senescence elicits an anti-Warburg effect. 2013 , 13, 2585-96	33
1541	Characterization of Cannabis sativa allergens. 2013 , 111, 32-7	50
1540	Haloferax volcanii archaeosortase is required for motility, mating, and C-terminal processing of the S-layer glycoprotein. 2013 , 88, 1164-75	41
1539	Mycobacterium tuberculosis utilizes a unique heterotetrameric structure for dehydrogenation of the cholesterol side chain. 2013 , 52, 2895-904	44

(2013-2013)

1538	Differential protein expression in mussels Mytilus galloprovincialis exposed to nano and ionic Ag. 2013 , 136-137, 79-90	74
1537	Unbiased characterization of the senescence-associated secretome using SILAC-based quantitative proteomics. 2013 , 965, 175-84	10
1536	Identification of novel biomarkers of abdominal aortic aneurysms by 2D-DIGE and MALDI-MS from AAA-thrombus-conditioned media. 2013 , 1000, 91-101	2
1535	CENP-A confers a reduction in height on octameric nucleosomes. 2013 , 20, 763-5	40
1534	Short-term proteomic dynamics reveal metabolic factory for active extrafloral nectar secretion by Acacia cornigera ant-plants. 2013 , 73, 546-54	25
1533	Surface-exposed glycoproteins of hyperthermophilic Sulfolobus solfataricus P2 show a common N-glycosylation profile. 2013 , 12, 2779-90	38
1532	Proteome profiling of human neutrophil granule subsets, secretory vesicles, and cell membrane: correlation with transcriptome profiling of neutrophil precursors. 2013 , 94, 711-21	151
1531	Virulence factors are released in association with outer membrane vesicles of Pseudomonas syringae pv. tomato T1 during normal growth. 2013 , 1834, 231-9	51
1530	Characterization of the novel broad-spectrum kinase inhibitor CTx-0294885 as an affinity reagent for mass spectrometry-based kinome profiling. 2013 , 12, 3104-16	40
1529	Comparative proteomic analysis of generative and sperm cells reveals molecular characteristics associated with sperm development and function specialization. 2013 , 12, 5058-71	16
1528	Human SIRT1 regulates DNA binding and stability of the Mcm10 DNA replication factor via deacetylation. 2013 , 41, 4065-79	23
1527	Asp-Selective Microwave-Supported Acid Proteolysis. 2013 , 225-236	
1526	Subcellular proteomics reveals a role for nucleo-cytoplasmic trafficking at the DNA replication origin activation checkpoint. 2013 , 12, 1436-53	13
1525	Two birds with one stone: doing metabolomics with your proteomics kit. 2013 , 13, 3371-86	19
1524	Regulation of H2O2 stress-responsive genes through a novel transcription factor in the protozoan pathogen Entamoeba histolytica. 2013 , 288, 4462-74	34
1523	The sirtuin SIRT6 regulates stress granule formation in C. elegans and mammals. 2013 , 126, 5166-77	46
1522	Purification and primary structure of a mannose/glucose-binding lectin from Parkia biglobosa Jacq. seeds with antinociceptive and anti-inflammatory properties. 2013 , 26, 470-8	18
1521	Dual LC-MS platform for high-throughput proteome analysis. 2013 , 12, 5963-70	14

1520	Cellular ERK phospho-form profiles with conserved preference for a switch-like pattern. 2013, 12, 637-46	17
1519	Shotgun proteomic analysis of wing discs from the domesticated silkworm (Bombyx mori) during metamorphosis. 2013 , 45, 1231-41	9
1518	Combining filter-aided sample preparation and pseudoshotgun technology to profile the proteome of a low number of early passage human melanoma cells. 2013 , 12, 1040-8	29
1517	Use of narrow mass-window, high-resolution extracted product ion chromatograms for the sensitive and selective identification of protein modifications. 2013 , 85, 4621-7	14
1516	Cell cycle regulation of microtubule interactomes: multi-layered regulation is critical for the interphase/mitosis transition. 2013 , 12, 3135-47	18
1515	Research resource: identification of novel coregulators specific for thyroid hormone receptor-IZ. 2013 , 27, 840-59	8
1514	Extensive mass spectrometry-based analysis of the fission yeast proteome: the Schizosaccharomyces pombe PeptideAtlas. 2013 , 12, 1741-51	21
1513	Identification and characterization of Porphyromonas gingivalis client proteins that bind to Streptococcus oralis glyceraldehyde-3-phosphate dehydrogenase. 2013 , 81, 753-63	17
1512	Reactive oxygen species (ROS) protection via cysteine oxidation in the epidermal cornified cell envelope. 2014 , 1195, 157-69	5
1511	Tissue-specific splicing of a ubiquitously expressed transcription factor is essential for muscle differentiation. 2013 , 27, 1247-59	73
1510	A SILAC-based approach identifies substrates of caspase-dependent cleavage upon TRAIL-induced apoptosis. 2013 , 12, 1436-50	23
1509	Proteomics approach to the study of cattle tick adaptation to white tailed deer. 2013 , 2013, 319812	10
1508	A regulatory circuit that involves HR23B and HDAC6 governs the biological response to HDAC inhibitors. 2013 , 20, 1306-16	37
1507	EVI1 oncoprotein interacts with a large and complex network of proteins and integrates signals through protein phosphorylation. 2013 , 110, E2885-94	32
1506	Ube2W conjugates ubiquitin to ⊞mino groups of protein N-termini. 2013 , 453, 137-45	69
1505	Heterozygous LmnadelK32 mice develop dilated cardiomyopathy through a combined pathomechanism of haploinsufficiency and peptide toxicity. 2013 , 22, 3152-64	45
1504	Chimeric protein complexes in hybrid species generate novel phenotypes. 2013 , 9, e1003836	36
1503	The chromodomain helicase Chd4 is required for Polycomb-mediated inhibition of astroglial differentiation. 2013 , 32, 1598-612	61

1502	Holocarboxylase synthetase catalyzes biotinylation of heat shock protein 72, thereby inducing RANTES expression in HEK-293 cells. 2013 , 305, C1240-5	8
1501	Endonuclease G mediates Bynuclein cytotoxicity during Parkinson's disease. 2013 , 32, 3041-54	63
1500	Insm1 controls development of pituitary endocrine cells and requires a SNAG domain for function and for recruitment of histone-modifying factors. 2013 , 140, 4947-58	32
1499	NRMT2 is an N-terminal monomethylase that primes for its homologue NRMT1. 2013 , 456, 453-62	29
1498	Functional proteomics of barley and barley chloroplasts - strategies, methods and perspectives. 2013 , 4, 52	16
1497	Mass spectrometry-based proteomics for the analysis of chromatin structure and dynamics. 2013 , 14, 5402-31	27
1496	Integrative "omics"-approach discovers dynamic and regulatory features of bacterial stress responses. 2013 , 9, e1003576	50
1495	TRIAD1 and HHARI bind to and are activated by distinct neddylated Cullin-RING ligase complexes. 2013 , 32, 2848-60	67
1494	Effects of the peptide pheromone plantaricin A and cocultivation with Lactobacillus sanfranciscensis DPPMA174 on the exoproteome and the adhesion capacity of Lactobacillus plantarum DC400. 2013 , 79, 2657-69	27
1493	HIPK2 kinase activity depends on cis-autophosphorylation of its activation loop. 2013 , 5, 27-38	50
1492	Stable isotope labeling in zebrafish allows in vivo monitoring of cardiac morphogenesis. 2013 , 12, 1502-12	19
1491	Systemic cold stress adaptation of Chlamydomonas reinhardtii. 2013 , 12, 2032-47	87
1490	Carboxyl group footprinting mass spectrometry and molecular dynamics identify key interactions in the HER2-HER3 receptor tyrosine kinase interface. 2013 , 288, 25254-25264	25
1489	Isolation, identification, and characterization of novel arenaviruses, the etiological agents of boid inclusion body disease. 2013 , 87, 10918-35	87
1488	Wnt3a-dependent and -independent protein interaction networks of chromatin-bound ⊡catenin in mouse embryonic stem cells. 2013 , 12, 1980-94	14
1487	Chromoplast-specific carotenoid-associated protein appears to be important for enhanced accumulation of carotenoids in hp1 tomato fruits. 2013 , 161, 2085-101	58
1486	Phosphoproteomic analysis of protein kinase C signaling in Saccharomyces cerevisiae reveals Slt2 mitogen-activated protein kinase (MAPK)-dependent phosphorylation of eisosome core components. 2013 , 12, 557-74	40
1485	Proteomic response of marine invertebrate larvae to ocean acidification and hypoxia during metamorphosis and calcification. 2013 , 216, 4580-9	24

1484	Multiple RNA interactions position Mrd1 at the site of the small subunit pseudoknot within the 90S pre-ribosome. 2013 , 41, 1178-90	18
1483	Helicobacter pylori DprA alleviates restriction barrier for incoming DNA. 2013 , 41, 3274-88	26
1482	Differences in sialic acid O-acetylation between human urinary and recombinant erythropoietins: a possible mass spectrometric marker for doping control. 2013 , 5, 877-89	11
1481	Human complement factor H is a reductase for large soluble von Willebrand factor multimersbrief report. 2013 , 33, 2524-8	31
1480	F-actin asymmetry and the endoplasmic reticulum-associated TCC-1 protein contribute to stereotypic spindle movements in the Caenorhabditis elegans embryo. 2013 , 24, 2201-15	13
1479	ClpS1 is a conserved substrate selector for the chloroplast Clp protease system in Arabidopsis. 2013 , 25, 2276-301	84
1478	Factor V activator from Daboia russelli russelli venom destabilizes 🛭 amyloid aggregate, the hallmark of Alzheimer disease. 2013 , 288, 30559-30570	14
1477	Defining the Escherichia coli SecA dimer interface residues through in vivo site-specific photo-cross-linking. 2013 , 195, 2817-25	16
1476	Glycoproteome of elongating cotton fiber cells. 2013 , 12, 3677-89	32
1475	The FTLD risk factor TMEM106B and MAP6 control dendritic trafficking of lysosomes. 2014 , 33, 450-67	92
1474	Histone biotinylation in Candida albicans. 2013 , 13, 529-39	9
1473	Comparison of detergent-based sample preparation workflows for LTQ-Orbitrap analysis of the Escherichia coli proteome. 2013 , 13, 2597-607	81
1472	Extensive proteomic remodeling is induced by eukaryotic translation elongation factor 1B deletion in Aspergillus fumigatus. 2013 , 22, 1612-22	8
1471	Global remodelling of cellular microenvironment due to loss of collagen VII. 2013 , 9, 657	71
1470	The C-terminal portion of the cleaved HT motif is necessary and sufficient to mediate export of proteins from the malaria parasite into its host cell. 2013 , 87, 835-50	31
1469	Proteolytic processing of osteopontin by PHEX and accumulation of osteopontin fragments in Hyp mouse bone, the murine model of X-linked hypophosphatemia. 2013 , 28, 688-99	89
1468	Enrichment specificity of micro and nano-sized titanium and zirconium dioxides particles in phosphopeptide mapping. 2013 , 48, 1188-98	9
1467	Kinetic enrichment of 34S during proteobacterial thiosulfate oxidation and the conserved role of SoxB in S-S bond breaking. 2013 , 79, 4455-64	22

1466	Posttranslational modifications in type I collagen from different tissues extracted from wild type and prolyl 3-hydroxylase 1 null mice. 2013 , 288, 24742-52	34
1465	Catalytic DNA with phosphatase activity. 2013 , 110, 5315-20	38
1464	Hsp70 and Hsp90 multichaperone complexes sequentially regulate thiazide-sensitive cotransporter endoplasmic reticulum-associated degradation and biogenesis. 2013 , 288, 13124-35	41
1463	Genome signature-based dissection of human gut metagenomes to extract subliminal viral sequences. 2013 , 4, 2420	60
1462	Protein phosphatase 4 is phosphorylated and inactivated by Cdk in response to spindle toxins and interacts with Eubulin. 2013 , 12, 2876-87	17
1461	Mutant p53 enhances MET trafficking and signalling to drive cell scattering and invasion. 2013 , 32, 1252-65	144
1460	JMJD1C demethylates MDC1 to regulate the RNF8 and BRCA1-mediated chromatin response to DNA breaks. 2013 , 20, 1425-33	73
1459	Comparative proteomics of two life cycle stages of stable isotope-labeled Trypanosoma brucei reveals novel components of the parasite's host adaptation machinery. 2013 , 12, 172-9	67
1458	ER stress potentiates insulin resistance through PERK-mediated FOXO phosphorylation. 2013, 27, 441-9	99
1457	Identification of CRM1-dependent Nuclear Export Cargos Using Quantitative Mass Spectrometry. 2013 , 12, 664-78	69
1456	Consistency of the proteome in primary human keratinocytes with respect to gender, age, and skin localization. 2013 , 12, 2509-21	29
1455	The nuclear cap-binding complex interacts with the U4/U6[U5 tri-snRNP and promotes spliceosome assembly in mammalian cells. 2013 , 19, 1054-63	42
1454	The heme a synthase Cox15 associates with cytochrome c oxidase assembly intermediates during Cox1 maturation. 2013 , 33, 4128-37	38
1453	Quantitative mass spectrometry-based proteomics in angiogenesis. 2013 , 7, 464-76	4
1452	A quantitative analysis of histone methylation and acetylation isoforms from their deuteroacetylated derivatives: application to a series of knockout mutants. 2013 , 48, 608-15	5
1451	Modified Clp protease complex in the ClpP3 null mutant and consequences for chloroplast development and function in Arabidopsis. 2013 , 162, 157-79	41
1450	Response of MC3T3-E1 osteoblasts, L929 fibroblasts, and J774 macrophages to fluoride surface-modified AZ31 magnesium alloy. 2013 , 101, 2753-62	29
1449	Comparative proteomic analysis of ductal breast carcinoma demonstrates an altered expression of chaperonins and cytoskeletal proteins. 2013 , 7, 1700-4	8

1448	Extracellular membrane vesicles from umbilical cord blood-derived MSC protect against ischemic acute kidney injury, a feature that is lost after inflammatory conditioning. 2013 , 2,	101
1447	Proteomic profiling and functional characterization of early and late shoulder osteoarthritis. 2013 , 15, R180	25
1446	14-3-3[mediates the cell fate decision-making pathways in response of hepatocellular carcinoma to Bleomycin-induced DNA damage. 2013 , 8, e55268	9
1445	Proteomic profiling of cereal aphid saliva reveals both ubiquitous and adaptive secreted proteins. 2013 , 8, e57413	73
1444	Cell cycle-regulated protein abundance changes in synchronously proliferating HeLa cells include regulation of pre-mRNA splicing proteins. 2013 , 8, e58456	11
1443	Ubiquitin-like protein from human placental extract exhibits collagenase activity. 2013 , 8, e59585	18
1442	Shotgun proteomic analysis on the diapause and non-diapause eggs of domesticated silkworm Bombyx mori. 2013 , 8, e60386	25
1441	Novel binding partners and differentially regulated phosphorylation sites clarify Eps8 as a multi-functional adaptor. 2013 , 8, e61513	10
1440	Osteoprotegerin in exosome-like vesicles from human cultured tubular cells and urine. 2013 , 8, e72387	40
1439	Immunoproteomic analysis of proteins expressed by two related pathogens, Burkholderia multivorans and Burkholderia cenocepacia, during human infection. 2013 , 8, e80796	24
1438	Structural determinants for protein adsorption/non-adsorption to silica surface. 2013, 8, e81346	78
1437	Molecular strategies of the Caenorhabditis elegans dauer larva to survive extreme desiccation. 2013 , 8, e82473	67
1436	Proteomic Workflows for Biomarker Identification Using Mass Spectrometry - Technical and Statistical Considerations during Initial Discovery. 2013 , 1, 109-127	15
1435	Biomarker discovery by plasma proteomics in familial Brugada Syndrome. 2013 , 18, 564-71	15
1434	Apocrine secretion in Drosophila salivary glands: subcellular origin, dynamics, and identification of secretory proteins. 2014 , 9, e94383	21
1433	Morphology and histochemistry of the aesthetasc-associated epidermal glands in terrestrial hermit crabs of the genus Coenobita (Decapoda: Paguroidea). 2014 , 9, e96430	15
1432	Purification and characterization of an extracellular, thermo-alkali-stable, metal tolerant laccase from Bacillus tequilensis SN4. 2014 , 9, e96951	98
1431	Oral vaccination with heat inactivated Mycobacterium bovis activates the complement system to protect against tuberculosis. 2014 , 9, e98048	41

1430	Physiological and proteomic analyses of Saccharum spp. grown under salt stress. 2014 , 9, e98463	30
1429	Proteomic changes of alveolar lining fluid in illnesses associated with exposure to inhaled non-infectious microbial particles. 2014 , 9, e102624	3
1428	In-cell intrabody selection from a diverse human library identifies C12orf4 protein as a new player in rodent mast cell degranulation. 2014 , 9, e104998	11
1427	Immunogenicity of intensively decellularized equine carotid arteries is conferred by the extracellular matrix protein collagen type VI. 2014 , 9, e105964	34
1426	A proteomic approach to investigating gene cluster expression and secondary metabolite functionality in Aspergillus fumigatus. 2014 , 9, e106942	30
1425	Computational and experimental analysis of the secretome of Methylococcus capsulatus (Bath). 2014 , 9, e114476	6
1424	Stubborn contaminants: influence of detergents on the purity of the multidrug ABC transporter BmrA. 2014 , 9, e114864	18
1423	Generation of a nanobody targeting the paraflagellar rod protein of trypanosomes. 2014 , 9, e115893	20
1422	Proteomic Identification of Nrf2-Mediated Phase II Enzymes Critical for Protection of Tao Hong Si Wu Decoction against Oxygen Glucose Deprivation Injury in PC12 Cells. 2014 , 2014, 945814	11
1421	SIRT1 deacetylates TopBP1 and modulates intra-S-phase checkpoint and DNA replication origin firing. 2014 , 10, 1193-202	33
1420	Caspase-3 and caspase-6 cleave STAT1 in leukemic cells. 2014 , 5, 2305-17	9
1419	C/EBP🛮 (CCAAT/enhancer-binding protein 🗓) mediates progesterone production through transcriptional regulation in co-operation with SF-1 (steroidogenic factor-1). 2014 , 460, 459-71	17
1418	Identification of importin ∄ specific transport cargoes using a proteomic screening approach. 2014 , 13, 1286-98	16
1417	Using SILAC proteomics to investigate the effect of the mycotoxin, alternariol, in the human H295R steroidogenesis model. 2014 , 30, 361-76	6
1416	Molecular cloning and in-silico characterization of high temperature stress responsive pAPX gene isolated from heat tolerant Indian wheat cv. Raj 3765. 2014 , 7, 713	12
1415	Analysis of root proteome unravels differential molecular responses during compatible and incompatible interaction between chickpea (Cicer arietinum L.) and Fusarium oxysporum f. sp. ciceri Race1 (Foc1). 2014 , 15, 949	32
1414	Class I major histocompatibility complex, the trojan horse for secretion of amyloidogenic [½-microglobulin. 2014 , 289, 3318-27	20
1413	Self-association of an insect I-1,3-glucan recognition protein upon binding laminarin stimulates prophenoloxidase activation as an innate immune response. 2014 , 289, 28399-410	24

1412	Processing of the l1 52/55k protein by the adenovirus protease: a new substrate and new insights into virion maturation. 2014 , 88, 1513-24	29
1411	Proteomic analysis implicates translationally controlled tumor protein as a novel mediator of occlusive vascular remodeling in pulmonary arterial hypertension. 2014 , 129, 2125-35	51
1410	Regulation of the Rhp26ERCC6/CSB chromatin remodeler by a novel conserved leucine latch motif. 2014 , 111, 18566-71	21
1409	SILAC-based proteomic quantification of chemoattractant-induced cytoskeleton dynamics on a second to minute timescale. 2014 , 5, 3319	15
1408	Detecting protein-protein interactions/complex components using mass spectrometry coupled techniques. 2014 , 1164, 1-13	9
1407	Proteomics of a fuzzy organelle: interphase chromatin. 2014 , 33, 648-64	41
1406	Phytoplasma effector SAP54 hijacks plant reproduction by degrading MADS-box proteins and promotes insect colonization in a RAD23-dependent manner. 2014 , 12, e1001835	122
1405	StableIsotope Labeling with Amino Acids in Cell Culture (SILAC)-based strategy for proteome-wide thermodynamic analysis of protein-ligand binding interactions. 2014 , 13, 1800-13	47
1404	Transcription-independent functions of an RNA polymerase II subunit, Rpb2, during genome rearrangement in the ciliate, Oxytricha trifallax. 2014 , 197, 839-49	17
1403	Identification of human tissue kallikrein 6 as a potential marker of laryngeal cancer based on the relevant secretory/releasing protein database. 2014 , 2014, 594093	9
1402	Isolation and structure characterization of an antioxidative glycopeptide from mycelial culture broth of a medicinal fungus. 2014 , 15, 17318-32	13
1401	Comprehensive cell-specific protein analysis in early and late pollen development from diploid microsporocytes to pollen tube growth. 2014 , 13, 295-310	44
1400	Plasma membrane localization is essential for Oryza sativa Pto-interacting protein 1a-mediated negative regulation of immune signaling in rice. 2014 , 166, 327-36	14
1399	Optimization of 2-dimensional gel electrophoresis for proteomic studies of solid tumor tissue samples. 2014 , 9, 626-32	6
1398	A partial proteome reference map of the wine lactic acid bacterium Oenococcus oeni ATCC BAA-1163. 2014 , 4, 130154	13
1397	Optimization and revision of the production process of the Necator americanus glutathione S-transferase 1 (Na-GST-1), the lead hookworm vaccine recombinant protein candidate. 2014 , 10, 1914-25	27
1396	Identification of candidate substrates for the Golgi Tul1 E3 ligase using quantitative diGly proteomics in yeast. 2014 , 13, 2871-82	25
1395	Changes in chemical components and cytotoxicity at different maturity stages of Pleurotus eryngii fruiting body. 2014 , 62, 12631-40	12

1394	Analytical utility of mass spectral binning in proteomic experiments by SPectral Immonium Ion Detection (SPIID). 2014 , 13, 1914-24	15
1393	Quantitative proteomics reveals differentially expressed proteins in murine preneoplastic intestine in a model of intestinal tumorigenesis induced by low dietary folate and MTHFR deficiency. 2014 , 14, 2558-65	8
1392	Evolutionary insights into premetazoan functions of the neuronal protein homer. 2014 , 31, 2342-55	37
1391	Phosphorylation of the kinase domain regulates autophosphorylation of myosin IIIA and its translocation in microvilli. 2014 , 53, 7835-45	6
1390	The changes of Proteome in MG-63 cells after induced by calcitonin gene-related peptide. 2014 , 453, 648-52	2
1389	Immunological behavior of in vitro digested egg-white lysozyme. 2014 , 58, 614-24	30
1388	Jack bean ⊕mannosidase: amino acid sequencing and N-glycosylation analysis of a valuable glycomics tool. 2014 , 24, 252-61	29
1387	Bone mineral density and expression of vitamin D receptor-dependent calcium uptake mechanisms in the proximal small intestine after bariatric surgery. 2014 , 101, 1566-75	19
1386	Mass spectrometry-based membrane proteomics in cancer biomarker discovery. 2014 , 14, 549-63	17
1385	Structure-kinetic relationship of carbapenem antibacterials permeating through E. coli OmpC porin. 2014 , 82, 2998-3012	22
1384	CDK5 is a major regulator of the tumor suppressor DLC1. 2014 , 207, 627-42	41
1383	The metabolic enzyme AdhE controls the virulence of Escherichia coli O157:H7. 2014 , 93, 199-211	40
1382	Identification and characterization of a basic thaumatin-like protein (TLP 2) as an allergen in sapodilla plum (Manilkara zapota). 2014 , 58, 894-902	4
1381	Posttranslational modifications of FERREDOXIN-NADP+ OXIDOREDUCTASE in Arabidopsis chloroplasts. 2014 , 166, 1764-76	24
1380	Esm1 modulates endothelial tip cell behavior and vascular permeability by enhancing VEGF bioavailability. 2014 , 115, 581-90	102
1379	Maf-dependent bacterial flagellin glycosylation occurs before chaperone binding and flagellar T3SS export. 2014 , 92, 258-72	26
1378	Immunoproteomics of processed beef proteins reveal novel galactose-⊞,3-galactose-containing allergens. 2014 , 69, 1308-15	50
1377	Proteomic approaches to sexual development mediated by antheridiogen in the fern Blechnum spicant L. 2014 , 14, 2061-71	13

1376	Integrated solid-phase extraction-capillary liquid chromatography (speLC) interfaced to ESI-MS/MS for fast characterization and quantification of protein and proteomes. 2014 , 13, 6169-75	18
1375	Proteome-wide search for PP2A substrates in fission yeast. 2014 , 14, 1367-80	6
1374	Analysis of differential expression patterns of mRNA and protein during cold-acclimation and de-acclimation in Arabidopsis. 2014 , 13, 3602-11	47
1373	Quantitative proteome analyses identify PrfA-responsive proteins and phosphoproteins in Listeria monocytogenes. 2014 , 13, 6046-57	21
1372	Mapping cell envelope and periplasm protein interactions of Escherichia coli respiratory formate dehydrogenases by chemical cross-linking and mass spectrometry. 2014 , 13, 5524-35	9
1371	Epidermal Cells. 2014 ,	
1370	Identification and characterization of a phage display-derived peptide for orthopoxvirus detection. 2014 , 406, 7611-21	10
1369	Recombinant filaggrin is internalized and processed to correct filaggrin deficiency. 2014 , 134, 423-429	36
1368	Structure of an unusual S-adenosylmethionine synthetase from Campylobacter jejuni. 2014 , 70, 442-50	4
1367	SILAC-pulse proteolysis: A mass spectrometry-based method for discovery and cross-validation in proteome-wide studies of ligand binding. 2014 , 25, 2073-83	31
1366	2-D and In Silico Analysis of Some Putative Drought-Induced Differential Boiling Soluble Proteins (hydrophilins) of Triticum aestivum. 2014 , 3, 386-394	
1365	TMEFF2 deregulation contributes to gastric carcinogenesis and indicates poor survival outcome. 2014 , 20, 4689-704	30
1364	ModM DNA methyltransferase methylome analysis reveals a potential role for Moraxella catarrhalis phasevarions in otitis media. 2014 , 28, 5197-207	60
1363	Carpal tunnel syndrome is associated with high fibrinogen and fibrinogen deposits. 2014 , 75, 276-85; discussion 285	1
1362	ESET methylates UBF at K232/254 and regulates nucleolar heterochromatin plasticity and rDNA transcription. 2014 , 42, 1628-43	19
1361	Exposure to mimivirus collagen promotes arthritis. 2014 , 88, 838-45	17
1360	Mitochondrial aldehyde dehydrogenase activation by Alda-1 inhibits atherosclerosis and attenuates hepatic steatosis in apolipoprotein E-knockout mice. 2014 , 3, e001329	38
1359	Proteomic Approach to the Reprogramming Machinery of the Mouse Oocyte. 2014 , 407-417	_

1358	Analysis of expressed genes of the bacterium 'Candidatus phytoplasma Mali' highlights key features of virulence and metabolism. 2014 , 9, e94391	23
1357	E-cadherin interactome complexity and robustness resolved by quantitative proteomics. 2014 , 7, rs7	114
1356	A comparative quantitative proteomic study identifies new proteins relevant for sulfur oxidation in the purple sulfur bacterium Allochromatium vinosum. 2014 , 80, 2279-92	32
1355	Protein expression, characterization, crystallization and preliminary X-ray crystallographic analysis of a Fic protein from Clostridium difficile. 2014 , 70, 827-31	4
1354	Proteomic and functional consequences of hexokinase deficiency in glucose-repressible Kluyveromyces lactis. 2014 , 13, 860-75	8
1353	Performance comparisons of nano-LC systems, electrospray sources and LC-MS-MS platforms. 2014 , 52, 120-7	13
1352	Proteome-wide identification of SUMO2 modification sites. 2014 , 7, rs2	142
1351	The Tudor domain of the PHD finger protein 1 is a dual reader of lysine trimethylation at lysine 36 of histone H3 and lysine 27 of histone variant H3t. 2014 , 426, 1651-60	17
1350	A unique insertion of low complexity amino acid sequence underlies protein-protein interaction in human malaria parasite orotate phosphoribosyltransferase and orotidine 5'-monophosphate decarboxylase. 2014 , 7, 184-92	6
1349	Reciprocal interacting effects of proteins and lipids during ex´vivo digestion of bovine milk. 2014 , 36, 6-13	20
1348	Proteomics identifies the composition and manufacturing recipe of the 2500-year old sourdough bread from Subeixi cemetery in China. 2014 , 105, 363-71	45
1347	Proteomic analysis of rat proximal tubule cells following stretch-induced apoptosis in an in vitro model of kidney obstruction. 2014 , 100, 125-35	8
1346	Substrate specificity analysis and novel substrates of the protein lysine methyltransferase NSD1. 2014 , 21, 226-37	41
1345	LC-MS/MS characterization of combined glycogenin-1 and glycogenin-2 enzymatic activities reveals their self-glucosylation preferences. 2014 , 1844, 398-405	10
1344	Advances in Computational Biology. 2014 ,	
1343	Recombinant expression of hydroxylated human collagen in Escherichia coli. 2014 , 98, 4445-55	41
1342	Dengue. 2014 ,	5
1341	Immobilization of trypsin onto multifunctional meso-/macroporous core-shell microspheres: a new platform for rapid enzymatic digestion. 2014 , 812, 65-73	25

1340	Interleukin-1-induced changes in the glioblastoma secretome suggest its role in tumor progression. 2014 , 99, 152-168	40
1339	Proteomic analysis of mycelium and secretome of different Botrytis cinerea wild-type strains. 2014 , 97, 195-221	59
1338	A systems-wide comparison of red rice (Oryza longistaminata) tissues identifies rhizome specific genes and proteins that are targets for cultivated rice improvement. 2014 , 14, 46	28
1337	[The influence of recombinant nucleophosmin 1 on artificial RNA internalization into human adenocarcinoma MCF-7 cells]. 2014 , 40, 55-63	
1336	Novel regulatory roles of omega-3 fatty acids in metabolic pathways: a proteomics approach. 2014 , 11, 6	25
1335	Comparative analysis of secretomes in basidiomycete fungi. 2014 , 102, 28-43	68
1334	Secretome profiling reveals the signaling molecules of apoptotic HCT116 cells induced by the dietary polyacetylene gymnasterkoreayne B. 2014 , 62, 2353-63	6
1333	Nascent chromatin capture proteomics determines chromatin dynamics during DNA replication and identifies unknown fork components. 2014 , 16, 281-93	225
1332	Proteomics evidence for kefir dairy in Early Bronze Age China. 2014 , 45, 178-186	92
1331	Proteomic characterization of seeds from yellow lupin (Lupinus luteus L.). 2014 , 14, 1543-6	16
1330	The membrane complexome of a new Pseudomonas strain during growth on lysogeny broth medium and medium containing glucose or phenol. 2014 , 4, 1-9	5
1329	Dendrimer-grafted graphene oxide nanosheets as novel support for trypsin immobilization to achieve fast on-plate digestion of proteins. 2014 , 122, 278-84	37
1328	Lysine biotinylation and methionine oxidation in the heat shock protein HSP60 synergize in the elimination of reactive oxygen species in human cell cultures. 2014 , 25, 475-82	11
1327	Quantitative proteomics identifies NCOA4 as the cargo receptor mediating ferritinophagy. 2014 , 509, 105-9	684
1326	The FLS2-associated kinase BIK1 directly phosphorylates the NADPH oxidase RbohD to control plant immunity. 2014 , 15, 329-38	424
1325	Shotgun Proteomics. 2014 ,	5
1324	House dust mite (Der p 10) and crustacean allergic patients may react to food containing Yellow mealworm proteins. 2014 , 65, 364-73	93
1323	Purification, characterization and partial sequence of a pro-inflammatory lectin from seeds of Canavalia oxyphylla Standl. & L. O. Williams. 2014 , 27, 117-23	12

1322	Complete posttranslational modification mapping of pathogenic Neisseria meningitidis pilins requires top-down mass spectrometry. 2014 , 14, 1141-51	23
1321	Spider genomes provide insight into composition and evolution of venom and silk. 2014 , 5, 3765	169
1320	Deletion of 30 murine cytochrome p450 genes results in viable mice with compromised drug metabolism. 2014 , 42, 1022-30	21
1319	Assaying microtubule nucleation by the Eubulin ring complex. 2014 , 540, 119-30	4
1318	CCL28 involvement in mucosal tissues protection as a chemokine and as an antibacterial peptide. 2014 , 44, 286-90	22
1317	Notch signaling regulates the phosphorylation of Akt and survival of lipopolysaccharide-activated macrophages via regulator of G protein signaling 19 (RGS19). 2014 , 219, 653-60	22
1316	A draft map of the human proteome. 2014 , 509, 575-81	1520
1315	Cysteine-rich positions outside the structural zinc motif of human papillomavirus E7 provide conformational modulation and suggest functional redox roles. 2014 , 53, 1680-96	17
1314	Proteomic analysis and polyamines, ethylene and reactive oxygen species levels of Araucaria angustifolia (Brazilian pine) embryogenic cultures with different embryogenic potential. 2014 , 34, 94-104	46
1313	Fermentation and proteome profiles of Lactobacillus plantarum strains during growth under food-like conditions. 2014 , 96, 366-80	63
1312	Quantitative proteomic dissection of a native 14-3-3[Interacting protein complex associated with hepatocellular carcinoma. 2014 , 46, 841-52	4
1311	Heteronemin, a marine sponge terpenoid, targets TDP-43, a key factor in several neurodegenerative disorders. 2014 , 50, 406-8	17
1310	Citrullination regulates pluripotency and histone H1 binding to chromatin. 2014 , 507, 104-8	264
1309	Bacteriophages use an expanded genetic code on evolutionary paths to higher fitness. 2014 , 10, 178-80	39
1308	HGA-2, a novel galactoside-binding lectin from the sea cucumber Holothuria grisea binds to bacterial cells. 2014 , 64, 435-42	14
1307	Mycobacterium tuberculosis DinG is a structure-specific helicase that unwinds G4 DNA: implications for targeting G4 DNA as a novel therapeutic approach. 2014 , 289, 25112-36	35
1306	Identification of a mosquitocidal toxin from Bacillus thuringiensis using mass spectrometry. 2014 , 30, 3273-7	6
1305	Resolubilization of precipitated intact membrane proteins with cold formic acid for analysis by mass spectrometry. 2014 , 13, 6001-12	35

1304	Functional mapping of the zebrafish early embryo proteome and transcriptome. 2014 , 13, 5536-50	23
1303	Broad-range glycosidase activity profiling. 2014 , 13, 2787-800	40
1302	Partner manipulation stabilises a horizontally transmitted mutualism. 2014 , 17, 185-92	29
1301	Reliable identification of cross-linked products in protein interaction studies by 13C-labeled p-benzoylphenylalanine. 2014 , 25, 1628-41	11
1300	Identification of isoform-specific dynamics in phosphorylation-dependent STAT5 dimerization by quantitative mass spectrometry and mathematical modeling. 2014 , 13, 5685-94	22
1299	Molecular cloning of two novel peroxidases and their response to salt stress and salicylic acid in the living fossil Ginkgo biloba. 2014 , 114, 923-36	12
1298	N-Formyl-7-amino-11-cycloamphilectene, a marine sponge metabolite, binds to tubulin and modulates microtubule depolymerization. 2014 , 10, 862-7	1
1297	In cell scalaradial interactome profiling using a bio-orthogonal clickable probe. 2014 , 50, 6043-5	13
1296	Growth arrest by the antitumor steroidal lactone withaferin A in human breast cancer cells is associated with down-regulation and covalent binding at cysteine 303 of □tubulin. 2014 , 289, 1852-65	81
1295	KAISO, a critical regulator of p53-mediated transcription of CDKN1A and apoptotic genes. 2014 , 111, 15078-83	41
1294	Protein interaction screening for the ankyrin repeats and suppressor of cytokine signaling (SOCS) box (ASB) family identify Asb11 as a novel endoplasmic reticulum resident ubiquitin ligase. 2014 , 289, 2043-54	30
1293	Fractionation profiling: a fast and versatile approach for mapping vesicle proteomes and protein-protein interactions. 2014 , 25, 3178-94	35
1292	Cleavage of E-cadherin and I-catenin by calpain affects Wnt signaling and spheroid formation in suspension cultures of human pluripotent stem cells. 2014 , 13, 990-1007	41
1291	Proteomic analysis of human tooth pulp: proteomics of human tooth. 2014 , 40, 1961-6	27
1290	A proteomic approach to Physcomitrella patens rhizoid exudates. 2014 , 171, 1671-8	9
1289	Exocytosis and Endocytosis. 2014 ,	
1288	Systematic nucleo-cytoplasmic trafficking of proteins following exposure of MCF7 breast cancer cells to estradiol. 2014 , 13, 1112-27	15
1287	Screening of missing proteins in the human liver proteome by improved MRM-approach-based targeted proteomics. 2014 , 13, 1969-78	22

1286	Newborn mouse lens proteome and its alteration by lysine 6 mutant ubiquitin. 2014 , 13, 1177-89	11
1285	Assessment of berberine as a multi-target antimicrobial: a multi-omics study for drug discovery and repositioning. 2014 , 18, 42-53	39
1284	Transglutaminase 2-dependent deamidation of glyceraldehyde-3-phosphate dehydrogenase promotes trophoblastic cell fusion. 2014 , 289, 4989-99	11
1283	Diversity within the O-linked protein glycosylation systems of acinetobacter species. 2014 , 13, 2354-70	44
1282	2DE-based approach for estimation of number of protein species in a cell. 2014 , 35, 895-900	14
1281	Ubiquitinated proteins in exosomes secreted by myeloid-derived suppressor cells. 2014 , 13, 5965-72	33
1280	A trans-outer membrane porin-cytochrome protein complex for extracellular electron transfer by Geobacter sulfurreducens PCA. 2014 , 6, 776-85	130
1279	Optimization of ultrasound-assisted extraction of protein from egg white using response surface methodology (RSM) and its proteomic study by MALDI-TOF-MS. 2014 , 4, 42608-42616	9
1278	Decreasing the amount of trypsin in in-gel digestion leads to diminished chemical noise and improved protein identifications. 2014 , 109, 16-25	38
1277	Biochemical and proteomic characterisation of haemolymph serum reveals the origin of the alkali-labile phosphate (ALP) in mussel (Mytilus galloprovincialis). 2014 , 11, 29-36	17
1276	Enzymatic protein digestion using a dissolvable polyacrylamide gel and its application to mass spectrometry-based proteomics. 2014 , 967, 36-40	9
1275	In-gel microwave-assisted acid hydrolysis of proteins combined with liquid chromatography tandem mass spectrometry for mapping protein sequences. 2014 , 86, 600-7	5
1274	Profiling of drug binding proteins by monolithic affinity chromatography in combination with liquid chromatography-tandem mass spectrometry. 2014 , 1359, 84-90	5
1273	Metaproteomics: Evaluation of protein extraction from activated sludge. 2014 , 14, 2535-9	38
1272	Interaction of Ddc1 and RPA with single-stranded/double-stranded DNA junctions in yeast whole cell extracts: Proteolytic degradation of the large subunit of replication protein A in ddc1l3trains. 2014 , 22, 30-40	3
1271	Proteomic response of mussels Mytilus galloprovincialis exposed to CuO NPs and Cu[]+: an exploratory biomarker discovery. 2014 , 155, 327-36	61
1270	Proteomic characterization of human coronary thrombus in patients with ST-segment elevation acute myocardial infarction. 2014 , 109, 368-81	18
1269	Stable Isotope Labeling by Amino Acids in Cell Culture (SILAC). 2014 ,	1

1268	The genomes, proteomes, and structures of three novel phages that infect the Bacillus cereus group and carry putative virulence factors. 2014 , 88, 11846-60	28
1267	Translation from a DMD exon 5 IRES results in a functional dystrophin isoform that attenuates dystrophinopathy in humans and mice. 2014 , 20, 992-1000	72
1266	S/T phosphorylation of DLL1 is required for full ligand activity in vitro but dispensable for DLL1 function in vivo during embryonic patterning and marginal zone B cell development. 2014 , 34, 1221-33	6
1265	Nicotinamidase/pyrazinamidase of Mycobacterium tuberculosis forms homo-dimers stabilized by disulfide bonds. 2014 , 94, 644-8	2
1264	Identification of a misfolded region in superoxide dismutase 1 that is exposed in amyotrophic lateral sclerosis. 2014 , 289, 28527-38	20
1263	Cryoconservation of peptide extracts from trypsin digestion of proteins for proteomic analysis in a hospital biobank facility. 2014 , 13, 1930-7	5
1262	Invasion of Solanum tuberosum L. by Aspergillus terreus: a microscopic and proteomics insight on pathogenicity. 2014 , 7, 350	19
1261	Profiling of human acquired immunity against the salivary proteins of Phlebotomus papatasi reveals clusters of differential immunoreactivity. 2014 , 90, 923-938	9
1260	Purification and characterization of three I-glycosidases exhibiting high glucose tolerance from Aspergillus niger ASKU28. 2014 , 78, 1167-76	11
1259	The architecture of a scrambled genome reveals massive levels of genomic rearrangement during development. 2014 , 158, 1187-1198	120
1258	Assessment of MS/MS search algorithms with parent-protein profiling. 2014 , 13, 1823-32	2
1257	Deciphering the proteomic signature of human endometrial receptivity. 2014 , 29, 1957-67	37
1256	Characterization of phosphorylation- and RNA-dependent UPF1 interactors by quantitative proteomics. 2014 , 13, 3038-53	20
1255	Assessment of in vivo antimicrobial activity of the carbene silver(I) acetate derivative SBC3 using Galleria mellonella larvae. 2014 , 27, 745-52	41
1254	Influence of p-cresol on the proteome of the autotrophic nitrifying bacterium Nitrosomonas eutropha C91. 2014 , 196, 497-511	12
1253	Phosphoketolases from Lactococcus lactis, Leuconostoc mesenteroides and Pseudomonas aeruginosa: dissimilar sequences, similar substrates but distinct enzymatic characteristics. 2014 , 98, 7855-67	7
1252	Proteomic analysis of salt stress and recovery in leaves of Vigna unguiculata cultivars differing in salt tolerance. 2014 , 33, 1289-306	30
1251	Proteomic Identification of a Candidate Sequence of Wheat Cytokinin-Binding Protein 1. 2014 , 33, 896-902	6

1250	From Amino Acids Profile to Protein Identification: Searching for Differences in Roe Deer Papilloma. 2014 , 77, 609-617	1
1249	Recognition of riboflavin and the capsular polysaccharide of Haemophilus influenzae type b by antibodies generated to the haptenic epitope D-ribitol. 2014 , 31, 247-58	3
1248	Nonvirus encoded proteins could be embedded into Bombyx mori cypovirus polyhedra. 2014 , 41, 2657-66	4
1247	Transcriptomics assisted proteomic analysis of Nicotiana occidentalis infected by Candidatus Phytoplasma mali strain AT. 2014 , 14, 1882-9	34
1246	Thermal and physical stresses induce a short-term immune priming effect in Galleria mellonella larvae. 2014 , 63, 21-6	35
1245	Vasorelaxant activity of Canavalia grandiflora seed lectin: A structural analysis. 2014 , 543, 31-9	15
1244	Quantification of cellular protein expression and molecular features of group 3 LEA proteins from embryos of Artemia franciscana. 2014 , 19, 329-41	25
1243	Dual inhibition of EGFR at protein and activity level via combinatorial blocking of PI4KII\hatas anti-tumor strategy. 2014 , 5, 457-68	13
1242	7B7: a novel antibody directed against the Ku70/Ku80 heterodimer blocks invasion in pancreatic and lung cancer cells. 2014 , 35, 6983-97	10
1241	Secretome weaponries of Cochliobolus lunatus interacting with potato leaf at different temperature regimes reveal a CL[xxxx]LHM - motif. 2014 , 15, 213	12
1240	The conserved upstream region of lscB/C determines expression of different levansucrase genes in plant pathogen Pseudomonas syringae. 2014 , 14, 79	8
1239	Proteomic analysis of post-nuclear supernatant fraction and percoll-purified membranes prepared from brain cortex of rats exposed to increasing doses of morphine. 2014 , 12, 11	14
1238	Proteomic response of Trichoderma aggressivum f. europaeum to Agaricus bisporus tissue and mushroom compost. 2014 , 118, 785-91	10
1237	Chromatin enrichment for proteomics. <i>Nature Protocols</i> , 2014 , 9, 2090-9	53
1236	Characterization of glycoproteins in pancreatic cyst fluid using a high-performance multiple lectin affinity chromatography platform. 2014 , 13, 289-99	24
1235	Metaproteomic analysis of a winter to spring succession in coastal northwest Atlantic Ocean microbial plankton. 2014 , 8, 1301-13	50
1234	StUbEx: Stable tagged ubiquitin exchange system for the global investigation of cellular ubiquitination. 2014 , 13, 4192-204	14
1233	"Out-gel" tryptic digestion procedure for chemical cross-linking studies with mass spectrometric detection. 2014 , 13, 527-35	6

1232	Optimization of a phenol extraction-based protein preparation method amenable to downstream 2DE and MALDI-MS based analysis of bacterial proteomes. 2014 , 14, 216-21	4
1231	A targeted in vivo SILAC approach for quantification of drug metabolism enzymes: regulation by the constitutive androstane receptor. 2014 , 13, 866-74	7
1230	Nuclear cytoplasmic trafficking of proteins is a major response of human fibroblasts to oxidative stress. 2014 , 13, 4398-423	11
1229	Characterization of lacrimal proline-rich protein 4 (PRR4) in human tear proteome. 2014 , 14, 1698-709	23
1228	Unexpected roles for ancient proteins: flavone 8-hydroxylase in sweet basil trichomes is a Rieske-type, PAO-family oxygenase. 2014 , 80, 385-95	23
1227	Carbonic anhydrases, EPF2 and a novel protease mediate CO2 control of stomatal development. 2014 , 513, 246-50	133
1226	Specific visualization and identification of phosphoproteome in gels. 2014 , 86, 6741-7	6
1225	David and Goliath: potent venom of an ant-eating spider (Araneae) enables capture of a giant prey. 2014 , 101, 533-40	34
1224	Binding of OTULIN to the PUB domain of HOIP controls NF-B signaling. 2014, 54, 349-61	121
1223	A recombinant subtilisin with keratinolytic and fibrin(ogen)olytic activity. 2014, 49, 948-954	3
1222	Comparative proteomics unveils cross species variations in Anabaena under salt stress. 2014 , 98, 254-70	68
1221	The two major isoforms of thyroid hormone receptor, TR# and TRI1, preferentially partner with distinct panels of auxiliary proteins. 2014 , 383, 80-95	5
1220	ERK-mediated phosphorylation of TFAM downregulates mitochondrial transcription: implications for Parkinson's disease. 2014 , 17, 132-40	43
1219	Heat shock and structural proteins associated with meat tenderness in Nellore beef cattle, a Bos indicus breed. 2014 , 96, 1318-24	63
1218	Comparative proteomic study in serum of patients with primary open-angle glaucoma and pseudoexfoliation glaucoma. 2014 , 98, 65-78	31
1217	Comparative proteomics for the characterization of the most relevant Amblyomma tick species as vectors of zoonotic pathogens worldwide. 2014 , 105, 204-16	15
1216	Integrated metabolomic and proteomic approaches dissect the effect of metal-resistant bacteria on maize biomass and copper uptake. 2014 , 48, 1184-93	56
1215	Structural characterization of a plant photosystem I and NAD(P)H dehydrogenase supercomplex. 2014 , 77, 568-76	62

1214	Extensive post-translational modification of active and inactivated forms of endogenous p53. 2014 , 13, 1-17	43
1213	Ubiquitin profiling in liver using a transgenic mouse with biotinylated ubiquitin. 2014 , 13, 3016-26	22
1212	Leishmania donovani eukaryotic initiation factor 5A: molecular characterization, localization and homology modelling studies. 2014 , 73, 37-46	3
1211	Transcription Factor Regulatory Networks. 2014 ,	
121 0	Pyruvate formate-lyase interacts directly with the formate channel FocA to regulate formate translocation. 2014 , 426, 2827-39	27
1209	N-glycan analysis of mannose/glucose specific lectin from Dolichos lablab seeds. 2014 , 69, 400-7	8
1208	Profiling lysine ubiquitination by selective enrichment of ubiquitin remnant-containing peptides. 2014 , 1174, 57-71	7
1207	Phosphorylation of multifunctional galectins by protein kinases CK1, CK2, and PKA. 2014 , 449, 109-17	1
1206	Mass spectrometry-based proteomics in Chest Medicine, Gerontology, and Nephrology: subgroups omics for personalized medicine. 2014 , 4, 25	11
1205	Quantitative phosphoproteomics unveils temporal dynamics of thrombin signaling in human endothelial cells. 2014 , 123, e22-36	27
1204	A repository of assays to quantify 10,000 human proteins by SWATH-MS. 2014 , 1, 140031	266
1203	The ChroP approach combines ChIP and mass spectrometry to dissect locus-specific proteomic landscapes of chromatin. 2014 ,	18
1202	A new approach for the comparative analysis of multiprotein complexes based on 15N metabolic labeling and quantitative mass spectrometry. 2014 ,	2
1201	Similarities in lindane induced alterations in protein expression profiling in different brain regions with neurodegenerative diseases. 2015 , 15, 3875-82	3
1200	Hepatic proteomic analysis revealed altered metabolic pathways in insulin resistant Akt1(+/-)/Akt2(-/-) mice. 2015 , 64, 1694-703	8
1199	Metaproteomics and metabolomics analyses of chronically petroleum-polluted sites reveal the importance of general anaerobic processes uncoupled with degradation. 2015 , 15, 3508-20	42
1198	Identification of novel microtubule-binding proteins by taxol-mediated microtubule stabilization and mass spectrometry analysis. 2015 , 6, 649-54	12
1197	Digestion, Purification, and Enrichment of Protein Samples for Mass Spectrometry. 2015 , 7, 201-222	10

1196	Experimental estimation of proteome size for cells and human plasma. 2015, 9, 305-311	1
1195	New HDAC6-mediated deacetylation sites of tubulin in the mouse brain identified by quantitative mass spectrometry. 2015 , 5, 16869	22
1194	Development of 'Redox Arrays' for identifying novel glutathionylated proteins in the secretome. 2015 , 5, 14630	13
1193	Functional and structural properties of a novel cellulosome-like multienzyme complex: efficient glycoside hydrolysis of water-insoluble 7-xylosyl-10-deacetylpaclitaxel. 2015 , 5, 13768	20
1192	Losartan ameliorates dystrophic epidermolysis bullosa and uncovers new disease mechanisms. 2015 , 7, 1211-28	102
1191	Expression of SERPINA3s in cattle: focus on bovSERPINA3-7 reveals specific involvement in skeletal muscle. 2015 , 5, 150071	13
1190	An Aquatic Microbial Metaproteomics Workflow: From Cells to Tryptic Peptides Suitable for Tandem Mass Spectrometry-based Analysis. 2015 ,	2
1189	Preoperative protein profiles in cerebrospinal fluid in elderly hip fracture patients at risk for delirium: A proteomics and validation study. 2015 , 4, 115-22	13
1188	High Concentration Trypsin Assisted Fast In-Gel Digestion for Phosphoproteome Analysis. 2015 , 43, 1452-145	582
1187	Deciphering the mode of action of a mutant Allium sativum Leaf Agglutinin (mASAL), a potent antifungal protein on Rhizoctonia solani. 2015 , 15, 237	14
1186	Characterization of human reflex tear proteome reveals high expression of lacrimal proline-rich protein 4 (PRR4). 2015 , 15, 3370-81	34
1185	Mass spectrometry-based analyses showing the effects of secretor and blood group status on salivary N-glycosylation. 2015 , 12, 29	9
1184	Generation of aroE overexpression mutant of Bacillus megaterium for the production of shikimic acid. 2015 , 14, 69	12
1183	Proteomic analysis of quail calcified eggshell matrix: a comparison to chicken and turkey eggshell proteomes. 2015 , 13, 22	20
1182	Hepatocytes respond differently to major dietary trans fatty acid isomers, elaidic acid and trans-vaccenic acid. 2015 , 13, 31	15
1181	Ixodes scapularis and Ixodes ricinus tick cell lines respond to infection with tick-borne encephalitis virus: transcriptomic and proteomic analysis. 2015 , 8, 599	48
1180	Amblyomma americanum tick saliva insulin-like growth factor binding protein-related protein 1 binds insulin but not insulin-like growth factors. 2015 , 24, 539-50	10
1179	Unveiling the optimal parameters for cellulolytic characteristics of Talaromyces verruculosus SGMNPf3 and its secretory enzymes. 2015 , 119, 88-98	6

1178	Muscle-Specific Variation in Buffalo (Bubalus bubalis) Meat Texture: Biochemical, Ultrastructural and Proteome Characterization. 2015 , 46, 254-261	8
1177	Growth condition-dependent cell surface proteome analysis of Enterococcus faecium. 2015 , 15, 3806-14	2
1176	Red blood cell storage affects the stability of cytosolic native protein complexes. 2015 , 55, 1927-36	20
1175	Enrichment of protein N-termini by charge reversal of internal peptides. 2015 , 15, 2470-8	21
1174	Yeast proteins Gar1p, Nop1p, Npl3p, Nsr1p, and Rps2p are natively methylated and are substrates of the arginine methyltransferase Hmt1p. 2015 , 15, 3209-18	27
1173	Colonic metaproteomic signatures of active bacteria and the host in obesity. 2015 , 15, 3544-52	56
1172	Protein disulfide isomerase as a novel target for cyclopentenone prostaglandins: implications for hypoxic ischemic injury. 2015 , 282, 2045-59	13
1171	In Cell Interactome of Oleocanthal, an Extra Virgin Olive Oil Bioactive Component. 2015 , 10, 1934578X150100)Q ₁
1170	Myeloma cells can corrupt senescent mesenchymal stromal cells and impair their anti-tumor activity. 2015 , 6, 39482-92	24
1169	Proteomic Characterisation of Two Strains of Mycoplasma mycoides Subsp. Mycoides of Differing Pathogenicity. 2015 , s13,	
1168	Terminal Mannose Residues in Seminal Plasma Glycoproteins of Infertile Men Compared to Fertile Donors. 2015 , 16, 14933-50	6
1167	Eucalyptus urograndis stem proteome is responsive to short-term cold stress. 2015 , 38, 191-8	13
1166	A deep proteomics perspective on CRM1-mediated nuclear export and nucleocytoplasmic partitioning. 2015 , 4,	125
1165	Honey Bee Infecting Lake Sinai Viruses. 2015 , 7, 3285-309	52
1164	Affinity proteomics to study endogenous protein complexes: pointers, pitfalls, preferences and perspectives. 2015 , 58, 103-19	39
1163	Molecular Mechanism Underlying the Entomotoxic Effect of Colocasia esculenta Tuber Agglutinin against Dysdercus cingulatus. 2015 , 6, 827-846	6
1162	Inflammatory Gene Expression Upon TGF-[]1-Induced p38 Activation in Primary Dupuytren's Disease Fibroblasts. 2015 , 2, 68	7
1161	Interrogation of the Substrate Profile and Catalytic Properties of the Phosphotriesterase from Sphingobium sp. Strain TCM1: An Enzyme Capable of Hydrolyzing Organophosphate Flame Retardants and Plasticizers. 2015 , 54, 7539-49	25

1160	Insights on predominant edible bamboo shoot proteins. 2015 , 14, 1511-1518	7
1159	The elicitin-like glycoprotein, ELI025, is secreted by the pathogenic oomycete Pythium insidiosum and evades host antibody responses. 2015 , 10, e0118547	17
1158	Mo-CBP3, an antifungal chitin-binding protein from Moringa oleifera seeds, is a member of the 2S albumin family. 2015 , 10, e0119871	38
1157	Comprehensive analysis of temporal alterations in cellular proteome of Bacillus subtilis under curcumin treatment. 2015 , 10, e0120620	1
1156	Proteomic Investigation of the Response of Enterococcus faecalis V583 when Cultivated in Urine. 2015 , 10, e0126694	18
1155	Transfer RNAs Mediate the Rapid Adaptation of Escherichia coli to Oxidative Stress. 2015 , 11, e1005302	66
1154	Altered Protein Expression in the Ileum of Mice Associated with the Development of Chronic Infections with Echinostoma caproni (Trematoda). 2015 , 9, e0004082	10
1153	Poly (A) Binding Protein Cytoplasmic 1 Is a Novel Co-Regulator of the Androgen Receptor. 2015 , 10, e012849	5 11
1152	Citrus tristeza virus (CTV) Causing Proteomic and Enzymatic Changes in Sweet Orange Variety "Westin". 2015 , 10, e0130950	17
1151	Prospection and Evaluation of (Hemi) Cellulolytic Enzymes Using Untreated and Pretreated Biomasses in Two Argentinean Native Termites. 2015 , 10, e0136573	18
1150	Proteomic Analysis of the Ubiquitin Landscape in the Drosophila Embryonic Nervous System and the Adult Photoreceptor Cells. 2015 , 10, e0139083	21
1149	A Metabolic Probe-Enabled Strategy Reveals Uptake and Protein Targets of Polyunsaturated Aldehydes in the Diatom Phaeodactylum tricornutum. 2015 , 10, e0140927	2
1148	Sperm Proteome Maturation in the Mouse Epididymis. 2015 , 10, e0140650	63
1147	Identification of B6T173 (ZmPrx35) as the prevailing peroxidase in highly insect-resistant maize (Zea mays, p84C3) kernels by activity-directed purification. 2015 , 6, 670	7
1146	Identification of a Novel 2S Albumin with Antitryptic Activity from Caryocar brasiliense Seeds. 2015 , 7,	1
1145	Proteome Analysis for Understanding Abiotic Stress (Salinity and Drought) Tolerance in Date Palm (Phoenix dactylifera L.). 2015 , 2015, 407165	26
1144	Tau stabilizes microtubules by binding at the interface between tubulin heterodimers. 2015 , 112, 7501-6	270
1143	Subunit Interactions within the Carbon-Phosphorus Lyase Complex from Escherichia coli. 2015 , 54, 3400-11	8

1142	Prmt5 is a regulator of muscle stem cell expansion in adult mice. 2015 , 6, 7140	71
1141	Helicobacter pylori vesicles carrying CagA localize in the vicinity of cell-cell contacts and induce histone H1 binding to ATP in epithelial cells. 2015 , 362,	23
1140	Acinetobacter strains carry two functional oligosaccharyltransferases, one devoted exclusively to type IV pilin, and the other one dedicated to O-glycosylation of multiple proteins. 2015 , 96, 1023-41	59
1139	The herpes simplex virus 1 UL51 protein interacts with the UL7 protein and plays a role in its recruitment into the virion. 2015 , 89, 3112-22	27
1138	Site-specific methylation of Notch1 controls the amplitude and duration of the Notch1 response. 2015 , 8, ra30	44
1137	Mitotic Control of Planar Cell Polarity by Polo-like Kinase 1. 2015 , 33, 522-34	32
1136	Infiltration of chitin by protein coacervates defines the squid beak mechanical gradient. 2015 , 11, 488-95	98
1135	Evidence for Two Distinct Binding Sites for Lipoprotein Lipase on Glycosylphosphatidylinositol-anchored High Density Lipoprotein-binding Protein 1 (GPIHBP1). 2015 , 290, 13919-34	15
1134	Profiling of urinary proteins in Karan Fries cows reveals more than 1550 proteins. 2015 , 127, 193-201	24
1133	Acute-phase protein behavior in dairy cattle herd naturally infected with Trypanosoma vivax. 2015 , 211, 141-5	6
1132	Determination of the Mercury Fraction Linked to Protein of Muscle and Liver Tissue of Tucunar (Cichla spp.) from the Amazon Region of Brazil. 2015 , 69, 422-30	18
1131	A Metalloproteomics Study on the Association of Mercury With Breast Milk in Samples From Lactating Women in the Amazon Region of Brazil. 2015 , 69, 223-9	16
1130	Vertebrate Hedgehog is secreted on two types of extracellular vesicles with different signaling properties. 2014 , 4, 7357	78
1129	The central nervous system transcriptome of the weakly electric brown ghost knifefish (Apteronotus leptorhynchus): de novo assembly, annotation, and proteomics validation. 2015 , 16, 166	14
1128	Dynamic digestive physiology of a female reproductive organ in a polyandrous butterfly. 2015 , 218, 1548-55	17
1127	Genetic encoding of the post-translational modification 2-hydroxyisobutyryl-lysine. 2015 , 13, 6479-81	12
1126	Isolation and Purification of Recombinant Serine/Threonine Protein Kinases of the Strain Bifidobacterium longum B379M and Investigation of Their Activity. 2015 , 80, 1303-11	4
1125	UPF0586 Protein C9orf41 Homolog Is Anserine-producing Methyltransferase. 2015 , 290, 17190-205	20

1124	The Drosophila Helicase Maleless (MLE) is Implicated in Functions Distinct From its Role in Dosage Compensation. 2015 , 14, 1478-88	12
1123	Proteomic analysis of the probiotic Lactobacillus reuteri CRL1098 reveals novel tolerance biomarkers to bile acid-induced stress. 2015 , 77, 599-607	19
1122	Novel Route for Agmatine Catabolism in Aspergillus niger Involves 4-Guanidinobutyrase. 2015 , 81, 5593-603	11
1121	The point mutation UCH-L1 C152A protects primary neurons against cyclopentenone prostaglandin-induced cytotoxicity: implications for post-ischemic neuronal injury. 2015 , 6, e1966	18
112 0	Purification and characterization of a cytochrome c with novel caspase-3 activation activity from the pathogenic fungus Rhizopus arrhizus. 2015 , 16, 21	5
1119	Identification of RNF168 as a PML nuclear body regulator. 2016 , 129, 580-91	12
1118	Delineating the glycoproteome of elongating cotton fiber cells. 2015 , 5, 717-25	3
1117	Proteomics Insights into the Biomass Hydrolysis Potentials of a Hypercellulolytic Fungus Penicillium funiculosum. 2015 , 14, 4342-58	37
1116	Structure of a fungal form of aspartate semialdehyde dehydrogenase from Cryptococcus neoformans. 2015 , 71, 1365-71	7
1115	Refining the Structural Model of a Heterohexameric Protein Complex: Surface Induced Dissociation and Ion Mobility Provide Key Connectivity and Topology Information. 2015 , 1, 477-487	49
1114	TET3 is recruited by REST for context-specific hydroxymethylation and induction of gene expression. 2015 , 11, 283-94	92
1113	Differences in urinary proteins related to surgical margin status after radical prostatectomy. 2015 , 34, 3247-55	7
1112	An enhanced in vivo stable isotope labeling by amino acids in cell culture (SILAC) model for quantification of drug metabolism enzymes. 2015 , 14, 750-60	6
1111	Feedback regulation on PTEN/AKT pathway by the ER stress kinase PERK mediated by interaction with the Vault complex. 2015 , 27, 436-42	26
1110	Nanostructured microfluidic digestion system for rapid high-performance proteolysis. 2015 , 15, 650-4	12
1109	Adaptation of Leishmania donovani to cutaneous and visceral environments: in vivo selection and proteomic analysis. 2015 , 14, 1033-59	15
1108	Purification, characterization and antibacterial potential of a lectin isolated from Apuleia leiocarpa seeds. 2015 , 75, 402-8	19
1107	Characterization of the gila monster (Heloderma suspectum suspectum) venom proteome. 2015 , 117, 1-11	20

1106	Proteomics analyses of Bacillus subtilis after treatment with plumbagin, a plant-derived naphthoquinone. 2015 , 19, 12-23	18
1105	A look behind the screens: characterization of the HSP70 family during osmotic stress in a non-model crop. 2015 , 119, 10-20	18
1104	Revealing the amino acid composition of proteins within an expanded genetic code. 2015 , 43, e8	52
1103	AMP-acetyl CoA synthetase from Leishmania donovani: identification and functional analysis of 'PX4GK' motif. 2015 , 75, 364-72	8
1102	Neuroproteomics tools in clinical practice. 2015 , 1854, 705-17	25
1101	The characterization of soybean oil body integral oleosin isoforms and the effects of alkaline pH on them. 2015 , 177, 288-94	44
1100	GFAP antibodies show protective effect on oxidatively stressed neuroretinal cells via interaction with ERP57. 2015 , 127, 298-304	16
1099	Hippocampal receptor complexes paralleling LTP reinforcement in the spatial memory holeboard test in the rat. 2015 , 283, 162-74	11
1098	Rapid analyses of proteomes and interactomes using an integrated solid-phase extraction-liquid chromatography-MS/MS system. 2015 , 14, 977-85	5
1097	Identification, cloning and heterologous expression of active [NiFe]-hydrogenase 2 from Citrobacter sp. SG in Escherichia coli. 2015 , 199, 1-8	4
1096	Changes in protein expression across laboratory and field experiments in Geobacter bemidjiensis. 2015 , 14, 1361-75	13
1095	Development and application of a quantitative multiplexed small GTPase activity assay using targeted proteomics. 2015 , 14, 967-76	11
1094	Optimization of a multi-stage, multi-subunit malaria vaccine candidate for the production in Pichia pastoris by the identification and removal of protease cleavage sites. 2015 , 112, 659-67	9
1093	Two distinct families of protein kinases are required for plant growth under high external Mg2+ concentrations in Arabidopsis. 2015 , 167, 1039-57	38
1092	Simultaneous dissection and comparison of IL-2 and IL-15 signaling pathways by global quantitative phosphoproteomics. 2015 , 15, 520-31	19
1091	Immuno-affinity purification of PglPGIP1, a polygalacturonase-inhibitor protein from pearl millet: studies on its inhibition of fungal polygalacturonases and role in resistance against the downy mildew pathogen. 2015 , 42, 1123-38	8
1090	Glycosylation patterns of kidney proteins differ in rat diabetic nephropathy. 2015 , 87, 963-74	21
1089	The pearl millet mitogen-activated protein kinase PgMPK4 is involved in responses to downy mildew infection and in jasmonic- and salicylic acid-mediated defense. 2015 , 87, 287-302	10

1088	Usefulness of DIGE for the detection of protein profile in retained and released bovine placental tissues. 2015 , 36, 246-9	11
1087	Spleen-specific isoforms of Pax5 and Ataxin-7 as potential proteomic markers of lymphoma-affected spleen. 2015 , 402, 181-91	3
1086	BcGs1, a glycoprotein from Botrytis cinerea, elicits defence response and improves disease resistance in host plants. 2015 , 457, 627-34	43
1085	Conservation of complete trimethylation of lysine-43 in the rotor ring of c-subunits of metazoan adenosine triphosphate (ATP) synthases. 2015 , 14, 828-40	23
1084	Arginine deprivation affects glioblastoma cell adhesion, invasiveness and actin cytoskeleton organization by impairment of Dactin arginylation. 2015 , 47, 199-212	29
1083	High density lipoproteins: Measurement techniques and potential biomarkers of cardiovascular risk. 2015 , 3, 175-88	96
1082	A two-stage spin cartridge for integrated protein precipitation, digestion and SDS removal in a comparative bottom-up proteomics workflow. 2015 , 118, 140-50	17
1081	Thiol-based regulation of glyceraldehyde-3-phosphate dehydrogenase in blood bank-stored red blood cells: a strategy to counteract oxidative stress. 2015 , 55, 499-506	19
1080	Evidence of histidine and aspartic acid phosphorylation in human prostate cancer cells. 2015 , 388, 161-73	7
1079	Proteomic identification and functional characterization of MYH9, Hsc70, and DNAJA1 as novel substrates of HDAC6 deacetylase activity. 2015 , 6, 42-54	44
1078	A comprehensive proteomic analysis of totarol induced alterations in Bacillus subtilis by multipronged quantitative proteomics. 2015 , 114, 247-62	19
1077	Changes in protein expression of pacific oyster Crassostrea gigas exposed in situ to urban sewage. 2015 , 22, 17267-79	12
1076	Urine sample preparation in 96-well filter plates to characterize inflammatory and infectious diseases of the urinary tract. 2015 , 845, 77-87	4
1075	ARGONAUTE2 cooperates with SWI/SNF complex to determine nucleosome occupancy at human Transcription Start Sites. 2015 , 43, 1498-512	33
1074	Ubiquitin-specific Protease 11 (USP11) Deubiquitinates Hybrid Small Ubiquitin-like Modifier (SUMO)-Ubiquitin Chains to Counteract RING Finger Protein 4 (RNF4). 2015 , 290, 15526-15537	22
1073	The stromal cell-surface protease fibroblast activation protein-Hocalizes to lipid rafts and is recruited to invadopodia. 2015 , 1853, 2515-25	15
1072	Stable isotope labeling by amino acids in cell culture based proteomics reveals differences in protein abundances between spiral and coccoid forms of the gastric pathogen Helicobacter pylori. 2015 , 126, 34-45	10
1071	Mitochondrial ATP synthasome: Expression and structural interaction of its components. 2015 , 464, 787-93	19

1070	Association of a characteristic membrane pattern of annexin A2 with high invasiveness and nodal status in colon adenocarcinoma. 2015 , 166, 196-206	11
1069	Discovery of compounds that protect tyrosine hydroxylase activity through different mechanisms. 2015 , 1854, 1078-89	12
1068	L-Rhamnose-binding lectin from eggs of the Echinometra lucunter: Amino acid sequence and molecular modeling. 2015 , 78, 180-8	9
1067	In-gel NHS-propionate derivatization for histone post-translational modifications analysis in Arabidopsis thaliana. 2015 , 886, 107-13	5
1066	Exploring the membrane proteome of the diazotropic cyanobacterium Anabaena PCC7120 through gel-based proteomics and in silico approaches. 2015 , 127, 161-8	3
1065	Dynamics of Energy and Electron Transfer in the FMO-Reaction Center Core Complex from the Phototrophic Green Sulfur Bacterium Chlorobaculum tepidum. 2015 , 119, 8321-9	21
1064	Facile Discovery of Cell-Surface Protein Targets of Cancer Cell Aptamers. 2015 , 14, 2692-700	26
1063	Cellular Proteome Dynamics during Differentiation of Human Primary Myoblasts. 2015 , 14, 3348-61	23
1062	Purification of TNFR-Fc produced in recombinant CHO cells: Characterization of product-related impurities. 2015 , 50, 1313-1317	3
1061	Proteomic Analysis of Connexin 43 Reveals Novel Interactors Related to Osteoarthritis. 2015 , 14, 1831-45	24
1060	Proteomic analysis of homocholine catabolic pathway in Pseudomonas sp. strain A9. 2015 , 50, 1735-1747	3
1059	Activation of Autophagic Flux against Xenoestrogen Bisphenol-A-induced Hippocampal Neurodegeneration via AMP kinase (AMPK)/Mammalian Target of Rapamycin (mTOR) Pathways. 2015 , 290, 21163-21184	56
1058	Proteomic Profiling and Functional Characterization of Multiple Post-Translational Modifications of Tubulin. 2015 , 14, 3292-304	25
1057	A Dual SILAC Proteomic Labeling Strategy for Quantifying Constitutive and Cell-Cell Induced Protein Secretion. 2015 , 14, 3229-38	11
1056	Structure of human ST8SiaIII sialyltransferase provides insight into cell-surface polysialylation. 2015 , 22, 627-35	55
1055	Novel pH-Stable Glycoside Hydrolase Family 3 I-Xylosidase from Talaromyces amestolkiae: an Enzyme Displaying Regioselective Transxylosylation. 2015 , 81, 6380-92	30
1054	ClpX stimulates the mitochondrial unfolded protein response (UPRmt) in mammalian cells. 2015 , 1853, 2580-91	42
1053	Increased alveolar soluble annexin V promotes lung inflammation and fibrosis. 2015 , 46, 1417-29	12

1052	Maternal stress predicts altered biogenesis and the profile of mitochondrial proteins in the frontal cortex and hippocampus of adult offspring rats. 2015 , 60, 151-62	44
1051	A negative feedback loop controls NMDA receptor function in cortical interneurons via neuregulin 2/ErbB4 signalling. 2015 , 6, 7222	36
1050	Organization of Subunits in the Membrane Domain of the Bovine F-ATPase Revealed by Covalent Cross-linking. 2015 , 290, 13308-20	33
1049	Centromere protein F includes two sites that couple efficiently to depolymerizing microtubules. 2015 , 209, 813-28	36
1048	Mechanisms of antibiotic resistance to enrofloxacin in uropathogenic Escherichia coli in dog. 2015 , 127, 365-76	29
1047	The DEAH-box helicase Dhr1 dissociates U3 from the pre-rRNA to promote formation of the central pseudoknot. 2015 , 13, e1002083	49
1046	Transcriptomic and Proteomic Profiling of Anabaena sp. Strain 90 under Inorganic Phosphorus Stress. 2015 , 81, 5212-22	28
1045	Impact of the antifungal protein PgAFP from Penicillium chrysogenum on the protein profile in Aspergillus flavus. 2015 , 99, 8701-15	32
1044	Proteomic challenges: sample preparation techniques for microgram-quantity protein analysis from biological samples. 2015 , 16, 3537-63	174
1043	Cadmium toxicity in diazotrophic Anabaena spp. adjudged by hasty up-accumulation of transporter and signaling and severe down-accumulation of nitrogen metabolism proteins. 2015 , 127, 134-46	38
1042	The Drosophila retinoblastoma binding protein 6 family member has two isoforms and is potentially involved in embryonic patterning. 2015 , 16, 10242-66	3
1041	A chromophore-containing agglutinin from Haliclona manglaris: purification and biochemical characterization. 2015 , 72, 1368-75	3
1040	Dissection of metabolic pathways in the Db/Db mouse model by integrative proteome and acetylome analysis. 2015 , 11, 908-22	15
1039	Differences in the resting platelet proteome and platelet releasate between healthy children and adults. 2015 , 123, 78-88	20
1038	Expression and purification of buffalo interferon-tau and efficacy of recombinant buffalo interferon-tau for in vitro embryo development. 2015 , 75, 186-96	5
1037	Structures, Functions, and Interactions of ClpT1 and ClpT2 in the Clp Protease System of Arabidopsis Chloroplasts. 2015 , 27, 1477-96	29
1036	Ubiquitin-Mediated Proteasomal Degradation of Oleosins is Involved in Oil Body Mobilization During Post-Germinative Seedling Growth in Arabidopsis. 2015 , 56, 1374-87	50
1035	Proteomic identification of plasma proteins as markers of growth promoter abuse in cattle. 2015 , 407, 4495-507	19

1034	TRAMM/TrappC12 plays a role in chromosome congression, kinetochore stability, and CENP-E recruitment. 2015 , 209, 221-34	22
1033	Development of blood transfusion product pathogen reduction treatments: a review of methods, current applications and demands. 2015 , 52, 19-34	79
1032	Identification and functional characterization of intracellular sialidase NeuA3 from Streptomyces avermitilis. 2015 , 50, 752-758	3
1031	The Plasmodium falciparum exportome contains non-canonical PEXEL/HT proteins. 2015 , 97, 301-14	23
1030	L-Plastin S-glutathionylation promotes reduced binding to 🛭 actin and affects neutrophil functions. 2015 , 86, 1-15	24
1029	Secretome analysis identifies novel signal Peptide peptidase-like 3 (Sppl3) substrates and reveals a role of Sppl3 in multiple Golgi glycosylation pathways. 2015 , 14, 1584-98	52
1028	Protein folding. Translational tuning optimizes nascent protein folding in cells. 2015 , 348, 444-8	140
1027	Comparative study of the protein profiles of Sunki mandarin and Rangpur lime plants in response to water deficit. 2015 , 15, 69	22
1026	Comparative proteomic analysis of Salmonella typhimurium LT2 and its hisG gene inactivated mutant. 2015 , 30, 48-56	1
1025	Phosphoproteomic analysis of wild-type and antimony-resistant Leishmania braziliensis lines by 2D-DIGE technology. 2015 , 15, 2999-3019	25
1024	Navigating through metaproteomics data: a logbook of database searching. 2015 , 15, 3439-53	81
1023	Validation of a novel shotgun proteomic workflow for the discovery of protein-protein interactions: focus on ZNF521. 2015 , 14, 1888-99	15
1022	Significantly enhanced heme retention ability of myoglobin engineered to mimic the third covalent linkage by nonaxial histidine to heme (vinyl) in synechocystis hemoglobin. 2015 , 290, 1979-93	12
1021	Dysregulation of parkin in the substantia nigra of db/db and high-fat diet mice. 2015 , 294, 182-92	46
1020	O-linked glycosylation of the mucin domain of the herpes simplex virus type 1-specific glycoprotein gC-1 is temporally regulated in a seed-and-spread manner. 2015 , 290, 5078-5091	15
1019	Application of multiplexed cysteine-labeled complex protein sample for 2D electrophoretic gel alignment. 2015 , 15, 1777-80	5
1018	Exploitation of complement regulatory proteins by Borrelia and Francisella. 2015 , 11, 1684-95	9
1017	Proteomics methods for discovering viral-host interactions. 2015 , 90, 21-7	5

1016	CRL3IBTK Regulates the Tumor Suppressor Pdcd4 through Ubiquitylation Coupled to Proteasomal Degradation. 2015 , 290, 13958-71	16
1015	Comparative proteomic analysis of biofilm and planktonic cells of Lactobacillus plantarum DB200. 2015 , 15, 2244-57	28
1014	A novel link between Fic (filamentation induced by cAMP)-mediated adenylylation/AMPylation and the unfolded protein response. 2015 , 290, 8482-99	65
1013	Phosphorylation of synaptic GTPase-activating protein (synGAP) by Ca2+/calmodulin-dependent protein kinase II (CaMKII) and cyclin-dependent kinase 5 (CDK5) alters the ratio of its GAP activity toward Ras and Rap GTPases. 2015 , 290, 4908-4927	48
1012	Comparative proteomic analysis of gamma-aminobutyric acid responses in hypoxia-treated and untreated melon roots. 2015 , 116, 28-37	12
1011	Proteomics beyond trypsin. 2015, 282, 2612-26	180
1010	Prolonged pre-incubation increases the susceptibility of Galleria mellonella larvae to bacterial and fungal infection. 2015 , 6, 458-65	20
1009	A physiological, biochemical and proteomic characterization of Saccharomyces cerevisiae trk1,2 transport mutants grown under limiting potassium conditions. 2015 , 161, 1260-70	5
1008	Evidence for restricted reactivity of ADAMDEC1 with protein substrates and endogenous inhibitors. 2015 , 290, 6620-9	7
1007	Surfactant-aided precipitation/on-pellet-digestion (SOD) procedure provides robust and rapid sample preparation for reproducible, accurate and sensitive LC/MS quantification of therapeutic protein in plasma and tissues. 2015 , 87, 4023-9	54
1006	Proteomic Profiling. 2015 ,	5
1005	Effects of clbR overexpression on enzyme production in Aspergillus aculeatus vary depending on the cellulosic biomass-degrading enzyme species. 2015 , 79, 488-95	12
1004	Lrp1/LDL Receptor Play Critical Roles in Mannose 6-Phosphate-Independent Lysosomal Enzyme Targeting. 2015 , 16, 743-59	41
1003	The Non-catalytic B Subunit of Coagulation Factor XIII Accelerates Fibrin Cross-linking. 2015 , 290, 12027-39	24
1002	eIF3 targets cell-proliferation messenger RNAs for translational activation or repression. 2015 , 522, 111-4	220
1001	Analysis of HIV-1 Gag protein interactions via biotin ligase tagging. 2015 , 89, 3988-4001	31
1000	SILAC-based quantification of changes in protein tyrosine phosphorylation induced by Interleukin-2 (IL-2) and IL-15 in T-lymphocytes. 2015 , 5, 53-8	10
999	A highly sensitive prenylation assay reveals in vivo effects of bisphosphonate drug on the Rab prenylome of macrophages outside the skeleton. 2015 , 6, 202-11	20

(2015-2015)

99	Homology-Driven Proteomics. 2015 , 14, 4823-33	31
99	Discovery of a Unique Clp Component, ClpF, in Chloroplasts: A Proposed Binary ClpF-ClpS1 Ad Complex Functions in Substrate Recognition and Delivery. 2015 , 27, 2677-91	aptor 52
99	Comparison of sodium dodecyl sulfate depletion techniques for proteome analysis by mass spectrometry. 2015 , 1418, 158-166	41
99	Proteogenomic Discovery of a Small, Novel Protein in Yeast Reveals a Strategy for the Detecti Unannotated Short Open Reading Frames. 2015 , 14, 5038-47	ion of 19
99	Cell type- and brain region-resolved mouse brain proteome. 2015 , 18, 1819-31	418
99	Analysis of proteins and potential bioactive peptides from tilapia (Oreochromis spp.) procession co-products using proteomic techniques coupled with BIOPEP database. 2015 , 19, 629-640	ng 33
99	Structural Aspects of N-Glycosylations and the C-terminal Region in Human Glypican-1. 2015 , 2	290, 22991-3008 ₁₄
99	791 The Green Gut: Chlorophyll Degradation in the Gut of Spodoptera littoralis. 2015 , 41, 965-74	2
99	Inactivation of the particulate methane monooxygenase (pMMO) in Methylococcus capsulatus (Bath) by acetylene. 2015 , 1854, 1842-1852	S 11
98	In silico and experimental validation of protein-protein interactions between PknI and Rv2159 from Mycobacterium tuberculosis. 2015 , 62, 283-293	c 8
98	Bacteria do not incorporate I-N-methylamino-L-alanine into their proteins. 2015 , 102, 55-61	31
98	Integration of Proteomics and Transcriptomics Data Sets for the Analysis of a Lymphoma B-Ce Line in the Context of the Chromosome-Centric Human Proteome Project. 2015 , 14, 3530-40	ll 9
98	First proteome study of sporadic flowering in bamboo species (Bambusa vulgaris and Dendrocalamus manipureanus) reveal the boom is associated with stress and mobile genetic elements. 2015 , 574, 255-64	4
98	Transcriptional Regulation, Metal Binding Properties and Structure of Pden1597, an Unusual Z Transport Protein from Paracoccus denitrificans. 2015 , 290, 11878-89	Zinc 16
98	Proteomic analysis of Dasarone induced cytotoxicity in human glioblastoma U251 cells. 2015 ,	115, 292-9 12
98	Activation of m1 muscarinic acetylcholine receptor induces surface transport of KCNQ channe through a CRMP-2-mediated pathway. 2015 , 128, 4235-45	els 10
98	UV-B stress induced metabolic rearrangements explored with comparative proteomics in thre Anabaena species. 2015 , 127, 122-33	e 39
98	Xylanase production by endophytic Aspergillus niger using pentose-rich hydrothermal liquor f sugarcane bagasse. 2015 , 33, 175-187	rom 10

980	ATGL and CGI-58 are lipid droplet proteins of the hepatic stellate cell line HSC-T6. 2015, 56, 1972-84	28
979	Expression and characterization of a new isoform of the 9 kDa allergenic lipid transfer protein from tomato (variety San Marzano). 2015 , 96, 64-71	6
978	Genomic and Proteomic Analyses Indicate that Banchine and Campoplegine Polydnaviruses Have Similar, if Not Identical, Viral Ancestors. 2015 , 89, 8909-21	37
977	Differences in biomass degradation between newly isolated environmental strains of Clostridium thermocellum and heterogeneity in the size of the cellulosomal scaffoldin. 2015 , 38, 424-32	14
976	Posttranslational Modifications of Baculovirus Protamine-Like Protein P6.9 and the Significance of Its Hyperphosphorylation for Viral Very Late Gene Hyperexpression. 2015 , 89, 7646-59	25
975	Analysis of the Role of the C-Terminal Tail in the Regulation of the Epidermal Growth Factor Receptor. 2015 , 35, 3083-102	47
974	Differences in Host Innate Responses among Coccidioides Isolates in a Murine Model of Pulmonary Coccidioidomycosis. 2015 , 14, 1043-53	8
973	A Duplicated ESAT-6 Region of ESX-5 Is Involved in Protein Export and Virulence of Mycobacteria. 2015 , 83, 4349-61	34
972	Depolymerization of lignosulfonates by submerged cultures of the basidiomycete Irpex consors and cloning of a putative versatile peroxidase. 2015 , 81, 8-15	8
971	Purification and primary structure of a novel mannose-specific lectin from Centrolobium microchaete Mart seeds. 2015 , 81, 600-7	15
970	Adrenergic Repression of the Epigenetic Reader MeCP2 Facilitates Cardiac Adaptation in Chronic Heart Failure. 2015 , 117, 622-33	44
969	Novel remodeling of the mouse heart mitochondrial proteome in response to acute insulin stimulation. 2015 , 25, 1152-8	
968	Characterization of the gila monster (Heloderma suspectum suspectum) venom proteome. 2015 , 3, 137-42	2
967	Data for the characterization of the HSP70 family during osmotic stress in banana, a non-model crop. 2015 , 3, 78-84	5
966	Oxidative proteome alterations during skeletal muscle ageing. 2015 , 5, 267-274	49
965	Identification of a Novel Splice Variant Isoform of TREM-1 in Human Neutrophil Granules. 2015 , 195, 5725-31	18
964	Spinach (Spinacia oleracea L.) modulates its proteome differentially in response to salinity, cadmium and their combination stress. 2015 , 97, 235-45	40
963	The role of protein and peptide separation before mass spectrometry analysis in clinical proteomics. 2015 , 1381, 1-12	51

(2015-2015)

962	coli. 2015 , 43, 530-43	15
961	The 🛮 lactamase gene regulator AmpR is a tetramer that recognizes and binds the D-Ala-D-Ala motif of its repressor UDP-N-acetylmuramic acid (MurNAc)-pentapeptide. 2015 , 290, 2630-43	51
960	Theonellasterone, a steroidal metabolite isolated from a Theonella sponge, protects peroxiredoxin-1 from oxidative stress reactions. 2015 , 51, 1591-3	6
959	Extracellular and cell-associated forms of Gluconobacter oxydans dextran dextrinase change their localization depending on the cell growth. 2015 , 456, 500-5	11
958	Reaction of human macrophages on protein corona covered TiO[hanoparticles. 2015, 11, 275-82	26
957	Elucidation of fluoranthene degradative characteristics in a newly isolated Achromobacter xylosoxidans DN002. 2015 , 175, 1294-305	36
956	Direct energy transfer from the major antenna to the photosystem II core complexes in the absence of minor antennae in liposomes. 2015 , 1847, 248-261	11
955	Enhancing of sugar cane bagasse hydrolysis by Annulohypoxylon stygium glycohydrolases. 2015 , 177, 247-54	17
954	Proteomic investigation of Sri Lankan hump-nosed pit viper (Hypnale hypnale) venom. 2015 , 93, 164-70	35
953	Blau syndrome-associated Nod2 mutation alters expression of full-length NOD2 and limits responses to muramyl dipeptide in knock-in mice. 2015 , 194, 349-57	27
952	Affinity chromatography revealed insights into unique functionality of two 14-3-3 protein species in developing maize kernels. 2015 , 114, 274-86	14
951	Insight into the primary mode of action of TiO2 nanoparticles on Escherichia coli in the dark. 2015 , 15, 98-113	71
950	Construction of a high-performance magnetic enzyme nanosystem for rapid tryptic digestion. 2014 , 4, 6947	64
949	Expression of tight-junction proteins in human proximal small intestinal mucosa before and after Roux-en-Y gastric bypass surgery. 2015 , 11, 45-53	40
948	Characterization of novel insect associated peptidases for hydrolysis of food proteins. 2015 , 240, 431-439	13
947	Proteomic identification of organic additives in the mortars of ancient Chinese wooden buildings. 2015 , 7, 143-149	28
946	A role for the Parkinson's disease protein DJ-1 as a chaperone and antioxidant in the anhydrobiotic nematode Panagrolaimus superbus. 2015 , 20, 121-37	9
945	A generic approach for "shotgun" analysis of the soluble proteome of plant cell suspension cultures. 2015 , 974, 48-56	1

944	Bdellovibrio bacteriovorus inhibits Staphylococcus aureus biofilm formation and invasion into human epithelial cells. 2014 , 4, 3811	48
943	Automated assignment of MS/MS cleavable cross-links in protein 3D-structure analysis. 2015 , 26, 83-97	130
942	Mercury fractionation in dourada (Brachyplatystoma rousseauxii) of the Madeira River in Brazil using metalloproteomic strategies. 2015 , 132, 239-44	37
941	Major proteomic changes associated with amyloid-induced biofilm formation in Pseudomonas aeruginosa PAO1. 2015 , 14, 72-81	26
940	Production of isomalto-oligosaccharides by cell bound ⊞glucosidase of Microbacterium sp 2015 , 60, 486-494	24
939	Articular chondrocyte network mediated by gap junctions: role in metabolic cartilage homeostasis. 2015 , 74, 275-84	45
938	Podoplanin is a component of extracellular vesicles that reprograms cell-derived exosomal proteins and modulates lymphatic vessel formation. 2016 , 7, 16070-89	51
937	EPH/ephrin profile and EPHB2 expression predicts patient survival in breast cancer. 2016 , 7, 21362-80	25
936	Orthologous Allergens and Diagnostic Utility of Major Allergen Alt a 1. 2016 , 8, 428-37	13
935	Indole affects the formation of multicellular aggregate structures in Pantoea agglomerans YS19. 2016 , 62, 31-7	14
934	Hepatitis B Virus Protein X Induces Degradation of Talin-1. 2016 , 8,	11
933	Insights into the Hypertensive Effects of Tityus serrulatus Scorpion Venom: Purification of an Angiotensin-Converting Enzyme-Like Peptidase. 2016 , 8,	10
932	Sample preparation for proteomic analysis using a GeLC-MS/MS strategy. 2016 , 3,	31
931	Characterization of recombinant human lysosomal beta-hexosaminidases produced in the methylotrophic yeast Pichia pastoris. 2016 , 21, 195	7
930	Shotgun Quantitative Proteomic Analysis of Proteins Responding to Drought Stress in Brassica rapa L. (Inbred Line "Chiifu"). 2016 , 2016, 4235808	6
929	Deciphering the Translation Initiation Factor 5A Modification Pathway in Halophilic Archaea. 2016 , 2016, 7316725	15
928	Aging-related elevation of sphingoid bases shortens yeast chronological life span by compromising mitochondrial function. 2016 , 7, 21124-44	18
927	Effects of Tityus stigmurus (Thorell 1876) (Scorpiones: Buthidae) venom in isolated perfused rat kidneys. 2016 , 88 Suppl 1, 665-75	7

(2016-2016)

926	TCR Triggering Induces the Formation of Lck-RACK1-Actinin-1 Multiprotein Network Affecting Lck Redistribution. 2016 , 7, 449	10
925	UV-B Radiation Stress Causes Alterations in Whole Cell Protein Profile and Expression of Certain Genes in the Rice Phyllospheric Bacterium Enterobacter cloacae. 2016 , 7, 1440	15
924	Functional Characterization of PknI-Rv2159c Interaction in Redox Homeostasis of. 2016 , 7, 1654	7
923	Proteomics-Based Analysis of Protein Complexes in Pluripotent Stem Cells and Cancer Biology. 2016 , 17, 432	2
922	Insight of Saffron Proteome by Gel-Electrophoresis. 2016 , 21, 167	8
921	Biochemical and cellular characterization of transcription factors binding to the hyperconserved core promoter-associated M4 motif. 2016 , 17, 693	5
92 0	Mycobacterium tuberculosis AtsG (Rv0296c), GlmU (Rv1018c) and SahH (Rv3248c) Proteins Function as the Human IL-8-Binding Effectors and Contribute to Pathogen Entry into Human Neutrophils. 2016 , 11, e0148030	7
919	Faecal Metaproteomic Analysis Reveals a Personalized and Stable Functional Microbiome and Limited Effects of a Probiotic Intervention in Adults. 2016 , 11, e0153294	59
918	Optimization of Liver Decellularization Maintains Extracellular Matrix Micro-Architecture and Composition Predisposing to Effective Cell Seeding. 2016 , 11, e0155324	52
917	Spermidine Suppresses Age-Associated Memory Impairment by Preventing Adverse Increase of Presynaptic Active Zone Size and Release. 2016 , 14, e1002563	62
916	Adaptive Remodeling of the Bacterial Proteome by Specific Ribosomal Modification Regulates Pseudomonas Infection and Niche Colonisation. 2016 , 12, e1005837	29
915	Monitoring Solution Structures of Peroxisome Proliferator-Activated Receptor []/[upon Ligand Binding. 2016 , 11, e0151412	12
914	Threonine 89 Is an Important Residue of Profilin-1 That Is Phosphorylatable by Protein Kinase A. 2016 , 11, e0156313	10
913	Proteomic Analysis of Outer Membrane Proteins from Salmonella Enteritidis Strains with Different Sensitivity to Human Serum. 2016 , 11, e0164069	8
912	Structural, Functional and Phylogenetic Analysis of Sperm Lysozyme-Like Proteins. 2016 , 11, e0166321	6
911	Quantitative Proteomics Uncovers Novel Factors Involved in Developmental Differentiation of Trypanosoma brucei. 2016 , 12, e1005439	60
910	A Ribonuclease Isolated from Wild Ganoderma Lucidum Suppressed Autophagy and Triggered Apoptosis in Colorectal Cancer Cells. 2016 , 7, 217	20
909	The Rice Eukaryotic Translation Initiation Factor 3 Subunit f (OseIF3f) Is Involved in Microgametogenesis. 2016 , 7, 532	4

908	The Aquaporin Splice Variant NbXIP1;1 Permeable to Boric Acid and Is Phosphorylated in the N-terminal Domain. 2016 , 7, 862	17
907	Circadian Profiling of the Arabidopsis Proteome Using 2D-DIGE. 2016 , 7, 1007	26
906	New Features on the Environmental Regulation of Metabolism Revealed by Modeling the Cellular Proteomic Adaptations Induced by Light, Carbon, and Inorganic Nitrogen in Chlamydomonas reinhardtii. 2016 , 7, 1158	6
905	Unbiased analysis of senescence associated secretory phenotype (SASP) to identify common components following different genotoxic stresses. 2016 , 8, 1316-29	133
904	20-Hydroxyecdysone stimulates nuclear accumulation of BmNep1, a nuclear ribosome biogenesis-related protein in the silkworm, Bombyx mori. 2016 , 25, 617-28	1
903	Plasma membrane proteomics in the maize primary root growth zone: novel insights into root growth adaptation to water stress. 2016 , 39, 2043-54	13
902	Isolation and characterisation of a novel alpha-amylase from the extreme haloarchaeon Haloterrigena turkmenica. 2016 , 92, 174-184	12
901	Prostate Cancer-Associated Kallikrein-Related Peptidase 4 Activates Matrix Metalloproteinase-1 and Thrombospondin-1. 2016 , 15, 2466-78	14
900	Expression changes of proteins associated with the development of preeclampsia in maternal plasma: A case-control study. 2016 , 16, 1581-9	18
899	Proteomic investigation of the secretome of Cellvibrio japonicus during growth on chitin. 2016 , 16, 1904-14	22
898	Aqueous Terminalia arjuna extract modulates expression of key atherosclerosis-related proteins in a hypercholesterolemic rabbit: A proteomic-based study. 2016 , 10, 750-9	4
897	Autoantibodies against TYMS and PDLIM1 proteins detected as circulatory signatures in Indian breast cancer patients. 2016 , 10, 564-73	13
896	Native Piezo2 Interactomics Identifies Pericentrin as a Novel Regulator of Piezo2 in Somatosensory Neurons. 2016 , 15, 2676-87	18
895	Crystal structure of a thiolase from Escherichia coli at 1.8 Iresolution. 2016 , 72, 534-44	6
894	Revealing oxidative damage to enzymes of carbohydrate metabolism in yeast: An integration of 2D DIGE, quantitative proteomics, and bioinformatics. 2016 , 16, 1889-903	9
893	Polyclonal antibodies for specific detection of tobacco host cell proteins can be efficiently generated following RuBisCO depletion and the removal of endotoxins. 2016 , 11, 507-18	15
892	Functional and structural characterization of domain truncated violaxanthin de-epoxidase. 2016 , 157, 414-21	1
891	Analysis of the effect of a novel therapeutic for type 2 diabetes on the proteome of a muscle cell line. 2016 , 16, 70-9	3

(2016-2016)

890	Proteomic analysis of the venom and venom sac of the woodwasp, Sirex noctilio - Towards understanding its biological impact. 2016 , 146, 195-206	16
889	In situ protein-SIP highlights Burkholderiaceae as key players degrading toluene by para ring hydroxylation in a constructed wetland model. 2016 , 18, 1176-86	57
888	The disulfide oxidoreductase SdbA is active in Streptococcus gordonii using a single C-terminal cysteine of the CXXC motif. 2016 , 99, 236-53	8
887	The function of the PduJ microcompartment shell protein is determined by the genomic position of its encoding gene. 2016 , 101, 770-83	24
886	Proteomic analysis reveals the differential histone programs between male germline cells and vegetative cells in Lilium davidii. 2016 , 85, 660-74	13
885	Far-western blotting as a solution to the non-specificity of the anti-erythropoietin receptor antibody. 2016 , 12, 1575-1580	O
884	Annexin A5 is the Most Abundant Membrane-Associated Protein in Stereocilia but is Dispensable for Hair-Bundle Development and Function. 2016 , 6, 27221	17
883	ATP-Dependent C-F Bond Cleavage Allows the Complete Degradation of 4-Fluoroaromatics without Oxygen. 2016 , 7,	27
882	An unexplored pathway for degradation of cholate requires a 7thydroxysteroid dehydratase and contributes to a broad metabolic repertoire for the utilization of bile salts in Novosphingobium sp. strain Chol11. 2016 , 18, 5187-5203	15
881	Identification of a novel putative interaction partner of the nucleoporin ALADIN. 2016 , 5, 1697-1705	11
880	Phosphorylation of FEZ1 by Microtubule Affinity Regulating Kinases regulates its function in presynaptic protein trafficking. 2016 , 6, 26965	18
879	Bulk cell density and Wnt/TGFbeta signalling regulate mesendodermal patterning of human pluripotent stem cells. 2016 , 7, 13602	74
878	Computer aided identification of a Hevein-like antimicrobial peptide of bell pepper leaves for biotechnological use. 2016 , 17, 999	4
877	Cloning of a novel endogenous promoter for foreign gene expression in Phaeodactylum tricornutum. 2016 , 59, 861-867	12
876	Single-target high-throughput transcription analyses reveal high levels of alternative splicing present in the FPPS/GGPPS from Plasmodium falciparum. 2015 , 5, 18429	6
875	Modern Proteomics (Sample Preparation, Analysis and Practical Applications. 2016,	10
874	Protein Structural Analysis via Mass Spectrometry-Based Proteomics. 2016 , 919, 397-431	21
873	The membrane scaffold SLP2 anchors a proteolytic hub in mitochondria containing PARL and the i-AAA protease YME1L. 2016 , 17, 1844-1856	94

872	Evidence that ubiquitylated H2B corrals hDot1L on the nucleosomal surface to induce H3K79 methylation. 2016 , 7, 10589	49
871	Heterogeneous regulation of bacterial natural product biosynthesis via a novel transcription factor. 2016 , 2, e00197	10
870	Glaucoma related Proteomic Alterations in Human Retina Samples. 2016 , 6, 29759	34
869	First insight into the proteome landscape of the porcine short posterior ciliary arteries: Key signalling pathways maintaining physiologic functions. 2016 , 6, 38298	8
868	Aspergillus flavipes methionine Eyase-dextran conjugates with enhanced structural, proteolytic stability and anticancer efficiency. 2016 , 133, S15-S24	20
867	Chronic Exposure of Marine Medaka (Oryzias melastigma) to 4,5-Dichloro-2-n-octyl-4-isothiazolin-3-one (DCOIT) Reveals Its Mechanism of Action in Endocrine Disruption via the Hypothalamus-Pituitary-Gonadal-Liver (HPGL) Axis. 2016 , 50, 4492-501	33
866	Changes in Relative Thylakoid Protein Abundance Induced by Fluctuating Light in the Diatom Thalassiosira pseudonana. 2016 , 15, 1649-58	17
865	Proteomic analysis of exosomal cargo: the challenge of high purity vesicle isolation. 2016 , 12, 1407-19	119
864	Purification, biochemical characterization and structural modelling of alkali-stable [-1,4-xylan xylanohydrolase from Aspergillus fumigatus R1 isolated from soil. 2016 , 16, 11	17
863	Application of Clinical Bioinformatics. 2016,	8
863	Application of Clinical Bioinformatics. 2016, Proteomic Profiling: Data Mining and Analyses. 2016, 133-173	8
		40
862	Proteomic Profiling: Data Mining and Analyses. 2016 , 133-173 Development of a new platform for secretory production of recombinant proteins in	
862	Proteomic Profiling: Data Mining and Analyses. 2016 , 133-173 Development of a new platform for secretory production of recombinant proteins in Corynebacterium glutamicum. 2016 , 113, 163-72 Mass spectrometry-based identification of allergens from Curvularia pallescens, a prevalent	40
862 861 860	Proteomic Profiling: Data Mining and Analyses. 2016, 133-173 Development of a new platform for secretory production of recombinant proteins in Corynebacterium glutamicum. 2016, 113, 163-72 Mass spectrometry-based identification of allergens from Curvularia pallescens, a prevalent aerospore in India. 2016, 1864, 869-79 Development of data for the identification and characterization of proteins found in Rhodnius	40
862 861 860 859	Proteomic Profiling: Data Mining and Analyses. 2016, 133-173 Development of a new platform for secretory production of recombinant proteins in Corynebacterium glutamicum. 2016, 113, 163-72 Mass spectrometry-based identification of allergens from Curvularia pallescens, a prevalent aerospore in India. 2016, 1864, 869-79 Development of data for the identification and characterization of proteins found in Rhodnius prolixus, Triatoma lecticularia and Panstrongylus herreri. 2016, 7, 844-7 Analysis of the dose-dependent stage-specific in vitro efficacy of a multi-stage malaria vaccine	40 14 2
862 861 860 859 858	Proteomic Profiling: Data Mining and Analyses. 2016, 133-173 Development of a new platform for secretory production of recombinant proteins in Corynebacterium glutamicum. 2016, 113, 163-72 Mass spectrometry-based identification of allergens from Curvularia pallescens, a prevalent aerospore in India. 2016, 1864, 869-79 Development of data for the identification and characterization of proteins found in Rhodnius prolixus, Triatoma lecticularia and Panstrongylus herreri. 2016, 7, 844-7 Analysis of the dose-dependent stage-specific in vitro efficacy of a multi-stage malaria vaccine candidate cocktail. 2016, 15, 279 Data on mass spectrometry based identification of allergens from sunflower (Helianthus annuus L.)	40 14 2 17

(2016-2016)

854	Resistance against Echinostoma caproni (Trematoda) secondary infections in mice is not dependent on the ileal protein production. 2016 , 140, 37-47		5
853	Hedgehog Signaling Strength Is Orchestrated by the mir-310 Cluster of MicroRNAs in Response to Diet. 2016 , 202, 1167-83		24
852	Functional Characterization of a Novel Member of the Amidohydrolase 2 Protein Family, 2-Hydroxy-1-Naphthoic Acid Nonoxidative Decarboxylase from Burkholderia sp. Strain BC1. 2016 , 198, 1755-1763		5
851	STAGE-diging: A novel in-gel digestion processing for proteomics samples. 2016 , 140, 48-54		12
850	PolDIP2 interacts with human PrimPol and enhances its DNA polymerase activities. 2016 , 44, 3317-29		40
849	Tetratricopeptide repeat factor XAB2 mediates the end resection step of homologous recombination. 2016 , 44, 5702-16		18
848	MS-analysis of SILAC-labeled MYC-driven B lymphoma cells overexpressing miR-17-19b. 2016 , 7, 349-53		1
847	Cross-talk between Dopachrome Tautomerase and Caveolin-1 Is Melanoma Cell Phenotype-specific and Potentially Involved in Tumor Progression. 2016 , 291, 12481-12500		4
846	Proteomic analysis reveals modulation of iron homeostasis and oxidative stress response in Pseudomonas aeruginosa PAO1 by curcumin inhibiting quorum sensing regulated virulence factors and biofilm production. 2016 , 145, 112-126		43
845	Endocrine Disruption throughout the Hypothalamus-Pituitary-Gonadal-Liver (HPGL) Axis in Marine Medaka (Oryzias melastigma) Chronically Exposed to the Antifouling and Chemopreventive Agent, 3,3'-Diindolylmethane (DIM). 2016 , 29, 1020-8		16
844	Identification of a Third Mn(II) Oxidase Enzyme in Pseudomonas putida GB-1. 2016 , 82, 3774-3782		38
843	Oms1 associates with cytochrome c oxidase assembly intermediates to stabilize newly synthesized Cox1. 2016 , 27, 1570-80		3
842	Molecular basis of PRC1 targeting to Polycomb response elements by PhoRC. 2016 , 30, 1116-27		51
841	Identification of a dairy product in the grass woven basket from Gumugou Cemetery (3800 BP, northwestern China). 2016 , 426, 158-165		30
840	Characterization of a highly potent antimicrobial peptide microcin N from uropathogenic Escherichia coli. 2016 , 363,		6
839	Molecular studies on structural changes and oligomerisation of violaxanthin de-epoxidase associated with the pH-dependent activation. 2016 , 129, 29-41		14
838	Six alternative proteases for mass spectrometry-based proteomics beyond trypsin. <i>Nature Protocols</i> , 2016 , 11, 993-1006	8.8	245
837	A Non-canonical Melanin Biosynthesis Pathway Protects Aspergillus terreus Conidia from Environmental Stress. 2016 , 23, 587-597		50

836	The EGFR-specific antibody cetuximab combined with chemotherapy triggers immunogenic cell death. 2016 , 22, 624-31	145
835	Identification of an OmpW homologue in Burkholderia pseudomallei, a protective vaccine antigen against melioidosis. 2016 , 34, 2616-21	18
834	Intergenic Variable-Number Tandem-Repeat Polymorphism Upstream of rocA Alters Toxin Production and Enhances Virulence in Streptococcus pyogenes. 2016 , 84, 2086-2093	14
833	Targeted Ablation of Periostin-Expressing Activated Fibroblasts Prevents Adverse Cardiac Remodeling in Mice. 2016 , 118, 1906-17	133
832	The different catalytic roles of the metal-binding ligands in human 4-hydroxyphenylpyruvate dioxygenase. 2016 , 473, 1179-89	9
831	Rqc1 and Ltn1 Prevent C-terminal Alanine-Threonine Tail (CAT-tail)-induced Protein Aggregation by Efficient Recruitment of Cdc48 on Stalled 60S Subunits. 2016 , 291, 12245-53	56
830	Community proteomics provides functional insight into polyhydroxyalkanoate production by a mixed microbial culture cultivated on fermented dairy manure. 2016 , 100, 7957-76	10
829	Gut Bacteria Metabolism Impacts Immune Recovery in HIV-infected Individuals. 2016 , 8, 203-216	63
828	Production of dengue virus envelope protein domain III-based antigens in tobacco chloroplasts using inducible and constitutive expression systems. 2016 , 91, 497-512	22
827	A Novel Fic (Filamentation Induced by cAMP) Protein from Clostridium difficile Reveals an Inhibitory Motif-independent Adenylylation/AMPylation Mechanism. 2016 , 291, 13286-300	10
826	Proteomic analysis of human tooth pulp proteomes - Comparison of caries-resistant and caries-susceptible persons. 2016 , 145, 127-136	14
825	Identification of syntrophic acetate-oxidizing bacteria in anaerobic digesters by combined protein-based stable isotope probing and metagenomics. 2016 , 10, 2405-18	96
824	Characterization of the Protein Components of Matrix Stones Sheds Light on S100-A8 and S100-A9 Relevance in the Inflammatory Pathogenesis of These Rare Renal Calculi. 2016 , 196, 911-8	9
823	Unraveling K63 Polyubiquitination Networks by Sensor-Based Proteomics. 2016 , 171, 1808-20	36
822	Sumoylation of eIF4A2 affects stress granule formation. 2016 , 129, 2407-15	24
821	Antimicrobial and Virulence-Modulating Effects of Clove Essential Oil on the Foodborne Pathogen Campylobacter jejuni. 2016 , 82, 6158-6166	39
820	Identification of low abundance cyclophilins in human plasma. 2016 , 16, 2815-2826	4
819	A quantitative proteomic approach to highlight Phragmites sp. adaptation mechanisms to chemical stress induced by a textile dyeing pollutant. 2016 , 573, 788-798	10

818	Data from quantitative label free proteomics analysis of rat spleen. 2016 , 8, 494-500	3
817	Post-translational modifications are enriched within protein functional groups important to bacterial adaptation within a deep-sea hydrothermal vent environment. 2016 , 4, 49	24
816	Global MS-Based Proteomics Drug Profiling. 2016 , 1449, 469-79	1
815	Physico-chemical characteristics and primary structure of an affinity-purified £D-galactose-specific, jacalin-related lectin from the latex of mulberry (Morus indica). 2016 , 609, 59-68	7
814	Approaches for Preparation and Biophysical Characterization of Transmembrane L-Barrels. 2016 , 49-116	1
813	Microbial assisted industrially important multiple enzymes from fish processing waste: purification, characterization and application for the simultaneous hydrolysis of lipid and protein molecules. 2016 , 6, 93602-93620	9
812	A chemical biology route to site-specific authentic protein modifications. 2016 , 354, 623-626	151
811	HIF-2phosphorylation by CK1promotes erythropoietin secretion in liver cancer cells under hypoxia. 2016 , 129, 4213-4226	20
810	Proteomics Analysis with a Nano Random Forest Approach Reveals Novel Functional Interactions Regulated by SMC Complexes on Mitotic Chromosomes. 2016 , 15, 2802-18	16
809	Quantitative Protein Sulfenic Acid Analysis Identifies Platelet Releasate-Induced Activation of Integrin 🛮 on Monocytes via NADPH Oxidase. 2016 , 15, 4221-4233	10
808	Visualizing the phage T4 activated transcription complex of DNA and E. coli RNA polymerase. 2016 , 44, 7974-88	7
807	DmicDechniques for Nanosafety. 2016 , 287-318	O
806	Identification of Bremia lactucae and Oidium neolycopersici proteins extracted for intact spore MALDI mass spectrometric biotyping. 2016 , 37, 2940-2952	5
805	Disulfide Bond Pattern of Transforming Growth Factor [-Induced Protein. 2016 , 55, 5610-5621	10
804	A combined proteomic and transcriptomic analysis of slime secreted by the southern bottletail squid, Sepiadarium austrinum (Cephalopoda). 2016 , 148, 170-82	11
803	Biomolecular proteomics discloses ATP synthase as the main target of the natural glycoside deglucoruscin. 2016 , 12, 3132-8	2
802	N-acetylcysteine with apocynin prevents hyperoxaluria-induced mitochondrial protein perturbations in nephrolithiasis. 2016 , 50, 1032-44	8
801	☐Boswellic acid, a bioactive substance used in food supplements, inhibits protein synthesis by targeting the ribosomal machinery. 2016 , 51, 821-7	5

800	SPATA2 promotes CYLD activity and regulates TNF-induced NF-B signaling and cell death. 2016 , 17, 1485-1497	76
799	Arabidopsis transcriptional repressor VAL1 triggers Polycomb silencing at FLC during vernalization. 2016 , 353, 485-8	136
798	Direct targeting of membrane fusion by SNARE mimicry: Convergent evolution of Legionella effectors. 2016 , 113, 8807-12	24
797	A possible serologic biomarker for maternal immune activation-associated neurodevelopmental disorders found in the rat models. 2016 , 113, 63-70	5
796	Direct Functional Interaction of the Kinesin-13 Family Member Kinesin-like Protein 2A (Kif2A) and Arf GAP with GTP-binding Protein-like, Ankyrin Repeats and PH Domains1 (AGAP1). 2016 , 291, 21350-21362	4
795	Abundant Lysine Methylation and N-Terminal Acetylation in Sulfolobus islandicus Revealed by Bottom-Up and Top-Down Proteomics. 2016 , 15, 3388-3404	23
794	Sequential Poly-ubiquitylation by Specialized Conjugating Enzymes Expands the Versatility of a Quality Control Ubiquitin Ligase. 2016 , 63, 827-39	45
793	High Sensitivity Crosslink Detection Coupled With Integrative Structure Modeling in the Mass Spec Studio. 2016 , 15, 3071-80	27
792	Distinct recruitment of human eIF4E isoforms to processing bodies and stress granules. 2016 , 17, 21	25
791	Quantitative Proteomics Analysis of Leukemia Cells. 2016 , 1465, 139-48	О
790	Adipocyte-secreted chemerin is processed to a variety of isoforms and influences MMP3 and chemokine secretion through an NFkB-dependent mechanism. 2016 , 436, 114-29	17
789	Minor intron splicing is regulated by FUS and affected by ALS-associated FUS mutants. 2016 , 35, 1504-21	69
788	Kank2 activates talin, reduces force transduction across integrins and induces central adhesion formation. 2016 , 18, 941-53	100
787	A Family of Negative Regulators Targets the Committed Step of de Novo Fatty Acid Biosynthesis. 2016 , 28, 2312-2325	29
786	Hydrophobic Interactions Contribute to Conformational Stabilization of Endoglycoceramidase II by Mechanism-Based Probes. 2016 , 55, 4823-35	6
785	An early dysregulation of FAK and MEK/ERK signaling pathways precedes the Damyloid deposition in the olfactory bulb of APP/PS1 mouse model of Alzheimer's disease. 2016 , 148, 149-58	36
7 ⁸ 4	Biochemical fate of vicilin storage protein during fermentation and drying of cocoa beans. 2016 , 90, 53-65	29
783	Carbene footprinting accurately maps binding sites in protein-ligand and protein-protein interactions. 2016 , 7, 13288	51

(2018-2016)

782	Proteomic based approach for characterizing 4-hydroxy-2-nonenal induced oxidation of buffalo () and goat () meat myoglobins. 2016 , 14, 18	5
781	Quantitative Protein Profiling of Chlamydia trachomatis Growth Forms Reveals Defense Strategies Against Tryptophan Starvation. 2016 , 15, 3540-3550	12
780	Manual of Cardiovascular Proteomics. 2016,	2
779	SUMO Signaling by Hypoxic Inactivation of SUMO-Specific Isopeptidases. 2016 , 16, 3075-3086	25
778	BRG1 interacts with GLI2 and binds Mef2c gene in a hedgehog signalling dependent manner during in vitro cardiomyogenesis. 2016 , 16, 27	1
777	Metaproteomic analysis of atmospheric aerosol samples. 2016 , 408, 6337-48	13
776	Abundant cysteine side reactions in traditional buffers interfere with the analysis of posttranslational modifications and protein quantification - How to compromise. 2016 , 30, 1823-8	8
775	PADI2-mediated citrullination is required for efficient oligodendrocyte differentiation and myelination.	1
774	Protein aggregation capture on microparticles enables multi-purpose proteomics sample preparation.	1
773	PRMT1-mediated methylation of the Large Drosha Complex regulates microRNA biogenesis.	1
772	Competitive Inhibitors of Ras Effector Binding.	1
772 771	Competitive Inhibitors of Ras Effector Binding. A conserved SUMO-Ubiquitin pathway directed by RNF4/SLX5-SLX8 and PIAS4/SIZ1 drives proteasomal degradation of topoisomerase DNA-protein crosslinks.	
	A conserved SUMO-Ubiquitin pathway directed by RNF4/SLX5-SLX8 and PIAS4/SIZ1 drives	1
771	A conserved SUMO-Ubiquitin pathway directed by RNF4/SLX5-SLX8 and PIAS4/SIZ1 drives proteasomal degradation of topoisomerase DNA-protein crosslinks.	1 5
771	A conserved SUMO-Ubiquitin pathway directed by RNF4/SLX5-SLX8 and PIAS4/SIZ1 drives proteasomal degradation of topoisomerase DNA-protein crosslinks. Plasmodium falciparumimmunodominant IgG epitopes in subclinical malaria. Novel functional insights revealed by distinct protein-protein interactions of the residual SWI/SNF	1 5 1
771 770 769	A conserved SUMO-Ubiquitin pathway directed by RNF4/SLX5-SLX8 and PIAS4/SIZ1 drives proteasomal degradation of topoisomerase DNA-protein crosslinks. Plasmodium falciparumimmunodominant IgG epitopes in subclinical malaria. Novel functional insights revealed by distinct protein-protein interactions of the residual SWI/SNF complex in SMARCA4-deficient small cell carcinoma of the ovary, hypercalcemic type.	1 5 1
771 770 769 768	A conserved SUMO-Ubiquitin pathway directed by RNF4/SLX5-SLX8 and PIAS4/SIZ1 drives proteasomal degradation of topoisomerase DNA-protein crosslinks. Plasmodium falciparumimmunodominant IgG epitopes in subclinical malaria. Novel functional insights revealed by distinct protein-protein interactions of the residual SWI/SNF complex in SMARCA4-deficient small cell carcinoma of the ovary, hypercalcemic type. Mass-spectrometry based proteomics reveals mitochondrial supercomplexome plasticity.	1 5 1 3

764	Flow virometric sorting and analysis of HIV quasispecies from plasma. 2017, 2, e90626	11
763	A specific phosphorylation regulates the protective role of A-crystallin in diabetes. 2018, 3,	18
762	Antigen-mediated regulation in monoclonal gammopathies and myeloma. 2018, 3,	28
761	Impaired plasma membrane localization of ubiquitin ligase complex underlies 3-M syndrome development. 2019 , 129, 4393-4407	6
760	Hyposialylated IgG activates endothelial IgG receptor FcRIIB to promote obesity-induced insulin resistance. 2018 , 128, 309-322	52
759	Efficient isolation of chloroplasts from in vitro shoots of Malus and Prunus. 2018 , 105, 171-176	1
758	The Calponin Family Member CHDP-1 Interacts with Rac/CED-10 to Promote Cell Protrusions. 2016 , 12, e1006163	6
757	Chromatin modifiers and recombination factors promote a telomere fold-back structure, that is lost during replicative senescence. 2020 , 16, e1008603	2
756	Comparative Proteomics Identifies Host Immune System Proteins Affected by Infection with Mycobacterium bovis. 2016 , 10, e0004541	9
755	Two highly conserved cysteine residues in HPV16 L2 form an intramolecular disulfide bond and are critical for infectivity in human keratinocytes. 2009 , 4, e4463	48
754	ESNOQ, proteomic quantification of endogenous S-nitrosation. 2010 , 5, e10015	30
753	Determination of the proteolytic cleavage sites of the amyloid precursor-like protein 2 by the proteases ADAM10, BACE1 and Elecretase. 2011 , 6, e21337	35
752	A thermophilic ionic liquid-tolerant cellulase cocktail for the production of cellulosic biofuels. 2012 , 7, e37010	87
751	Genes for the major structural components of Thermotogales species' togas revealed by proteomic and evolutionary analyses of OmpA and OmpB homologs. 2012 , 7, e40236	13
750	Proteomic investigation of falciparum and vivax malaria for identification of surrogate protein markers. 2012 , 7, e41751	47
749	Down-regulation of small rubber particle protein expression affects integrity of rubber particles and rubber content in Taraxacum brevicorniculatum. 2012 , 7, e41874	60
748	Human mesenchymal stem cell expression program upon extended ex-vivo cultivation, as revealed by 2-DE-based quantitative proteomics. 2012 , 7, e43523	43
747	Comparative proteome analysis of Milnesium tardigradum in early embryonic state versus adults in active and anhydrobiotic state. 2012 , 7, e45682	21

(2014-2013)

746	Identification and functional characterization of a novel monotreme- specific antibacterial protein expressed during lactation. 2013 , 8, e53686	12
745	A natural-like synthetic small molecule impairs bcr-abl signaling cascades and induces megakaryocyte differentiation in erythroleukemia cells. 2013 , 8, e57650	11
744	Culturing on Wharton's jelly extract delays mesenchymal stem cell senescence through p53 and p16INK4a/pRb pathways. 2013 , 8, e58314	32
743	Selective selC-independent selenocysteine incorporation into formate dehydrogenases. 2013 , 8, e61913	12
742	Localization of HPV-18 E2 at mitochondrial membranes induces ROS release and modulates host cell metabolism. 2013 , 8, e75625	52
741	Amyloid beta(1-40)-induced astrogliosis and the effect of genistein treatment in rat: a three-dimensional confocal morphometric and proteomic study. 2013 , 8, e76526	23
740	Characterization of angiotensin-converting enzyme 2 ectodomain shedding from mouse proximal tubular cells. 2014 , 9, e85958	42
739	Structural basis of thermal stability of the tungsten cofactor synthesis protein MoaB from Pyrococcus furiosus. 2014 , 9, e86030	3
738	A systems biology approach to the characterization of stress response in Dermacentor reticulatus tick unfed larvae. 2014 , 9, e89564	33
737	Quantitative proteomic analysis of gene regulation by miR-34a and miR-34c. 2014 , 9, e92166	20
736	The S. pombe translation initiation factor eIF4G is Sumoylated and associates with the SUMO protease Ulp2. 2014 , 9, e94182	6
735	Molecular characterization and expression of a novel alcohol oxidase from Aspergillus terreus MTCC6324. 2014 , 9, e95368	5
734	Structural studies of an anti-inflammatory lectin from Canavalia boliviana seeds in complex with dimannosides. 2014 , 9, e97015	19
733	SIRT1 mediates FOXA2 breakdown by deacetylation in a nutrient-dependent manner. 2014 , 9, e98438	22
73²	Comprehensive identification of SUMO2/3 targets and their dynamics during mitosis. 2014 , 9, e100692	17
731	Proteomic analysis of chinook salmon (Oncorhynchus tshawytscha) ovarian fluid. 2014 , 9, e104155	25
730	Proteome analysis of human sebaceous follicle infundibula extracted from healthy and acne-affected skin. 2014 , 9, e107908	40
729	Structural and functional characterization of cleavage and inactivation of human serine protease inhibitors by the bacterial SPATE protease EspP#rom enterohemorrhagic E. coli. 2014 , 9, e111363	8

728	NAD(P)H-hydrate dehydratase- a metabolic repair enzyme and its role in Bacillus subtilis stress adaptation. 2014 , 9, e112590	9
727	Two cathepsins B are responsible for the yolk protein hydrolysis in Culex quinquefasciatus. 2015 , 10, e0118736	7
726	Production of functional human vitamin A transporter/RBP receptor (STRA6) for structure determination. 2015 , 10, e0122293	3
725	The pro-apoptotic BH3-only protein Bim interacts with components of the translocase of the outer mitochondrial membrane (TOM). 2015 , 10, e0123341	21
724	Quantitative Proteomics of an Amphibian Pathogen, Batrachochytrium dendrobatidis, following Exposure to Thyroid Hormone. 2015 , 10, e0123637	4
723	Redox proteomics of the inflammatory secretome identifies a common set of redoxins and other glutathionylated proteins released in inflammation, influenza virus infection and oxidative stress. 2015 , 10, e0127086	52
722	Evaluating the Hypoxia Response of Ruffe and Flounder Gills by a Combined Proteome and Transcriptome Approach. 2015 , 10, e0135911	12
721	Genetically and Phenotypically Distinct Pseudomonas aeruginosa Cystic Fibrosis Isolates Share a Core Proteomic Signature. 2015 , 10, e0138527	20
720	Search for Allergens from the Pollen Proteome of Sunflower (Helianthus annuus L.): A Major Sensitizer for Respiratory Allergy Patients. 2015 , 10, e0138992	26
719	An Enzyme from Aristolochia indica Destabilizes Fibrin-🏿 Amyloid Co-Aggregate: Implication in Cerebrovascular Diseases. 2015 , 10, e0141986	5
718	Transcriptional and Proteomic Profiling of Aspergillus flavipes in Response to Sulfur Starvation. 2015 , 10, e0144304	26
717	Proteomic Analysis of the Schistosoma mansoni Miracidium. 2016 , 11, e0147247	25
716	Identification of Immunoreactive Leishmania infantum Protein Antigens to Asymptomatic Dog Sera through Combined Immunoproteomics and Bioinformatics Analysis. 2016 , 11, e0149894	20
715	The Maltase Involved in Starch Metabolism in Barley Endosperm Is Encoded by a Single Gene. 2016 , 11, e0151642	15
714	The dsRNA Virus Papaya Meleira Virus and an ssRNA Virus Are Associated with Papaya Sticky Disease. 2016 , 11, e0155240	24
713	Mutation in the Pro-Peptide Region of a Cysteine Protease Leads to Altered Activity and Specificity-A Structural and Biochemical Approach. 2016 , 11, e0158024	5
712	Ribosomopathy-like properties of murine and human cancers. 2017 , 12, e0182705	19
711	Analysis of the SUMO2 Proteome during HSV-1 Infection. 2015 , 11, e1005059	51

(2015-2016)

710	Interactions of Prototype Foamy Virus Capsids with Host Cell Polo-Like Kinases Are Important for Efficient Viral DNA Integration. 2016 , 12, e1005860	5
709	Lactoferrin binding protein B - a bi-functional bacterial receptor protein. 2017 , 13, e1006244	16
708	Seizure protein 6 controls glycosylation and trafficking of kainate receptor subunits GluK2 and GluK3. 2020 , 39, e103457	13
707	Linc-MYH configures INO80 to regulate muscle stem cell numbers and skeletal muscle hypertrophy. 2020 , 39, e105098	4
706	Intrinsically disordered protein PID-2 modulates Z granules and is required for heritable piRNA-induced silencing in the Caenorhabditis elegans embryo. 2021 , 40, e105280	6
7°5	[Experimental estimation of proteome size for cells and human plasma]. 2015 , 61, 279-85	7
704	[Influence of cultivation conditions on the proteomic profile of Mycobacterium tuberculosis H37RV]. 2017 , 63, 334-340	2
703	Quantitative proteomics of rat livers shows that unrestricted feeding is stressful for proteostasis with implications on life span. 2016 , 8, 1735-58	14
702	Nuclear Nox4 interaction with prelamin A is associated with nuclear redox control of stem cell aging. 2018 , 10, 2911-2934	19
701	LAIR-1 suppresses cell growth of ovarian cancer cell via the PI3K-AKT-mTOR pathway. 2020 , 12, 16142-16154	3
701 700	LAIR-1 suppresses cell growth of ovarian cancer cell via the PI3K-AKT-mTOR pathway. 2020 , 12, 16142-16154 Plasma membrane proteomics identifies biomarkers associated with MMSET overexpression in T(4;14) multiple myeloma. 2013 , 4, 1008-18	24
	Plasma membrane proteomics identifies biomarkers associated with MMSET overexpression in	
700	Plasma membrane proteomics identifies biomarkers associated with MMSET overexpression in T(4;14) multiple myeloma. 2013 , 4, 1008-18 Quantitative proteomics reveals Piccolo as a candidate serological correlate of recovery from	
700 699	Plasma membrane proteomics identifies biomarkers associated with MMSET overexpression in T(4;14) multiple myeloma. 2013, 4, 1008-18 Quantitative proteomics reveals Piccolo as a candidate serological correlate of recovery from Guillain-Barrßyndrome. 2016, 7, 74582-74591 High-throughput proteome analysis reveals targeted TRPM8 degradation in prostate cancer. 2017,	24
700 699 698	Plasma membrane proteomics identifies biomarkers associated with MMSET overexpression in T(4;14) multiple myeloma. 2013, 4, 1008-18 Quantitative proteomics reveals Piccolo as a candidate serological correlate of recovery from Guillain-Barr[syndrome. 2016, 7, 74582-74591 High-throughput proteome analysis reveals targeted TRPM8 degradation in prostate cancer. 2017, 8, 12877-12890 Tick-host conflict: immunoglobulin E antibodies to tick proteins in patients with anaphylaxis to tick	24 2 12
700 699 698	Plasma membrane proteomics identifies biomarkers associated with MMSET overexpression in T(4;14) multiple myeloma. 2013, 4, 1008-18 Quantitative proteomics reveals Piccolo as a candidate serological correlate of recovery from Guillain-Barr yndrome. 2016, 7, 74582-74591 High-throughput proteome analysis reveals targeted TRPM8 degradation in prostate cancer. 2017, 8, 12877-12890 Tick-host conflict: immunoglobulin E antibodies to tick proteins in patients with anaphylaxis to tick bite. 2017, 8, 20630-20644 A systematic approach for peptide characterization of B-cell receptor in chronic lymphocytic	24 2 12 39
700 699 698 697	Plasma membrane proteomics identifies biomarkers associated with MMSET overexpression in T(4;14) multiple myeloma. 2013, 4, 1008-18 Quantitative proteomics reveals Piccolo as a candidate serological correlate of recovery from Guillain-BarrGyndrome. 2016, 7, 74582-74591 High-throughput proteome analysis reveals targeted TRPM8 degradation in prostate cancer. 2017, 8, 12877-12890 Tick-host conflict: immunoglobulin E antibodies to tick proteins in patients with anaphylaxis to tick bite. 2017, 8, 20630-20644 A systematic approach for peptide characterization of B-cell receptor in chronic lymphocytic leukemia cells. 2017, 8, 42836-42846 Analyzing the influence of kinase inhibitors on DNA repair by differential proteomics of	24 2 12 39 5

692	YBX1/YB-1 induces partial EMT and tumourigenicity through secretion of angiogenic factors into the extracellular microenvironment. 2015 , 6, 13718-30	53
691	miR-200c dampens cancer cell migration via regulation of protein kinase A subunits. 2015 , 6, 23874-89	19
690	Molecular profiling of cetuximab and bevacizumab treatment of colorectal tumours reveals perturbations in metabolic and hypoxic response pathways. 2015 , 6, 38166-80	13
689	The levels of serine proteases in colon tissue interstitial fluid and serum serve as an indicator of colorectal cancer progression. 2016 , 7, 32592-606	19
688	⊕efensin HD5 Stabilizes Capsid/Core Interactions. 2019 , 4, 196-234	7
687	Identification and mapping of central pair proteins by proteomic analysis. 2020 , 17, 71-85	16
686	Diversity of ejaculated sperm proteins in Moxot bucks () evaluated by multiple extraction methods. 2018 , 15, 84-92	1
685	Evaluation of the proteomic profiles of ejaculated spermatozoa from Saanen bucks (). 2019 , 16, 902-913	2
684	Identification of Cysteine Ubiquitylation Sites on the Sec23A Protein of the COPII Complex Required for Vesicle Formation from the ER. 2017 , 11, 36-46	8
683	Identification of RNase-sensitive LINE-1 Ribonucleoprotein Interactions by Differential Affinity Immobilization. 2019 , 9,	3
682	Biochemical Pulldown of mRNAs and Long Noncoding RNAs from Cellular Lysates Coupled with Mass Spectrometry to Identify Protein Binding Partners. 2020 , 10, e3639	1
681	Analysis of K-Ras Interactions by Biotin Ligase Tagging. 2017 , 14, 225-239	7
680	Assessment of Heterotrophic Nitrification Capacity in Bacillus spp. and its Potential Application in the Removal of Nitrogen from Aquaculture Water. 2019 , 13, 1893-1908	2
679	Plasma gelsolin protein: a candidate biomarker for hepatitis B-associated liver cirrhosis identified by proteomic approach. 2010 , 8 Suppl 3, s105-12	8
678	Oxidative stress and caspase-mediated fragmentation of cytoplasmic domain of erythrocyte band 3 during blood storage. 2012 , 10 Suppl 2, s55-62	23
677	Analysis of Nickel-Binding Proteins from Various Animal Sera. 2018 , 62, 59-66	2
676	BACE2 distribution in major brain cell types and identification of novel substrates. 2018 , 1, e201800026	27
675	Fibril-induced glutamine-/asparagine-rich prions recruit stress granule proteins in mammalian cells. 2019 , 2,	6

(2018-2016)

674	Proteomics analysis of the response of the marine bacterium Marinobacter adhaerens HP15 to the diatom Thalassiosira weissflogii. 2016 , 78, 65-79	10
673	Structural Analysis of Jumbo Coliphage phAPEC6. 2020 , 21,	5
672	Purification and Characterization of Recombinant Expressed Apple Allergen Mal d 1. 2020, 4,	4
671	N-terminal VP1 Truncations Favor = 1 Norovirus-Like Particles. 2020 , 9,	8
670	Lipid Droplet Isolation for Quantitative Mass Spectrometry Analysis. 2017,	2
669	Changes in Protein Expression in Peanut Leaves in the Response to Progressive Water Stress. 2015 , 18, 19-26	2
668	Comparative proteomic analysis of sequential isolates of Mycobacterium tuberculosis from a patient with pulmonary tuberculosis turning from drug sensitive to multidrug resistant. 2015 , 141, 27-45	36
667	Comparative Proteomics Reveals Set of Oxidative Stress and Thaumatin-Like Proteins Associated with Resistance to Late Blight of Tomato. 2018 , 09, 789-816	1
666	Shotgun analysis on the peritrophic membrane of the silkworm Bombyx mori. 2012 , 45, 665-70	18
665	P1 peptidase of Pea seed-borne mosaic virus contains non-canonical C2H2 zinc finger and may act in a truncated form. 2014 , 3, 1	3
664	Sodium taurocholate cotransporting polypeptide is a functional receptor for human hepatitis B and D virus. 2012 , 1, e00049	1216
663	Coordination of peptidoglycan synthesis and outer membrane constriction during Escherichia coli cell division. 2015 , 4,	127
662	ETO family protein Mtgr1 mediates Prdm14 functions in stem cell maintenance and primordial germ cell formation. 2015 , 4, e10150	40
661	The MAP kinase pathway coordinates crossover designation with disassembly of synaptonemal complex proteins during meiosis. 2016 , 5, e12039	21
660	BRAF activates PAX3 to control muscle precursor cell migration during forelimb muscle development. 2016 , 5,	12
659	Oral transfer of chemical cues, growth proteins and hormones in social insects. 2016 , 5,	61
658	Anti-nociceptive action of peripheral mu-opioid receptors by G-beta-gamma protein-mediated inhibition of TRPM3 channels. 2017 , 6,	57
657	SETD3 protein is the actin-specific histidine -methyltransferase. 2018 , 7,	50

656	Endothelial PKA activity regulates angiogenesis by limiting autophagy through phosphorylation of ATG16L1. 2019 , 8,	15
655	Evolution of Yin and Yang isoforms of a chromatin remodeling subunit precedes the creation of two genes. 2019 , 8,	4
654	TRF1 averts chromatin remodelling, recombination and replication dependent-break induced replication at mouse telomeres. 2020 , 9,	14
653	A small protein encoded by a putative lncRNA regulates apoptosis and tumorigenicity in human colorectal cancer cells. 2020 , 9,	16
652	The tricuspid valve also maladapts as shown in sheep with biventricular heart failure. 2020 , 9,	2
651	An evolving computational platform for biological mass spectrometry: workflows, statistics and data mining with MASSyPup64. 2015 , 3, e1401	16
650	Proteomics alterations in chicken jejunum caused by 24 h fasting. 2019 , 7, e6588	4
649	Proteomic analysis and interactions network in leaves of mycorrhizal and nonmycorrhizal sorghum plants under water deficit. 2020 , 8, e8991	4
648	The New Omics Era into Systems Approaches: What Is the Importance of Separation Techniques?. 2021 , 1336, 1-15	
647	An Approach to Measuring Protein Turnover in Human Induced Pluripotent Stem Cell Organoids by Mass Spectrometry.	
646	Molecular Characterization of Novel x-Type HMW Glutenin Subunit 1B 🛭 16.5 in Wheat. 2021 , 10,	
645	Extraction, purification by cation exchange supermacroporous cryogel and physico-chemical characterization of <code>tonglutin</code> from lupin seeds (Lupinus albus L.). 2021 ,	O
644	<u>°⊞100 (1800)</u> 11 (1800)	
643	A possible role of gas-phase electrophoretic mobility molecular analysis (nES GEMMA) in extracellular vesicle research. 2021 , 413, 7341-7352	O
642	Regulation of electrogenic Na /HCO cotransporter 1 (NBCe1) function and its dependence on m-TOR mediated phosphorylation of Ser. 2021 ,	0
641	Inhibition of Serine Protease, Amylase and Growth of Phytopathogenic Fungi by Antimicrobial Peptides from Capsicum chinense Fruits. 2021 , 1	О
640	Nuclear PHGDH promotes neutrophil recruitment to drive liver cancer progression.	1
639	Nuclear import and chaperoning of monomeric histones H3 and H4 is mediated by Imp5, NASP and the HAT1 complex.	

638	Structural and functional consequences of NEDD8 phosphorylation. 2021, 12, 5939	2
637	Genetically encoded dihydroxyphenylalanine coupled with tyrosinase for strain promoted labeling. 2021 , 50, 116460	
636	Clinicopathological and Fecal Proteome Evaluations in 16 Dogs Presenting Chronic Diarrhea Associated with Lymphangiectasia. 2021 , 8,	2
635	Small extracellular vesicles from malignant ascites of patients with advanced ovarian cancer provide insights into the dynamics of the extracellular matrix. 2021 , 15, 3596-3614	1
634	Increased abundance of Cbl E3 ligases alters PDGFR signaling in recessive dystrophic epidermolysis bullosa. 2021 , 103-104, 58-73	O
633	Development of a Platform for Producing Recombinant Protein Components of Epitope Vaccines for the Prevention of COVID-19. 2021 , 86, 1275-1287	1
632	Drug affinity responsive target stability (DARTS) accelerated small molecules target discovery: Principles and application. 2021 , 194, 114798	5
631	Identification of SUMO Targets Associated With the Pluripotent State in Human Stem Cells. 2021 , 20, 100164	1
630	Relationship of Motility Activation to Lipid Composition, Protein Profile, and Swelling Rate of Burbot Lota lota Spermatozoon Following Change of Temperature and Osmolality. 2021 , 8,	
629	Selection of Specific Nanobodies against Lupine Allergen Lup an 1 for Immunoassay Development. 2021 , 10,	O
628	Progressive chromatin silencing of ABA biosynthesis gene permits seed germination in Arabidopsis.	0
627	The Specific Elongation Factor to Selenocysteine Incorporation in Escherichia coli: Unique tRNA Recognition and its Interactions. 2021 , 433, 167279	1
626	Introduction. 2011 , 241-243	
625	Sample Preparation and In Gel Tryptic Digestion for Mass Spectrometry Experiments. 2011 , 289-291	O
624	Eggs. 2013 , 305-321	
623	Proteomics analysis of contact-initiated eph receptor-ephrin signaling. 2013, 1066, 1-16	
622	CHAPTER 11:Next Generation Proteomics: PTMs in Space and Time. 2014 , 233-256	
621	Proteomic analysis of perfusate from in situ rat placenta perfusion. 2014 , 3, 1	

620	Partial Purification and Characterization of the Rat Parotid Gland Protein Kinase Catalyzing Phosphorylation of Matured Destrin at Ser-2. 2014 , 02, 100-112	
619	Candidates for New Molecules Controlling Allorecognition in Hydractinia symbiolongicarpus. 2014 , 259-263	1
618	Proteomics Methods. 2016 , 219-237	1
617	Identification of a novel putative interaction partner of the nucleoporin ALADIN.	
616	Lipid metabolic perturbation is an early-onset phenotype in adult spin mutants: a Drosophila model for lysosomal storage disorders.	
615	Regulation of eIF4F complex by the peptidyl prolyl isomerase FKBP7 in taxane-resistant prostate cancer.	
614	Platelet Proteomics and its Applications to Study Platelet-Related Disorders. 2017, 157-170	
613	Post-translational thioamidation of methyl-coenzyme M reductase, a key enzyme in methanogenic and methanotrophic Archaea.	
612	Intermolecular disulfide-bond formation in human FICD modulates the activity of the hyperactive E234G mutant.	
611	Translational repression of the Drosophila nanos mRNA involves the RNA helicase Belle and RNA coating by Me31B and Trailer hitch.	О
610	MS Western, a Method of Multiplexed Absolute Protein Quantification is a Practical Alternative to Western Blotting.	О
609	Structure and function of the intermembrane space domain of mammalian FoF1 ATP synthase.	
608	Codon-Dependent Translational Accuracy Controls Protein Quality in Escherichia coli but not in Saccharomyces cerevisiae.	
607	A Proteomic Approach to Evaluate the Effects of Endogenous Expression of Cryptogein Gene in Crypt-Transgenic Plants of Bacopa monnieri. 2017 , 4,	
606	Giant flagellins form thick flagellar filaments in two species of marine Eproteobacteria.	
605	Extraction of Antigenic Membrane Proteins from Salmonella Using Detergent and Phase Partition Method. 2017 , 13, 47-52	O
604	Long-read sequencing of nascent RNA reveals coupling among RNA processing events.	
603	Osteoglycin: A Novel Coordinator of Bone and Glucose Homeostasis.	1

602	Proteomic Profiling of Mammalian COPII Vesicles.	1
601	SETD3 protein is the actin-specific histidine N-methyltransferase.	
600	Identification of endogenous Adenomatous polyposis coli interaction partners and 	0
599	GTSF-1 is required for the formation of a functional RNA-dependent RNA Polymerase complex in C. elegans.	1
598	IDENTIFICATION OF IMMUNOGENIC PROTEINS OF STRAINS OF BACILLUS ANTHRACIS IN MALDI TOF MS. 2018 , 52-57	
597	Systematic Elucidation and Validation of OncoProtein-Centric Molecular Interaction Maps.	
596	Transcription apparatus of the yeast killer DNA plasmids: Architecture, function, and evolutionary origin.	
595	Crystallization and structure analysis of the core motif of the Pks13 acyltransferase domain from. 2018 , 6, e4728	3
594	Luciferase of the Japanese syllid polychaete Odontosyllis umdecimdonta.	2
593	Kunitz type protease inhibitor EgKI-1 from the canine tapeworm Echinococcus granulosus as a promising anti-cancer therapeutic.	O
592	A synthetic non-histone substrate provides insight into substrate targeting by the Gcn5 HAT and sirtuin HDACs.	
591	Regional diversity in the postsynaptic proteome of the mouse brain.	
590	Reconstitution of mammalian Cleavage Factor II involved in 3[processing of mRNA precursors.	
589	Pleotropic effects of mutations in the effector domain of influenza A virus NS1 protein.	
588	Extreme variation in rates of evolution in the plastid Clp protease complex.	
587	Quantitative proteomics of the 2016 WHONeisseria gonorrhoeaereference strains surveys vaccine candidates and antimicrobial resistance determinants.	
586	Analysing protein post-translational modform regions by linear programming.	
585	A folded conformation of MukBEF and Cohesin.	2

Profiling of the Muscle-Specific Dystroglycan Complexome Identifies Novel Muscular Dystrophy 584 Factors. Preparation of Samples for a Mass Spectrometry-Based Method to Identify Allergenic Proteins. 583 2019, 2020, 223-237 Spatial Regulation of Polo-like Kinase Activity during C. elegans Meiosis by the Nucleoplasmic 582 HAL-2/HAL-3 Complex. Endothelial PKA targets ATG16L1 to regulate angiogenesis by limiting autophagy. 581 A homozygous genome-edited Sept2-EGFP fibroblast cell line. 580 HCF-2 inhibits cell proliferation and activates differentiation-gene expression programs. 579 578 Discovery of functional alternatively spliced PKM transcripts in human cancers. O Biosynthesis of an Anti-Addiction Agent from the Iboga Plant. 577 TRF1 prevents permissive DNA damage response, recombination and Break Induced Replication at 576 telomeres. Bound-state diffusion due to binding to flexible polymers in a selective biofilter. 575 Mutation of Ebola virus VP35 Ser129 uncouples interferon antagonist and replication functions. 574 Novel Proteomic changes in Yeast Mitochondria provide insights into mitochondrial functioning 573 upon over-expression of human p53. ipaA triggers vinculin oligomerization to strengthen cell adhesion during Shigella invasion. 572 1 Affinity Proteomic Analysis of the Human Exosome and Its Cofactor Complexes. 2020, 2062, 291-325 2 571 NHerminal acetylation of proteins by NatA and NatB serves distinct physiological roles 570 inSaccharomyces cerevisiae. ARP-T1 is a ciliogenesis protein associated with a novel ciliopathy in inherited basal cell cancer, 569 Bazex-DuprEChristol Syndrome. Detection of Multisite Phosphorylation of Intrinsically Disordered Proteins Using Quantitative 568 Mass-Spectrometry. 2020, 2141, 819-833 Gel electrophoresis for phosphorylated proteins: a brief introduction. 2020, 64, 13-17

566	Lysine Acetylation Reshapes The Downstream Signaling Landscape of Vav1 in Lymphocytes.	O
565	Discovery of plasma protein biomarkers related to Alzheimer disease, sex and APOE genotype.	O
564	Parkinson disease-related phosphorylation at Tyr39 rearranges Bynuclein amyloid fibril structure revealed by cryo-EM.	
563	Serratia marcescenssecretes proteases and chitinases with larvicidal activity againstAnopheles dirus.	
562	Genomic innovation of ATD alleviates mistranslation associated with multicellularity in Animalia. 2020 , 9,	0
561	YTHDF1 drives intestinal immune response against bacterial infection.	
560	The Receptor Kinase BRI1 promotes cell proliferation in Arabidopsis by phosphorylation- mediated inhibition of the growth repressing peptidase DA1.	1
559	Mitochondrial Enzymes of the Urea Cycle Cluster at the Inner Mitochondrial Membrane.	
558	PIWIL1 Promotes Gastric Cancer via a piRNA-Independent Mechanism.	
557	The derlin Dfm1 promotes retrotranslocation of folded protein domains from the endoplasmic reticulum.	
556	Purification and Characterization of Natural Solid-Substrate Degrading and Alcohol Producing Hyperthermostable Alkaline Amylase from Bacillus cereus (sm-sr14). 2020 , 21, 872-881	
555	Protein tyrosine phosphatase-PEST (PTP-PEST) mediates hypoxia-induced endothelial autophagy and angiogenesis through AMPK activation.	O
554	Cyclin-dependent kinase 2 (Cdk2) controls phosphatase-regulated signaling and function in platelets.	
553	Src activates retrograde membrane traffic through phosphorylation of GBF1.	
552	Changes in hemoglobin function and isoform expression during embryonic development in the American alligator,. 2021 , 321, R869-R878	O
551	Proteomics analysis reveals several metabolic alterations in cyanobacterium Anabaena sp. NC-K1 in response to alpha-cypermethrin exposure. 2021 , 1	O
550	Binding of cytochrome P450 27C1, a retinoid desaturase, to its accessory protein adrenodoxin. 2021 , 714, 109076	О
549	Biomarkers in a socially exchanged /fluid reflect colony maturity, behavior, and distributed metabolism. 2021 , 10,	2

548	Comparative Structural and Compositional Analyses of Cow, Buffalo, Goat and Sheep Cream. 2021 , 10,	О
547	Chromatin modifiers and recombination factors promote a telomere fold-back structure, that is lost during replicative senescence.	
546	Insights into the proteomic profile and gene expression of Lutzomyia longipalpis-derived Lulo cell line. 2020 , 115, e200113	
545	Dietary Monoterpenoids As a New Class of Allosteric Human Aryl Hydrocarbon Receptor Antagonists.	
544	Early induction of antibacterial activities distinguishes response of mice to infection with non-permissive from response to permissive Salmonella.	
543	The Bark Beetle (Curculionidae: Scolytinae) Has Digestive Capacity to Degrade Complex Substrates: Functional Characterization and Heterologous Expression of an <code>HAmylase</code> . 2020 , 22,	Ο
542	Branching and Mixing: New Signals of the Ubiquitin Signaling System.	
541	Leaf proteome modulation and cytological features of seagrass Cymodocea nodosa in response to long-term high CO exposure in volcanic vents. 2020 , 10, 22332	1
540	The Phosphorylation Status of NPH3 Affects Photosensory Adaptation During the Phototropic Response.	1
539	Coupling Liquid Chromatography and Tandem Mass Spectrometry to Electrophoresis for In-Depth Analysis of Glycosaminoglycan Drugs: Heparin and the Multicomponent Sulodexide. 2021 , 93, 1433-1442	1
538	The SUMOylation pathway suppresses arbovirus replication in Aedes aegypti cells. 2020 , 16, e1009134	1
537	Influences of acid and ethanol stresses on Oenococcus oeni SD-2a and its proteomic and transcriptional responses. 2021 , 101, 2892-2900	3
536	Identification of SUMO targets required to maintain human stem cells in the pluripotent state.	
535	Co-option of a seed-like proteome by oil-rich tubers.	Ο
534	Fatty acid and proteomic analysis of Sterculia striata nut. 2020 , 40, 489-495	
533	Using Caenorhabditis elegans to produce functional secretory proteins of parasitic nematodes. 2022 , 225, 106176	
532	Cell size matters: Nano- and micro-plastics preferentially drive declines of large marine phytoplankton due to co-aggregation. 2022 , 424, 127488	2
531	Uterine infusion of conceptus fragments changes the protein profile from cyclic mares. 2020 , 17, e20200552	

530	Isolation of the Pistil-Stimulated Pollen Tube Secretome. 2020 , 2160, 41-72	1
529	Tracing the In Vivo Fate of Nanoparticles with a Non-SelfBiological Identity.	
528	A recombinant gp145 Env glycoprotein from HIV-1 expressed in two different cell lines: effects on glycosylation and antigenicity.	
527	Unprecedentedly efficient CUG initiation of an overlapping reading frame inPOLGmRNA yields novel protein POLGARF.	1
526	The IDR-containing protein PID-2 affects Z granules and is required for piRNA-induced silencing in the embryo.	
525	Histone variants in archaea and the evolution of combinatorial chromatin complexity.	1
524	ND3 Cys39 in complex I is exposed during mitochondrial respiration. 2021 ,	4
523	Galectin-1 Cooperates with Yersinia Outer Protein (Yop) P to Thwart Protective Immunity by Repressing Nitric Oxide Production. 2021 , 11,	O
522	Mesowestern Blot: Simultaneous Analysis of Hundreds of Sub-Microliter Lysates.	
521	MPK3- and MPK6-mediated VLN3 phosphorylation regulates actin dynamics during stomatal immunity in Arabidopsis. 2021 , 12, 6474	2
520	Purification and characterization of a highly thermostable GlcNAc-binding lectin from Collaea speciosa seeds. 2021 ,	
519	Pyocin-mediated antagonistic interactions in Pseudomonas spp. isolated in James Ross Island, Antarctica. 2021 ,	O
518	Abca8b promotes myelination via regulation of chondroitin sulfate proteoglycan 4 localization in oligodendrocyte precursor cells in mice. 2021 , 100147	O
517	TOC1 clock protein phosphorylation controls complex formation with NF-YB/C to repress hypocotyl growth. 2021 , e108684	4
516	The TFIIH Complex is Required to Establish and Maintain Mitotic Chromosome Structure.	
515	A new thermostable rhizopuspepsin: Purification and biochemical characterisation. 2021 , 112, 18-18	1
514	Comprehensive Atlas of the Myelin Basic Protein Interaction Landscape. 2021 , 11,	3
513	Transcription factor recruitment by parallel G-quadruplexes to promote transcription: the case of herpes simplex virus-1 ICP4.	1

Selective cross-linking of coinciding protein assemblies by in-gel cross-linking mass-spectrometry.

511	The tricuspid valve also maladapts: A multiscale study in sheep with biventricular heart failure.	
510	Mitochondrial, cell cycle control and neuritogenesis alterations in an iPSC-based neurodevelopmental model for schizophrenia.	О
509	Comparative Proteomic Profiles of Typical Strain and Genetically Altered Variant of Vibrio cholerae O1, Biovar El Tor. 2020 , 150-153	O
508	Promiscuous DNA cleavage by HpyAII endonuclease is modulated by the HNH catalytic residues. 2020 , 40,	
507	Identification of Stress-related Proteins during the Growth and Development of Piper nigrumL 2020 , 549, 012072	1
506	IM30 IDPs form a membrane protective carpet upon super-complex disassembly.	O
505	Proteomic analysis reveals Utf1 as a neurogenesis-associated new Sumo target.	
504	Age-Associated Insolubility of Parkin in Human Midbrain is Linked to Redox Balance and Sequestration of Reactive Dopamine Metabolites.	
503	N-terminal VP1 truncations favor T=1 norovirus-like particles.	
502	Tissue fractionation by hydrostatic pressure cycling technology: the unified sample preparation technique for systems biology studies. 2008 , 19, 189-99	27
501	Antibiotics and probiotics in chronic pouchitis: a comparative proteomic approach. 2010, 16, 30-41	11
500	Mass spectrometry-based proteomics for translational research: a technical overview. 2012 , 85, 59-73	20
499	Porcine salivary analysis by 2-dimensional gel electrophoresis in 3 models of acute stress: a pilot study. 2014 , 78, 127-32	3
498	Proteomic analysis of synovial fluid as an analytical tool to detect candidate biomarkers for knee osteoarthritis. 2015 , 8, 9975-89	19
497	Analysis of the effects of preservative-free tafluprost on the tear proteome. 2016 , 8, 4025-4039	6
496	Nuclear uptake of an amino-terminal fragment of apolipoprotein E4 promotes cell death and localizes within microglia of the Alzheimer's disease brain. 2017 , 9, 40-57	10
495	Morpho-Physiological and Proteomic Response of Bt-Cotton and Non-Bt Cotton to Drought Stress. 2021 , 12, 663576	

494	Formation of resting cells is accompanied with enrichment of ferritin in marine diatom Phaeodactylum tricornutum. 2022 , 61, 102567	О
493	Structure and activity of a novel robust peroxidase from Alkanna frigida cell culture. 2021 , 194, 113022	O
492	Proteomics and Interspecies Interaction Analysis Revealed Abscisic Acid Signalling to Be the Primary Driver for Oil Palm's Response against Red Palm Weevil Infestation 2021 , 10,	О
491	Smooth muscle-specific MMP17 (MT4-MMP) regulates the intestinal stem cell niche and regeneration after damage. 2021 , 12, 6741	4
490	Epitope-coated polymer particles elicit neutralising antibodies against Plasmodium falciparum sporozoites. 2021 , 6, 141	O
489	Comparative proteomic analysis of parasites isolated from visceral and cutaneous leishmaniasis patients. 2021 , 1-8	
488	Proteomic profiling of cryopreserved Trichormus variabilis using various cryoprotectants. 2021 , 104, 23-23	
487	CD47 interactions with exportin-1 limit the targeting of mG-modified RNAs to extracellular vesicles. 2021 , 1	2
486	Transcriptional activity and epigenetic regulation of transposable elements in the symbiotic fungus. 2021 ,	1
485	Focal adhesion kinase inhibitor TAE226 combined with Sorafenib slows down hepatocellular carcinoma by multiple epigenetic effects. 2021 , 40, 364	3
484	Expanding the Scope of Polyoxometalates as Artificial Proteases towards Hydrolysis of Insoluble Proteins. 2021 ,	0
483	Cellular Energy Sensor SNF1-Realted Protein Kinase 1 Represses E2F-Dependent G1-S Transition and Arabidopsis Growth.	
482	Iso-seco-tanapartholide activates Nrf2 signaling pathway through Keap1 modification and oligomerization to exert anti-inflammatory effects 2021 ,	1
481	Study of Glutathione S-transferase-P1 in cancer blood plasma after extraction by affinity magnetic nanoparticles and monitoring by MALDI-TOF, IM-Q-TOF and LC-ESI-Q-TOF MS 2021 , 1190, 123091	1
480	High-Performance Liquid ChromatographyMass Spectrometry in Peptide and Protein Analysis. 1-58	
479	Direct capture and selective elution of a secreted polyglutamate-tagged nanobody using bare magnetic nanoparticles 2022 , e2100577	O
478	Acid stress responses of and isolated from fermented sorghum gruel and their application in food fermentation 2022 ,	
477	Proteome Profiling of Cells Exposed to Nitrosative Stress 2022 , 7, 3470-3482	O

476	Analysis of plasma proteins using 2D gels and novel fluorescent probes: in search of blood based biomarkers for Alzheimer's disease 2022 , 20, 2	1
475	Quantitative proteomics revealed new functions of ALKBH4 2021 , e2100231	
474	Fine-tuned method to extract high purified proteins from the seagrass Halophila stipulacea to be used for proteome analyses. 1-9	
473	Selective multi-kinase inhibition sensitizes mesenchymal pancreatic cancer to immune checkpoint blockade by remodeling the tumor microenvironment 2022 ,	1
472	Synthesis and physicochemical characterization of zinc-lactoferrin complexes 2022,	1
471	Novel Peptide Motifs Containing Asp-Glu-Gly Target PY and Thromboxane A2 Receptors to Inhibit Platelet Aggregation and Thrombus Formation 2022 ,	1
470	Exploring the beneficial effects of Aloe vera on the kidneys of diabetic rats at the protein level. 2022 , 3, 100013	
469	Non canonical scaffold-type ligase complex mediates protein UFMylation.	O
468	Proteomic cellular signatures of kinase inhibitor-induced cardiotoxicity 2022, 9, 18	0
467	modulates host energy metabolism by ADP-ribosylation of ADP/ATP translocases 2022 , 11,	6
466	Revisiting the Non-Coding Nature of Pospiviroids 2022 , 11,	2
465	Exploring the Interactome of Cytochrome P450 2E1 in Human Liver Microsomes with Chemical Crosslinking Mass Spectrometry 2022 , 12,	1
464	Comparative Analysis of Type 1 and Type Z Protein Phosphatases Reveals D615 as a Key Residue for Ppz1 Regulation 2022 , 23,	O
463	Invariable Ribosome Stoichiometry During Murine Erythroid Differentiation: Implications for Understanding Ribosomopathies 2022 , 9, 805541	O
462	Angiopoietin-2-induced lymphatic endothelial cell migration drives lymphangiogenesis via the 🛭 integrin-RhoA-formin axis 2022 , 1	2
461	Dimerization of SARS-CoV-2 nucleocapsid protein affects sensitivity of ELISA based diagnostics of COVID-19 2022 , 200, 428-437	1
460	Protocol to characterize mitochondrial supercomplexes from mouse tissues by combining BN-PAGE and MS-based proteomics 2022 , 3, 101135	О
459	Desolvation-induced formation of recombinant camel serum albumin-based nanocomposite for glutathione colorimetric determination. 2022 , 357, 131417	2

458	Identification of industrial detergent enzymes by SDS-PAGE and MALDI-TOF mass spectrometry.	О
457	Affinity Purification Followed by Liquid Chromatography-Tandem Mass Spectrometry to Identify Proteins Interacting with ABA Signaling Components 2022 , 2462, 181-189	
456	Common Polymorphism That Protects From Cardiovascular Disease Increases Fibronectin Processing and Secretion 2022 , CIRCGEN121003428	0
455	SMYD5 is a histone H3-specific methyltransferase mediating mono-methylation of histone H3 lysine 36 and 37 2022 , 599, 142-147	2
454	Protein Level Defense Responses of Theobroma cacao Interaction With Phytophthora palmivora. 2022 , 4,	
453	Recharacterization of the Mammalian Cytosolic Type 2 (R)-Hydroxybutyrate Dehydrogenase (BDH2) as 4-Oxo-L-Proline Reductase (EC 1.1.1.104) 2022 , 101708	O
452	Membrane-associated cytoplasmic granules carrying the Argonaute protein WAGO-3 enable paternal epigenetic inheritance in Caenorhabditis elegans 2022 , 24, 217-229	3
451	Targeting NAAA counters dopamine neuron loss and symptom progression in mouse models of Parkinson's disease.	
450	Proteomic analysis of the mitochondrial glucocorticoid receptor interacting proteins reveals pyruvate dehydrogenase and mitochondrial 60 kDa heat shock protein as potent binding partners 2022 , 257, 104509	1
449	CYLD deficiency enhances metabolic reprogramming and tumor progression in nasopharyngeal carcinoma via PFKFB3 2022 , 532, 215586	0
448	Human cellular homeostasis buffers trans-acting translational effects of heterologous gene expression with very different codon usage bias.	0
447	Src activates retrograde membrane traffic through phosphorylation of GBF1. 2021, 10,	2
446	Is divalent magnesium cation the best cofactor for bacterial 🛭 galactosidase?. 2018, 43, 941-945	
445	Macromolecular properties and partial amino acid sequence of a Kunitz-type protease inhibitor from okra (seeds. 2019 , 44,	
444	A Mechanistic Understanding of Polyethylene Biodegradation by the Marine Bacterium Alcanivorax.	
443	The impact of the soluble protein fraction and kernel hardness on wheat flour starch digestibility.	
442	Data-Independent Acquisition Enables Robust Quantification of 400 Proteins in Non-Depleted Canine Plasma 2022 , 10,	1
441	Novel Exosome Biomarker Candidates for Alzheimer's Disease Unravelled Through Mass Spectrometry Analysis 2022 , 1	2

440	Identification of distinct cytotoxic granules as the origin of supramolecular attack particles in T lymphocytes 2022 , 13, 1029	6
439	Host Defense Peptides LL-37 and Lactoferrin Trigger ET Release from Blood-Derived Circulating Monocytes 2022 , 10,	O
438	Targeting tumor endothelial hyperglycolysis enhances immunotherapy through remodeling tumor microenvironment. 2022 ,	1
437	Mechanistic insights into the functioning of GMP synthetase: a two-subunit, allosterically regulated, ammonia tunnelling enzyme.	
436	Conformational Rearrangements in the Redox Cycling of NADPH-Cytochrome P450 Reductase from Explored with FRET and Pressure-Perturbation Spectroscopy 2022 , 11,	О
435	Zinc-binding proteins in stallion seminal plasma as potential sperm function regulators. 2022,	O
434	IRON REGULATORY PROTEIN (IRP)-MEDIATED IRON HOMEOSTASIS IS CRITICAL FOR NEUTROPHIL DEVELOPMENT AND DIFFERENTIATION IN THE BONE MARROW.	
433	SufB intein splicing in Mycobacterium tuberculosis is influenced by two remote conserved N-extein histidines 2022 , 42,	
432	Novel Phage, vB_Sen_STGO-35-1, Characterization and Evaluation in Chicken Meat 2022, 10,	1
431	Proteomic Analysis of Intracellular and Membrane-Associated Fractions of Canine () Epididymal Spermatozoa and Sperm Structure Separation 2022 , 12,	O
430	Analysis of laccase-like enzymes secreted by fungi isolated from a cave in northern Spain 2022, 11, e1279	1
429	Na,K-ATPase ∄ and ⊡subunits show distinct localizations in the nervous tissue of the large milkweed bug 2022 , 1	O
428	Pyk2 Regulates MAMs and Mitochondrial Dynamics in Hippocampal Neurons 2022, 11,	1
427	Sulphoraphane Affinity-Based Chromatography for the Purification of Myrosinase from Seeds 2022 , 12,	О
426	Proteome Analysis of Vacuoles Isolated from Fig (Ficus carica L.) Flesh during Fruit Development 2022 ,	О
425	Recombinant pro-CTSD (cathepsin D) enhances SNCA/岳ynuclein degradation in 岳ynucleinopathy models 2022 ,	1
424	The TFIIH complex is required to establish and maintain mitotic chromosome structure 2022, 11,	1
423	Comprehensive interactome analysis for the sole adenylyl cyclase Cyr1 of Candida albicans.	

422	EhVps23, an ESCRT-I Member, Is a Key Factor in Secretion, Motility, Phagocytosis and Tissue Invasion by 2022 , 12, 835654	1
421	An approach to measuring protein turnover in human induced pluripotent stem cell organoids by mass spectrometry 2022 ,	1
420	Hydrogen Peroxide Induced Antioxidant-Coupled Redox Regulation of Germination in Rice: Redox Metabolic, Transcriptomic and Proteomic Evidences. 1	1
419	Proteomic Analysis Reveals Enzymes for I-D-Glucan Formation and Degradation in TMW 1.2112 2022 , 23,	
418	Gel electrophoresis/electroelution sorting fractionator combined with filter aided sample preparation for deep proteomic analysis 2022 ,	
417	Protein arginine and lysine methylation in Trypanosoma cruzi.	
416	A Nanobody-Based Toolset to Monitor and Modify the Mitochondrial GTPase Miro1 2022 , 9, 835302	0
415	Legionella pneumophila temporally regulates the activity of ADP/ATP translocases by reversible ADP-ribosylation. 2022 , 1, 51-65	1
414	Capturing a rhodopsin receptor signalling cascade across a native membrane 2022,	4
413	The tobacco phosphatidylethanolamine-binding protein NtFT4 increases the lifespan of by interacting with the proteostasis network 2022 , 14,	
412	Allosteric transitions of rabbit skeletal muscle lactate dehydrogenase induced by pH-dependent dissociation of the tetrameric enzyme 2022 ,	1
411	Proteomic landscape subtype and clinical prognosis of patients with the cognitive impairment by Japanese encephalitis infection 2022 , 19, 77	Ο
410	Caspar, an adapter for VAPB and TER94, modulates the progression of ALS8 by regulating IMD/NFB mediated glial inflammation in a drosophila model of human disease 2022 ,	
409	Advances in mass spectrometry-based epitope mapping of protein therapeutics 2022 , 215, 114754	Ο
408	Cpmer: A new conserved eEF1A2-binding partner that regulates Eomes translation and cardiomyocyte differentiation 2022 ,	0
407	Discovery of a signaling feedback circuit that defines interferon responses in myeloproliferative neoplasms 2022 , 13, 1750	Ο
406	The plastoglobule-localized protein AtABC1K6 is a Mn-dependent kinase necessary for timely transition to reproductive growth 2022 , 101762	1
405	Feedlot diets containing different starch levels and additives change the cecal proteome involved in cattle's energy metabolism and inflammatory response 2022 , 12, 5691	1

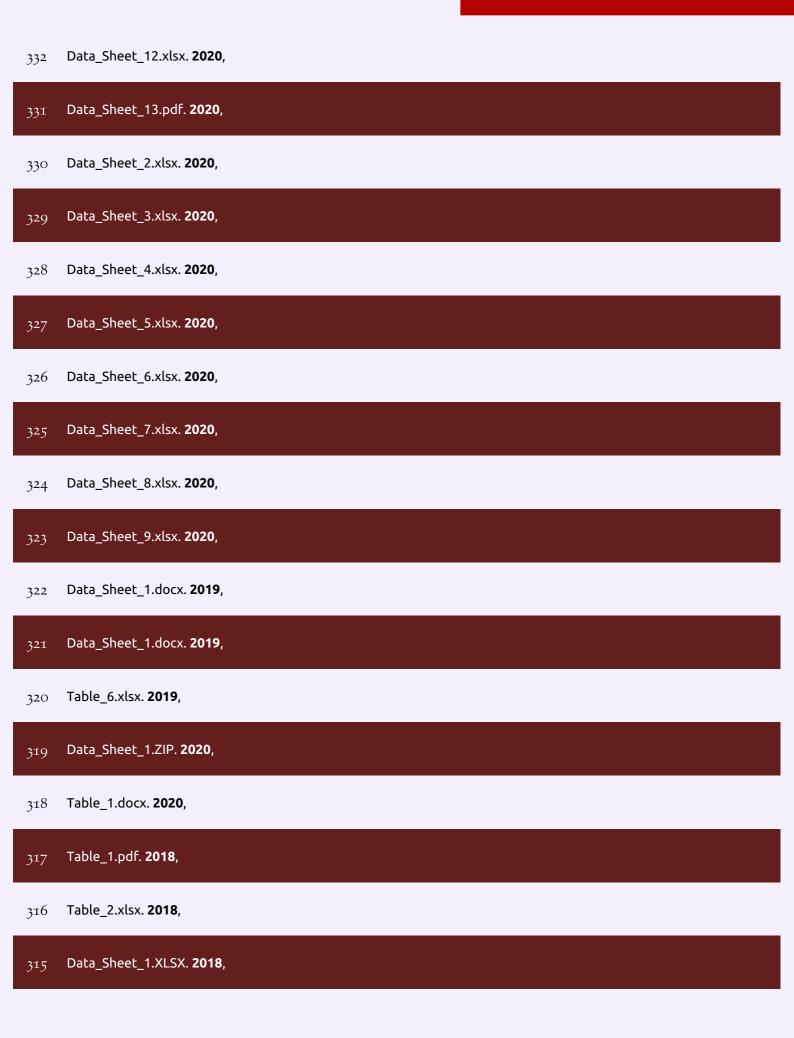
404	Structural, functional and proteomic differences of proteins extracted from white garlic and Laba garlic 2022 , 155, 111047	1
403	Tyrosine-sulfated dermatopontin shares multiple binding sites and recognition determinants on triple-helical collagens with proteins implicated in cell adhesion and collagen folding, fibrillogenesis, cross-linking, and degradation 2022 , 140771	O
402	Role of the nucleotide excision repair pathway proteins (UvrB and UvrD2) in recycling UdgB, a base excision repair enzyme in Mycobacterium smegmatis 2022 , 113, 103316	O
401	Combined proteomic strategies for in-depth venomic analysis of the beaked sea snake (Hydrophis schistosus) from Songkhla Lake, Thailand 2022 , 259, 104559	1
400	Technical report: In-gel sample preparation prior to proteomic analysis of bovine faeces increases protein identifications by removal of high molecular weight glycoproteins 2022 , 261, 104573	1
399	Unravelling gradient layers of microbial communities, proteins, and chemical structure in aerobic granules 2022 , 829, 154253	O
398	Gel Electrophoresis Chip Using Joule Heat Self-Dissipation, Short Run Time, and Online Dynamic Imaging 2021 ,	3
397	A nanobody-based toolset to monitor and modify the mitochondrial GTPase Miro1.	
396	A Lactic Acid Bacteria Consortium Impacted the Content of Casein-Derived Biopeptides in Dried Fresh Cheese 2021 , 27,	O
395	Protein Chemistry Combined with Mass Spectrometry for Protein Structure Determination 2021 ,	4
394	A dominant mutation in II-AMYLASE1 disrupts nighttime control of starch degradation in Arabidopsis leaves 2021 ,	O
393	Storage protein composition during germination and its association with physiological seed quality in common bean. 44, e53434	2
392	Trojan horse treatment based on PEG-coated extracellular vesicles to deliver doxorubicin to melanoma and 2021 , 1-16	5
391	Identification of Abscisic Acid-Dependent Phosphorylated Basic Helix-Loop-Helix Transcription Factors in Guard Cells of by Mass Spectrometry 2021 , 12, 735271	O
390	The phospho-docking protein 14-3-3 regulates microtubule-associated proteins in oocytes including the chromosomal passenger Borealin.	
389	Proteomic Analysis of Subchronic Furan Exposure in the Liver of Male Fischer F344 Rats 2022 , 50, 47-59	
388	The Mitochondrial Routing of the Kv1.3 Channel 2022 , 12, 865686	1
387	Proteolysis of adaptor protein Mmr1 during budding is necessary for mitochondrial homeostasis in Saccharomyces cerevisiae 2022 , 13, 2005	

386 Yeast Secretes High Amounts of Human Calreticulin without Cellular Stress. 2022, 44, 1768-1787 Application of Proteogenomics to Urine Analysis towards the Identification of Novel Biomarkers of 385 Prostate Cancer: An Exploratory Study.. 2022, 14, Immunoproteomic analysis of the secretome of bovine-adapted strains of Staphylococcus aureus 384 О demonstrates a strain-specific humoral response.. 2022, 249, 110428 Obtaining Complete Human Proteomes.. 2022, 383 The Lysosome Origin of Biosilica Machinery in the Demospongiae Model Petrosia ficiformis (Poiret, 382 1789). 2022, 9, Table_1.docx. 2019, 381 380 Data_Sheet_1.PDF. 2019, Data_Sheet_1.DOCX. 2018, 379 Image_1.TIF. 2018, 378 Image_2.TIF. 2018, 377 Table_1.XLSX. **2018**, 376 Video_1.MP4. 2018, 375 Video_2.MP4. 2018, 374 Video_3.MOV. **2018**, 373 Table_1.PDF. 2018, 372 Table_2.XLSX. **2018**, 371 Table_3.PDF. 2018, 370 Table_4.PDF. 2018, 369



(2020-2020)

Table_1.DOCX. 2020, 350 Data_Sheet_1.PDF. 2018, 349 Table_1.XLSX. 2020, 348 Table_2.docx. 2020, 347 346 Data_Sheet_1.PDF. 2019, Data_Sheet_1.docx. 2020, 345 DataSheet_1.pdf. 2020, 344 Table_1.xlsx. **2020**, 343 Table_2.xlsx. 2020, 342 Table_3.xlsx. **2020**, 341 Table_4.xlsx. 2020, 340 Table_1.xlsx. 2020, 339 338 Table_2.xlsx. 2020, Data_Sheet_1.PDF. 2020, 337 Data_Sheet_1.pdf. 2018, 336 Data_Sheet_1.pdf. 2020, 335 Data_Sheet_10.xlsx. 2020, 334 Data_Sheet_11.xlsx. 2020, 333



(2018-2018)

Data_Sheet_2.XLSX. 2018, 314 Data_Sheet_3.XLSX. 2018, 313 Data_Sheet_4.XLSX. 2018, 312 Data_Sheet_5.XLSX. 2018, 311 Data_Sheet_6.XLSX. 2018, 310 Image_1.TIF. 2018, 309 308 Image_2.TIF. 2018, Image_3.TIF. 2018, 307 Image_4.TIF. 2018, 306 Image_5.TIF. 2018, 305 Image_6.TIF. 2018, 304 Image_7.TIF. 2018, 303 302 Image_8.TIF. 2018, Table_1.PDF. 2018, 301 Table_2.PDF. 2018, 300 299 Image_1.pdf. **2018**, Image_2.pdf. 2018, 298 Image_3.pdf. 2018, 297

296	Table_1.pdf. 2018 ,
295	DataSheet_1.pdf. 2020 ,
294	Table_1.xls. 2020 ,
293	Data_Sheet_1.xlsx. 2019 ,
292	Data_Sheet_2.xlsx. 2019 ,
291	Table_1.docx. 2019 ,
290	Table_1.xls. 2018 ,
289	Table_2.xls. 2018 ,
288	Mycobacterium tuberculosis Transcription Factor EmbR Regulates the Expression of Key Virulence Factors That Aid in and Survival 2022 , e0383621
287	Morpho-Physiological and Proteomic Response of Bt-Cotton and Non-Bt Cotton to Drought Stress. 2021, 12, 663576
286	Sugar transporter Slc37a2 regulates bone metabolism via a dynamic tubular lysosomal network in osteoclasts.
285	Progressive chromatin silencing of ABA biosynthesis genes permits seed germination in Arabidopsis 2022 ,
284	Pre-existing Ab against vimentin leads to false-positive HLA Ab results in two pediatric heart transplant candidates 2022 , e14302
283	The Anti-Glucocorticoid Receptor Antibody Clone 5E4: Raising Awareness of Unspecific Antibody Binding 2022 , 23,
282	Structure and mechanism of a novel cytomegaloviral DCAF mediating interferon antagonism.
281	A mucin protein predominantly expressed in the female-specific symbiotic organ of the stinkbug Plautia stali 2022 , 12, 7782
280	Cell membrane enolase of Aedes albopictus C6/36 cells is involved in the entrance mechanism of dengue virus (DENV). 2022 , 25, 101924
279	Sample Preparation Matters for Peptide Mapping to Evaluate Deamidation of Adeno-Associated Virus (AAV) Capsid Proteins using LC-MS/MS 2022 ,

278	nicotinic acetylcholine receptor subunits and their native interactions with insecticidal peptide toxins 2022 , 11,	0
277	Human OTULIN haploinsufficiency impairs cell-intrinsic immunity to staphylococcal £oxin 2022, eabm6380	1
276	A Single Amino Acid Residue Controls Acyltransferase Activity in a Polyketide Synthase from Toxoplasma gondii. 2022 , 104443	1
275	Functional analysis of recombinant menthone menthol reductase by chiral GC and GC-MS. 2022 , 184, 115075	
274	Influence of Short and Medium Distance Road Transport on the Acute Phase Proteins in Horses.	
273	Juxtaposition of Bub1 and Cdc20 on phosphorylated Mad1 during catalytic mitotic checkpoint complex assembly.	Ο
272	A structural basis for prion strain diversity.	О
271	A Chloroplast Protein Atlas Reveals Novel Structures and Spatial Organization of Biosynthetic Pathways.	О
270	The Nse5/6-like SIMC1-SLF2 Complex Localizes SMC5/6 to Viral Replication Centers.	О
269	Thermophilic Geobacillus WSUCF1 Secretome for Saccharification of Ammonia Fiber Expansion and Extractive Ammonia Pretreated Corn Stover. 2022 , 13,	
268	The Caenorhabditis elegans TDRD5/7-like protein, LOTR-1, interacts with the helicase ZNFX-1 to balance epigenetic signals in the germline. 2022 , 18, e1010245	
267	5屆omiR-183-5p +2 elicits tumor suppressor activity in a negative feedback loop with E2F1. 2022 , 41,	
266	A Mechanistic Understanding of Polyethylene Biodegradation by the Marine Bacterium Alcanivorax. 2022 , 129278	1
265	Liquid chromatography coupled to tandem mass spectrometry for comprehensive quantification of crustacean tropomyosin and arginine kinase in food matrix. 2022 , 140, 109137	1
264	In-silico Studies Calculated a New Chitin Oligomer Binding Site Inside Vicilin: A Potent Antifungal and Insecticidal Agent. 2022 , 20, 155932582211082	
263	The gastric mucosa of Atlantic salmon (Salmo salar) is abundant in highly active chitinases.	
262	In Silico and In Vitro Analyses of Angiotensin-I Converting Enzyme Inhibitory and Antioxidant Activities of Enzymatic Protein Hydrolysates from Taiwan Mackerel (Scomber australasicus) Steaming Juice. 2022 , 11, 1785	2
261	A YAP/TAZ-TEAD signalling module links endothelial nutrient acquisition to angiogenic growth.	1

260	A Reduced F 420 -Dependent Nitrite Reductase in an Anaerobic Methanotrophic Archaeon.	1
259	Omics Analyses of Trichomonas vaginalis Actin and Tubulin and Their Participation in Intercellular Interactions and Cytokinesis. 2022 , 13, 1067	
258	Impact of Ferrous Sulfate on Thylakoidal Multiprotein Complexes, Metabolism and Defence of Brassica juncea L. under Arsenic Stress. 2022 , 11, 1559	
257	The phospho-docking protein 14-3-3 regulates microtubule-associated proteins in oocytes including the chromosomal passenger Borealin. 2022 , 18, e1009995	O
256	NuRD complex recruitment to Thpok mediates CD4 + T cell lineage differentiation. 2022 , 7,	O
255	Zika Virus Strains and Dengue Virus Induce Distinct Proteomic Changes in Neural Stem Cells and Neurospheres.	
254	Tandem immuno-purification of affinity-tagged proteins from mouse testis extracts for MS analysis. 2022 , 3, 101452	О
253	Androglobin, a chimeric mammalian globin, is required for male fertility. 11,	1
252	Control of CRK-RAC1 activity by the miR-1/206/133 miRNA family is essential for neuromuscular junction function. 2022 , 13,	
251	Enhanced Carbonylation of Photosynthetic and Glycolytic Proteins in Antibiotic Timentin-Treated Tobacco In Vitro Shoot Culture. 2022 , 11, 1572	O
250	LncRNA EPR-induced METTL7A1 modulates target gene translation.	О
249	Epithelial protein lost in neoplasm (EPLIN)-lis a novel substrate of ornithine decarboxylase antizyme 1, mediating cellular migration.	
248	Biochip Surfaces Containing Recombinant Cell-Binding Domains of Fibronectin. 2022, 12, 880	
247	Alternative transcript splicing regulates UDP-glucosyltransferase-catalyzed detoxification of DIMBOA in the fall armyworm (Spodoptera frugiperda). 2022 , 12,	O
246	HSP90 and Aha1 modulate microRNA maturation through promoting the folding of Dicer1.	1
245	Deletion of AA9 Lytic Polysaccharide Monooxygenases Impacts A. nidulans Secretome and Growth on Lignocellulose.	
244	Protein oxidation marker, \(\hat{\text{\text{\text{B}mino}}}\) adipic acid, impairs proteome of differentiated human enterocytes: Underlying toxicological mechanisms. 2022 , 1870, 140797	О
243	Label-free quantitative proteomic analysis of the mechanism of salt stress promoting selenium enrichment in Lactobacillus rhamnosus. 2022 , 265, 104663	

242	Complete secretion of recombinant Bacillus subtilis levansucrase in Pichia pastoris for production of high molecular weight levan. 2022 , 214, 203-211	0
241	Horizontal Integration: OMICS IMass Spectrometry-Based Proteomics in Systems Biology Research. 2022 ,	
240	An activity-based probe targeting the streptococcal virulence factor C5a peptidase.	О
239	Investigation of Structural Features of Two Related Lipases and the Impact on Fatty Acid Specificity in Vegetable Fats. 2022 , 23, 7072	1
238	Characterization and Genomic Analysis of a New Phage Infecting Helicobacter pylori. 2022, 23, 7885	0
237	Cell-free production of personalized therapeutic phages targeting multidrug-resistant bacteria. 2022 ,	1
236	Heterogeneous glycosylation and methylation of the Aeromonas caviae flagellin. 2022, 11,	
235	2.7 Eryo-EM structure of ex vivo RML prion fibrils. 2022 , 13,	3
234	Effect of incubation period on the glycosylated protein content in germinated and ungerminated seeds of mung bean (Vigna radiata (L.) Wilczek). 2022 ,	1
233	Phagocytosis of Plasmodium falciparum ring-stage parasites predicts protection against malaria. 2022 , 13,	1
232	Influence of short and medium distance road transport on the acute phase proteins in horses. 2022, 104061	
231	Revealing the difference of hmylase and CYP6AE76 gene between polyphagous Conogethes punctiferalis and oligophagous C. pinicolalis by multiple-omics and molecular biological technique. 2022 , 23,	
230	Identification of Microproteins in Saccharomyces cerevisiae under Different Stress Conditions.	О
229	Structure of Arabidopsis SOQ1 lumenal region unveils C-terminal domain essential for negative regulation of photoprotective qH.	0
228	Electronic cigarette liquids impair metabolic cooperation and alter proteomic profiles in V79 cells. 2022 , 23,	
227	Dysregulated Protein Phosphorylation in a Mouse Model of FTLD-Tau.	
226	Novel ⊞ein peptide fractions with in vitro cytotoxic activity against hepatocarcinoma. 2022 , 135, 48-59	О
225	Recognition of specific immunogenic antigens with potential diagnostic value in multi-drug resistant Mycobacterium tuberculosis inducing humoral immunity in MDR-TB patients. 2022 , 103, 105328	

224	Towards the purification of IgY from egg yolk by centrifugal partition chromatography. 2022 , 299, 121697	1
223	Recombinant AcnB, NrdR and RibD of Acinetobacter baumannii and their potential interaction with DNA adenine methyltransferase AamA. 2022 , 199, 106134	О
222	Structural analyses of human ryanodine receptor type 2 channels reveal the mechanisms for sudden cardiac death and treatment. 2022 , 8,	2
221	Coordinated control of the ADP-heptose/ALPK1 signalling network by the E3 ligases TRAF6, TRAF2/c-IAP1 and LUBAC.	
220	Super-enhancer hypermutation alters oncogene expression in B cell lymphoma. 2022, 607, 808-815	2
219	Proteogenomics identification of TBBPA degraders in anaerobic bioreactor. 2022 , 119786	
218	Comprehensive and systematic characterization of multi-functionalized cisplatin nano-conjugate: from the chemistry and proteomic biocompatibility to the animal model. 2022 , 20,	2
217	Discovering host protein interactions specific for SARS-CoV-2 RNA genome.	О
216	A Proteomic Platform Unveils the Brain Glycogen Phosphorylase as a Potential Therapeutic Target for Glioblastoma Multiforme. 2022 , 23, 8200	
215	Proteotoxicity caused by perturbed protein complexes underlies hybrid incompatibility in yeast. 2022 , 13,	O
214	Neuropilin 1 and its inhibitory ligand mini-tryptophanyl-tRNA synthetase inversely regulate VE-cadherin turnover and vascular permeability. 2022 , 13,	2
213	Dynamic states of eIF6 and SDS variants modulate interactions with uL14 of the 60S ribosomal subunit.	
212	Direct control of lysosomal catabolic activity by mTORC1 through regulation of V-ATPase assembly. 2022 , 13,	О
211	Cutaneous manifestations in Costello syndrome: HRAS p.Gly12Ser affects RIN1-mediated integrin trafficking in immortalized epidermal keratinocytes.	1
2 10	ERABD, an isoform of estrogen receptor alpha, promotes breast cancer proliferation and endocrine resistance. 2022 , 8,	1
209	Mesowestern Blot: Simultaneous Analysis of Hundreds of Submicroliter Lysates. 2022 , 7, 28912-28923	
208	Proteomics and Biochemical Analyses of Secreted Proteins Revealed a Novel Mechanism by Which ADAM12S Regulates the Migration of Gastric Cancer Cells.	
207	An Attenuated Strain of Human Cytomegalovirus for the Establishment of a Subviral Particle Vaccine. 2022 , 10, 1326	1

206	Drug affinity-responsive target stability unveils filamins as biological targets for artemetin, an anti-cancer flavonoid. 9,	
205	Human-specific gene CT47 blocks PRMT5 degradation to lead to meiosis arrest. 2022 , 8,	
204	TAOK2 represses translation via phosphorylation of eEF2 and ameliorates exaggerated protein synthesis in a mouse model of 16p11.2 microdeletion-driven autism.	
203	Mercury metalloproteomic profile in muscle tissue of Arapaima gigas from the Brazilian Amazon. 2022 , 194,	1
202	Purification of Human □and [Actin from Budding Yeast.	
201	Targeting of microvillus protein Eps8 by the NleH effector kinases from enteropathogenic E. coli. 2022 , 119,	О
200	N-glycans Profiling in Pilocarpine Induced Status Epilepticus in Immature Rats. 2022 , 69, 1-4	
199	Vitamin A Deficiency Alters the Phototransduction Machinery and Distinct Non-Vision-Specific Pathways in the Drosophila Eye Proteome. 2022 , 12, 1083	О
198	The AEhelix of CYP11A1 remodels mitochondrial cristae. 2022 , 29,	0
197	Identification of Transferrin Receptor 1 (TfR1) Overexpressed in Lung Cancer Cells, and Internalization of Magnetic Au-CoFe2O4 Core-Shell Nanoparticles Functionalized with Its Ligand in a Cellular Model of Small Cell Lung Cancer (SCLC). 2022 , 14, 1715	О
196	Tensin3 interaction with talin drives the formation of fibronectin-associated fibrillar adhesions. 2022 , 221,	2
195	Ectosomes and exosomes modulate neuronal spontaneous activity. 2022 , 269, 104721	1
194	SUMOylation of SYNJ2BP-COX16 promotes breast cancer progression through DRP1-mediated mitochondrial fission. 2022 , 547, 215871	0
193	Amyloid fibril formation by §1- and \(\text{D}\)casein implies that fibril formation is a general property of casein proteins. 2022 , 1870, 140854	2
192	Identification of Pinelliae Rhizoma and its counterfeit species based on enzymatic signature peptides from toxic proteins. 2022 , 107, 154451	o
191	Comparative maternal protein profiling of mouse biparental and uniparental embryos. 2022, 11,	1
190	Mechanistic Insights into the Functioning of a Two-Subunit GMP Synthetase, an Allosterically Regulated, Ammonia Channeling Enzyme. 2022 , 61, 1988-2006	0
189	A non-canonical scaffold-type E3 ligase complex mediates protein UFMylation.	O

188	INFOGEST Digestion Assay of Raw and Roasted Hazelnuts and Its Impact on Allergens and Their IgE Binding Activity. 2022 , 11, 2914	1
187	A Novel Role of Secretory Cytosolic Tryparedoxin Peroxidase in Delaying Apoptosis of Leishmania -Infected Macrophages.	Ο
186	Both AMP-activated and cAMP-dependent protein kinase regulate the expression of heat shock protein 70-2 gene in Neopyropia yezoensis. 9,	Ο
185	Bacterial Membrane Vesicles as a Novel Strategy for Extrusion of Antimicrobial Bismuth Drug in Helicobacter pylori.	О
184	Production of a viral surface protein in Nannochloropsis oceanica for fish vaccination against infectious pancreatic necrosis virus. 2022 , 106, 6535-6549	0
183	Two-Dimensional Blue Native/SDS Polyacrylamide Gel Electrophoresis for Analysis of Brazilian Bothrops Snake Venoms. 2022 , 14, 661	O
182	Evaluation of using the rice in Mekong Delta for beer making: nutritional, heat resistant, protease resistant and inhibitor properties of protein.	0
181	Targeting the USP7/RRM2 axis drives senescence and sensitizes melanoma cells to HDAC/LSD1 inhibitors. 2022 , 40, 111396	O
180	VAL1 acts as an assembly platform co-ordinating co-transcriptional repression and chromatin regulation at Arabidopsis FLC. 2022 , 13,	0
179	The Eucalyptus grandis chloroplast proteome: Seasonal variations in leaf development. 2022 , 17, e0265134	О
179 178	The Eucalyptus grandis chloroplast proteome: Seasonal variations in leaf development. 2022 , 17, e0265134 Development and Characterization of Type I, Type II, and Type III LIM-Kinase Chemical Probes.	0
178	Development and Characterization of Type I, Type II, and Type III LIM-Kinase Chemical Probes. Divergent regulation of KCNQ1/E1 by targeted recruitment of protein kinase A to distinct sites on	1
178 177	Development and Characterization of Type I, Type II, and Type III LIM-Kinase Chemical Probes. Divergent regulation of KCNQ1/E1 by targeted recruitment of protein kinase A to distinct sites on the channel complex.	0
178 177 176	Development and Characterization of Type I, Type II, and Type III LIM-Kinase Chemical Probes. Divergent regulation of KCNQ1/E1 by targeted recruitment of protein kinase A to distinct sites on the channel complex. A specific role for importin-5 and NASP in the import and nuclear hand-off of monomeric H3. 11,	1 0
178 177 176	Development and Characterization of Type I, Type II, and Type III LIM-Kinase Chemical Probes. Divergent regulation of KCNQ1/E1 by targeted recruitment of protein kinase A to distinct sites on the channel complex. A specific role for importin-5 and NASP in the import and nuclear hand-off of monomeric H3. 11, Characterizing the differential distribution and targets of Sumo paralogs in the mouse brain. Leveraging the Structure of DNAJA1 to Discover Novel Potential Pancreatic Cancer Therapies.	1 0 1
178 177 176 175	Development and Characterization of Type I, Type II, and Type III LIM-Kinase Chemical Probes. Divergent regulation of KCNQ1/E1 by targeted recruitment of protein kinase A to distinct sites on the channel complex. A specific role for importin-5 and NASP in the import and nuclear hand-off of monomeric H3. 11, Characterizing the differential distribution and targets of Sumo paralogs in the mouse brain. Leveraging the Structure of DNAJA1 to Discover Novel Potential Pancreatic Cancer Therapies. 2022, 12, 1391	1 O O

170	O-GlcNAcylation enhances CPS1 catalytic efficiency for ammonia and promotes ureagenesis. 2022 , 13,	1
169	A seed-like proteome in oil-rich tubers.	O
168	Concurrent inhibition of CDK2 adds to the anti-tumour activity of CDK4/6 inhibition in GIST.	2
167	Coordinated control of the ADP-heptose/ALPK1 signalling network by the E3 ligases TRAF6, TRAF2/c-IAP1 and LUBAC.	Ο
166	High-yield production in Escherichia coli and convenient purification of a candidate vaccine against SARS-CoV-2.	0
165	Characterization of the Secretome of Pathogenic Candida glabrata and Their Effectiveness against Systemic Candidiasis in BALB/c Mice for Vaccine Development. 2022 , 14, 1989	O
164	Evaluation of the Fecal Proteome in Healthy and Diseased Cheetahs (Acinonyx jubatus) Suffering from Gastrointestinal Disorders. 2022 , 12, 2392	1
163	Role of Intracellular and Extracellular Annexin A1 in MIA PaCa-2 Spheroids Formation and Drug Sensitivity. 2022 , 14, 4764	Ο
162	Glycan analysis of Lamin A/C protein at G2/M and S phases of the cell cycle.	Ο
161	On the role of cell surface associated, mucin-like glycoproteins in the pennate diatom Craspedostauros australis (Bacillariophyceae).	1
160	Secretome analysis of an environmental isolate Enterobacter sp. S-33 identifies proteins related to pathogenicity. 2022 , 204,	Ο
159	Lysosomal enzyme trafficking factor LYSET enables nutritional usage of extracellular proteins. 2022 , 378,	2
158	A fibrinogen-related Lectin from Echinometra lucunter represents a new FReP family in Echinodermata phylum. 2022 ,	Ο
157	Proteomic profiling of extracellular vesicles suggests Collectin10 as potential biomarker in relapsing head and neck squamous cell carcinoma. 2022 , 4, 9-17	Ο
156	Probing the sORF-encoded peptides of Deinococcus radiodurans in response to extreme stress. 2022 , 100423	О
155	Supranutritional Supplementation of Vitamin E Influences Myoglobin Post-Translational Modifications in Postmortem Beef Longissimus Lumborum Muscle. 2022 , 6,	Ο
154	Proteomics Unveils Post-Mortem Changes in Beef Muscle Proteins and Provides Insight into Variations in Meat Quality Traits of Crossbred Young Steers and Heifers Raised in Feedlot. 2022 , 23, 12259	1
153	Quantitative proteomics and biological activity of extracellular vesicles engineered to express SARS-CoV-2 spike protein. 2022 , 1,	1

152	Advantages of label free method in comparison with 2DE proteomic analysis of Butyrivibrio fibrisolvens 3071 grown on different carbon sources. 2022 , 21, 1508-1519	Ο
151	Genome-wide mapping of fluoroquinolone-stabilized DNA gyrase cleavage sites displays drug specific effects that correlate with bacterial persistence.	О
150	Molecular Mechanisms Mediating the Transfer of Disease-Associated Proteins and Effects on Neuronal Activity. 2022 , 1-26	1
149	Comprehensive Interactome Analysis for the Sole Adenylyl Cyclase Cyr1 of Candida albicans.	O
148	Subcellular localization of type IV pili regulates bacterial multicellular development. 2022, 13,	2
147	Proteomic consequences of TDA1 deficiency in Saccharomyces cerevisiae: Protein kinase Tda1 is essential for Hxk1 and Hxk2 serine 15 phosphorylation. 2022 , 12,	O
146	Algal photosystem I dimer and high-resolution model of PSI-plastocyanin complex. 2022, 8, 1191-1201	2
145	New In Vivo Approach to Broaden the Thioredoxin Family Interactome in Chloroplasts. 2022 , 11, 1979	Ο
144	NADPH Oxidase 5 (NOX5) Overexpression Promotes Endothelial Dysfunction via Cell Apoptosis, Migration, and Metabolic Alterations in Human Brain Microvascular Endothelial Cells (hCMEC/D3). 2022 , 11, 2147	0
143	Meat Quality and Muscle Tissue Proteome of Crossbred Bulls Finished under Feedlot Using Wet Distiller Grains By-Product. 2022 , 11, 3233	1
142	Juxtaposition of Bub1 and Cdc20 on phosphorylated Mad1 during catalytic mitotic checkpoint complex assembly. 2022 , 13,	0
141	A galactoside-specific Dalbergieae legume lectin from seeds of Vataireopsis araroba (Aguiar) Ducke.	0
140	Discovery and characterization of a new class of O-linking oligosaccharyltransferases from the Moraxellaceae family.	0
139	The HSP90 inhibitor 17-AAG induced calcium-mediated apoptosis in filarial parasites.	O
138	A pilot study to show that asymptomatic sexually transmitted infections alter the foreskin epithelial proteome. 13,	0
137	Nociceptor neurons direct goblet cells via a CGRP-RAMP1 axis to drive mucus production and gut barrier protection. 2022 , 185, 4190-4205.e25	3
136	Targeted Proteomic Analysis of Small GTPases in Radioresistant Breast Cancer Cells. 2022 , 94, 14925-14930	0
135	Effects of Hst3p inhibition in Candida albicans: a genome-wide H3K56 acetylation analysis. 12,	O

134	Interdependence of fucoxanthin biosynthesis and fucoxanthin-chlorophyll a/c binding proteins in Phaeodactylum tricornutum under different light intensities.	1
133	Overexpression of the plastidal pseudo-proteaseAtFtsHi3confers drought tolerance without penalizing growth.	О
132	Metalloproteomic approach to liver tissue of rats exposed to mercury. 2023 , 312, 137222	1
131	Protein Digestion for 2D-DIGE Analysis. 2023 , 339-349	1
130	Design and directed evolution of noncanonical 🛭 stereoselective metalloglycosidases. 2022, 13,	О
129	Kallikrein proteoforms and reproductive parameters in stallion are conditioned by climate. 2022 , 12,	О
128	The Predicted Splicing Variant c.11+5G>A in RPE65 Leads to a Reduction in mRNA Expression in a Cell-Specific Manner. 2022 , 11, 3640	O
127	The calcium-antagonist activity of the material released by olive pollen (PMR), tested on Ca2+-cytosolic of PE/CA-PJ15 cells.	О
126	Spatial regulation of the glycocalyx component Podocalyxin is a switch for pro-metastatic function.	О
125	Target Mechanisms of the Cyanotoxin Cylindrospermopsin in Immortalized Human Airway Epithelial Cells. 2022 , 14, 785	1
124	The photosystem I supercomplex from a primordial green algaOstreococcus tauriharbors three light-harvesting complex trimers.	О
123	The Nse5/6-like SIMC1-SLF2 complex localizes SMC5/6 to viral replication centers. 11,	O
122	Electrophoretic Detection of Black Market Myostatin Propeptide.	О
121	Conformational change of the Bordetella response regulator BvgA accompanies its activation of the B. pertussis virulence gene fhaB. 2022 ,	О
120	Bordetella pertussis whole cell immunization protects against Pseudomonas aeruginosa infections. 2022 , 7,	О
119	Energy sensor AMPK gamma regulates translation via phosphatase PPP6C independent of AMPK alpha. 2022 ,	О
118	Quantification of Protein Palmitoylation by Cysteine-SILAC. 2023, 59-69	O
117	Pseudo-phosphorylation of essential light chains affects the functioning of skeletal muscle myosin. 2022 , 106936	О

116	Mechanistic evaluation of chromium bioremediation in Acinetobacter junii strain b2w: A proteomic approach. 2023 , 328, 116978	0
115	The impact of the soluble protein fraction and kernel hardness on wheat flour starch digestibility. 2023 , 406, 135047	O
114	Analytical Characterization of Host Cell Proteins (HCPs). 2022 , 493-495	0
113	Calredoxin regulates the chloroplast NADPH-dependent thioredoxin reductase inChlamydomonas reinhardtii.	O
112	Protein Analysis of A. halleri and N. caerulescens Hyperaccumulators When Exposed to Nano and Ionic Forms of Cd and Zn. 2022 , 12, 4236	O
111	Human antibody recognition and neutralization mode on the NTD and RBD domains of SARS-CoV-2 spike protein. 2022 , 12,	1
110	SNF1 -related protein kinase 1 represses Arabidopsis growth through post-translational modification of E2Fa in response to energy stress.	0
109	LZTR1 mutation mediates oncogenesis through stabilization of EGFR and AXL.	O
108	Capture and mass spectrometry analysis of effector-substrate complexes using genetically incorporated photo-crosslinkers in host cells. 2022 , 3, 101882	О
107	Enhancing Cutaneous Wound Healing Based on Human Induced Neural Stem Cell-derived Exosomes. Volume 17, 5991-6006	O
106	Proteomic Profiling of Major Peanut Allergens and Their Post-Translational Modifications Affected by Roasting. 2022 , 11, 3993	2
105	Analysis of Golgi Protein Acetylation Using In Vitro Assays and Parallel Reaction Monitoring Mass Spectrometry. 2023 , 721-741	O
104	A Dual Detergent Strategy to Capture a Bacterial Outer Membrane Proteome in Peptidiscs for Characterization by Mass Spectrometry and Binding Assays.	O
103	Lysine deserts prevent adventitious ubiquitylation of ubiquitin-proteasome components.	O
102	Antibacterial Effects of ZnO Nanodisks: Shape Effect of the Nanostructure on the Lethality in Escherichia coli.	0
101	ZNF524 directly interacts with telomeric DNA and supports telomere integrity.	O
100	Biodegradation of Punicalagin into Ellagic Acid by Selected Probiotic Bacteria: A Study of the Underlying Mechanisms by MS-Based Proteomics.	1
99	Isolation, characterization and genome analysis of an orphan phage FoX4 of the new Foxquatrovirus genus. 2022 , 22,	O

98	Different Molecular Forms of TFF3 in the Human Respiratory Tract: Heterodimerization with IgG Fc Binding Protein (FCGBP) and Proteolytic Cleavage in Bronchial Secretions. 2022 , 23, 15359	1
97	ACTR5 controls CDKN2A and tumor progression in an INO80-independent manner. 2022 , 8,	Ο
96	A transcriptional switch controls sex determination in Plasmodium falciparum. 2022 , 612, 528-533	Ο
95	Ectopic CH60 mediates HAPLN1-induced cell survival signaling in multiple myeloma. 2023 , 6, e202201636	Ο
94	Affinity-Based Interactome Analysis of Endogenous LINE-1 Macromolecules. 2023, 215-256	Ο
93	Non-targeted metabolomics identifies erythronate accumulation in cancer cells.	Ο
92	Pseudomonas aeruginosa H3-T6SS Combats H2O2 Stress by Diminishing the Amount of Intracellular Unincorporated Iron in a Dps-Dependent Manner and Inhibiting the Synthesis of PQS. 2023 , 24, 1614	Ο
91	In-depth structural proteomics integrating mass spectrometry and polyacrylamide gel electrophoresis. 2,	Ο
90	Sample preparation for structural mass spectrometry via polyacrylamide gel electrophoresis. 2022,	0
89	GlnH, a Novel Antigen That Offers Partial Protection against Verocytotoxigenic Escherichia coli Infection. 2023 , 11, 175	Ο
88	Differential Serum Proteomic Signatures between Acute Aortic Dissection and Acute Myocardial Infarction. 2023 , 11, 161	0
87	Cancer-associated fibroblasts produce matrix-bound vesicles that influence endothelial cell function.	Ο
86	Genome-wide mapping of fluoroquinolone-stabilized DNA gyrase cleavage sites displays drug specific effects that correlate with bacterial persistence.	0
85	PML mutants resistant to arsenic induced degradation fail to generate the appropriate SUMO and ubiquitin signals required for RNF4 and p97 recruitment.	O
84	Mapping of functional SARS-CoV-2 receptors in human lungs establishes differences in variant binding and SLC1A5 as a viral entry modulator of hACE2. 2023 , 87, 104390	0
83	Attachment of the RNA degradosome to the bacterial inner cytoplasmic membrane prevents wasteful degradation of rRNA in ribosome assembly intermediates. 2023 , 21, e3001942	Ο
82	Structural and functional analysis of a tandem repeat galacturonic acid-binding lectin from the sea hare Aplysia californica. 2023 , 132, 108513	0
81	Dynamic states of eIF6 and SDS variants modulate interactions with uL14 of the 60S ribosomal subunit.	Ο

80	Multi-omics approach reveals elevated potential of bacteria for biodegradation of imidacloprid. 2023 , 221, 115271	О
79	The effects of mercury exposure on Amazonian fishes: An investigation of potential biomarkers. 2023 , 316, 137779	O
78	The p97/VCP segregase is essential for arsenic-induced degradation of PML and PML-RARA. 2023 , 222,	О
77	Myristoylated Neuronal Calcium Sensor-1 captures the ciliary vesicle at distal appendages.	O
76	Drug-induced eRF1 degradation promotes readthrough and reveals a new branch of ribosome quality control.	О
75	Protein-Based Biological Materials: Molecular Design and Artificial Production.	O
74	Analysis of Mammalian Circadian Clock Protein Complexes Over a Circadian Cycle. 2023 , 102929	0
73	Heteroleptic Copper(II) Complexes Containing 2?-Hydroxy-4-(Dimethylamino)Chalcone Show Strong Antiproliferative Activity. 2023 , 15, 307	O
72	Absolute quantification of photoreceptor outer segment proteins.	0
71	Nematode gene annotation by machine-learning-assisted proteotranscriptomics enables proteome-wide evolutionary analysis. 2023 , 33, 112-128	Ο
70	Cell division tracing combined with single-cell transcriptomics reveals new cell types and differentiation paths in the regenerating mouse lung.	0
69	Gum Arabic influences the activity of antioxidant enzymes during androgenesis in barley anthers.	O
68	ChipFilter: Microfluidic Based Comprehensive Sample Preparation Methodology for Metaproteomics.	О
67	An efficient in-gel digestion method on small amounts of protein sample from large intact gel pieces. 2200121	O
66	Microphysiological system recapitulating the pathophysiology of adipose tissue in obesity. 2023,	0
65	New lectin isolated from the tropical sponge Haliclona (Reniera) implexiformis (Hechtel, 1965) shows antibiofilm effect. 2023 , 95,	O
64	Eye proteome ofDrosophila melanogaster.	О
63	Structural and mechanistic insights into fungal 🖟 1,3-glucan synthase FKS1. 2023 , 616, 190-198	O

62	Endothelial FAT1 inhibits angiogenesis by controlling YAP/TAZ protein degradation via E3 ligase MIB2. 2023 , 14,	Ο
61	Venomous Noodles: evolution of toxins in Nemertea through positive selection and gene duplication.	O
60	Compartmentalization of the SUMO/RNF4 pathway by SLX4 drives DNA repair. 2023,	0
59	Microcosm-omics centric investigation reveals elevated bacterial degradation of imidacloprid. 2023 , 324, 121402	O
58	Proteomic dissection of the role of GliZ in gliotoxin biosynthesis in Aspergillus fumigatus. 2023 , 166, 103795	О
57	Proteomics in bovine semitendinosus muscle to assess emerging strategies based on papain injection and ultrasounds on meat tenderization process. 2023 , 200, 109147	O
56	Study on the mechanism and pharmacokinetics of HB-NC4 based on C5b-9 target in the treatment of osteoarthritis. 2023 , 1869, 166699	0
55	Physiology and proteomics analyses reveal the response mechanisms of Rhizophora mucronata seedlings to prolonged complete submergence. 2023 , 25, 420-432	Ο
54	Induction and sustenance of antibacterial activities distinguishes response of mice toSalmonellaTyphi from response toSalmonellaTyphimurium. 2023 , 81,	0
53	Mycelial and secretome proteomic dynamics of L. squarrosulus AF5 in azo dye degradation. 2023 , 11, 109374	O
52	Dysregulation of metalloproteins in ischemic heart disease patients with systolic dysfunction. 2023 , 232, 123435	0
51	Regioselective protein oxidative cleavage enabled by enzyme-like recognition of an inorganic metal oxo cluster ligand. 2023 , 14,	Ο
50	RNA-DNA hybrids prevent resection at dysfunctional telomeres. 2023 , 42, 112077	1
49	Ultrastructural and proteomic evidence for the presence of a putative nucleolus in an Archaeon. 14,	O
48	Acute phase proteins levels in horses, after a single carbohydrate overload, associated with cecal alkalinization. 10,	0
47	Disruption of Staphylococcus aureus Biofilms with Purified Moringa oleifera Leaf Extract Protein. 2023 , 30, 116-125	O
46	Spatial regulation of the glycocalyx component podocalyxin is a switch for prometastatic function. 2023 , 9,	0
45	Myosin post-translational modifications and function in the presence of myopathy-linked truncating MYH2 mutations. 2023 , 324, C769-C776	Ο

44	McrD binds asymmetrically to methyl-coenzyme M reductase improving active site accessibility during assembly.	0
43	Structural mechanism of CRL4-instructed STAT2 degradation via a novel cytomegaloviral DCAF receptor. 2023 , 42,	О
42	Expression, purification, and characterisation of the p53 binding domain of Retinoblastoma binding protein 6 (RBBP6). 2023 , 18, e0277478	0
41	Shuffled ATG8 interacting motifs form an ancestral bridge between UFMylation and autophagy.	О
40	The production of Newcastle disease virus-like particles in Nicotiana benthamiana as potential vaccines. 14,	0
39	Low-scale production and purification of a biologically active optimized form of the antitumor protein growth arrest specific 1 (GAS1) in a mammalian system for post-translational analysis. 2023 , 193, 108858	o
38	Sugar transporter Slc37a2 regulates bone metabolism in mice via a tubular lysosomal network in osteoclasts. 2023 , 14,	О
37	Pseudomonas aeruginosa Dps (PA0962) Functions in H2O2 Mediated Oxidative Stress Defense and Exhibits In Vitro DNA Cleaving Activity. 2023 , 24, 4669	О
36	H3K4me3 regulates RNA polymerase II promoter-proximal pause-release. 2023 , 615, 339-348	0
35	DAXX adds a de novo H3.3K9me3 deposition pathway to the histone chaperone network. 2023 , 83, 1075	-1092. e 9
34	Diatom adhesive trail proteins acquired by horizontal gene transfer from bacteria serve as primers for marine biofilm formation.	О
33	Re-engineering a lost trait:IPD3, a master regulator of arbuscular mycorrhizal symbiosis, affects genes for immunity and metabolism of non-host Arabidopsis when restored long after its evolutionary loss.	o
32	Post-mortem muscle proteome of crossbred bulls and steers: Relationships with carcass and meat quality. 2023 , 278, 104871	О
31	Characterizing the differential distribution and targets of Sumo1 and Sumo2 in the mouse brain. 2023 , 26, 106350	O
30	The human sperm proteomelloward a panel for male fertility testing.	О
29	Bottom-Up Proteomics: Advancements in Sample Preparation. 2023 , 24, 5350	0
28	Profile-based proteomic investigation of unintended effects on transgenic and gamma radiation induced mutant soybean plants.	0
27	The mechanical arthropod vectorStomoxys calcitransinfluences the outcome of lumpy skin disease virus infection in cattle.	0

26	Proteomic Alterations in Human Dermal Fibroblasts under Photo-Induced Pollution Caused by Excessive Solar Irradiations such as Infra-Red, Blue Light, UVA and UVB. 2023 , 13, 16-32	O
25	The level of arylphorin in the haemolymph of Spodoptera mauritia Boisd. (Lepidoptera: Noctuidae) larvae is increased by the insecticide, pyriproxyfen.	O
24	Neuron-specific protein expression at striatal excitatory synapses.	O
23	Fecal Protein Profile in Eight Dogs Suffering from Acute Uncomplicated Diarrhea before and after Treatment. 2023 , 10, 233	o
22	SARS-CoV-2 NSP12 associates with the TRiC complex and the P323L substitution is a host adaption.	O
21	Identification of Myelin Basic Protein Proximity Interactome Using TurboID Labeling Proteomics. 2023 , 12, 944	0
20	Proteomics Reveals Damaging Effect of Alpha-Cypermethrin Exposure in a Non-Target Freshwater Microalga Chlorella sp. NC-MKM. 2023 , 80,	O
19	ZCCHC17 modulates neuronal RNA splicing and supports cognitive resilience in Alzheimer⊠ disease.	O
18	The photosystem I supercomplex from a primordial green alga Ostreococcus tauri harbors three light-harvesting complex trimers. 12,	O
17	Development of modern immunization agent against bovine papillomavirus type 1 infection based on BPV1 L1 recombinant protein. 10,	O
16	Deregulated Transcription and Proteostasis in Adult mapt Knockout Mouse. 2023 , 24, 6559	O
15	Expression of Xanthorhodopsin in Escherichia coli.	O
14	Protein Phosphatase 2A Regulates Phenotypic and Metabolic Alteration of Microglia Cells in HFD-Associated Vascular Dementia Mice via TNF-Arg-1 Axis.	О
13	Mitochondrial, cell cycle control and neuritogenesis alterations in an iPSC-based neurodevelopmental model for schizophrenia.	O
12	Dimerisation of European robin cryptochrome 4a.	0
11	Shigella IpaA mediates actin bundling through diffusible vinculin oligomers with activation imprint. 2023 , 42, 112405	O
10	Viral pIC-pocketing: RSV sequestration of eIF4F Initiation Complexes into bi-phasic biomolecular condensates.	0
9	The composition and functionality of bacterial membrane vesicles (bMVs) in Escherichia coli 🗈 time course comparison study in different media.	O

8	Dosage sensitivity to Pumilio1 variants in the mouse brain reflects distinct molecular mechanisms.	0
7	FACI is a novel clathrin adaptor protein 2-binding protein that facilitates low-density lipoprotein endocytosis. 2023 , 13,	O
6	A novel method for the component identification of human blood products: Mass spectrometric analysis of human fibrinogen digested after SDS-PAGE in-gel digestion. 2023 , 123718	0
5	A VEL3 histone deacetylase complex establishes a maternal epigenetic state controlling progeny seed dormancy. 2023 , 14,	O
4	Elevated Nuclear PHGDH Synergistically Functions with cMyc to Reshape the Immune Microenvironment of Liver Cancer.	0
3	An Assassin Secret: Multifunctional Cytotoxic Compounds in the Predation Venom of the Assassin Bug Psytalla horrida (Reduviidae, Hemiptera). 2023 , 15, 302	O
2	Targeted Proteomic Profiling Revealed Roles of Small GTPases during Osteogenic Differentiation.	0
1	Regulation of adaptive growth decisions via phosphorylation of the TRAPPII complex in Arabidopsis.	Ο